Universidade de Aveiro Secção Autónoma de Ciências da Saúde
2012

Ana Patrícia da Fonseca Tenreiro

Avaliação dos efeitos do Abeta através de um modelo sinaptossomal

Evaluating the effects of Abeta using a synaptosomal model

Universidade de Aveiro Secção Autónoma de Ciências da Saúde
2012

Ana Patrícia da Fonseca Tenreiro

Avaliação dos efeitos do Abeta através de um modelo sinaptossomal

Evaluating the effects of Abeta using a synaptosomal model

Dissertação apresentada à Universidade de Aveiro para cumprimento dos requisitos necessários à obtenção do grau de Mestre em Biomedicina Molecular, realizada sob a orientação científica da Professora Doutora Sandra Maria Tavares da Costa Rebelo, Professora Auxiliar Convidada da Secção Autónoma de Ciências da Saúde da Universidade de Aveiro.

Este trabalho contou com o apoio do Centro de Biologia Celular (CBC) da Universidade de Aveiro, e é financiado por fundos FEDER através do Programa Operacional Factores de Competitividade – COMPETE e por Fundos nacionais da FCT – Fundação para a Ciência e a Tecnologia no âmbito dos projetos PTDC/QUI-BIQ/101317/2008 e PEst-OE/SAU/UI0482/2011.

Dedico este trabalho aos meus pais e irmão, por todas as oportunidades que me deram e me conduziram até este momento.

o júri

presidente

Professora Doutora Odete Abreu Beirão da Cruz e Silva
Professora Auxiliar com Agregação da Secção Autónoma de Ciências da Saúde da Universidade de Aveiro

Professora Doutora Sandra Maria Tavares da Costa Rebelo
Professora Auxiliar Convidada da Secção Autónoma de Ciências da Saúde da Universidade de Aveiro

Doutora Maria de Fátima Camões Sobral Bastos
Investigadora do Centro de Biologia Celular da Universidade de Aveiro

agradecimentos

À Professora Sandra Rebelo agradeço pela forma como me orientou, pelos ensinamentos constantes, pelo entusiasmo e motivação.

À Professora Odete da Cruz e Silva pela oportunidade de trabalhar no Laboratório de Neurociências e por toda a disponibilidade prestada.

A todos os colegas do Laboratório de Neurociências, Laboratório de Transdução de Sinais, Laboratório de Biogénese de Organelos e Laboratório de Investigação Clínica.

Aos Investigadores do CBC pelo apoio científico sem o qual o sucesso do trabalho experimental não teria sido possível, bem como ao CBC por todos os equipamentos e reagentes de base.

À FCT pelo financiamento dos projetos PTDC/QUI-BIC/101317/2008 e PEst-OE/SAU/UI0482/2011.

À Filipa um Muito Obrigada pela ajuda na parte prática, apoio e preocupação nos momentos de mais trabalho. Obrigada Mariana por estares sempre pronta para ajudar!

À Oliveira, Ana, Sara, Rocha e Mónica pela disponibilidade e simpatia.

À Lili e à Regina pela amizade e companheirismo ao longo destes cinco anos.

À minha Família, em especial aos meus pais e irmão por todo o amor, carinho e entusiasmo que me transmitem em cada dia.

palavras-chave

Doença de Alzheimer, Abeta, Proteina precursora de amilóde de Alzheimer (PPA), fosforilação da PPA, Tau, fosforilação da Tau, sinaptossomas, proteinas fosfatases.

resumo

A Doença de Alzheimer (DA) é uma doença neurodegenerativa caracterizada pela presença de placas senis extracelulares (PSs), compostas principalmente pelo péptido Abeta, pelas tranças neurofibrilhares intracelulares (TNFs) compostas pela Tau hiperfosforilada, e pela disfunção sináptica. Assim, na DA estão envolvidas proteínas cuja expressão está alterada como a proteína precursora de amilóide de Alzheimer (PPA) e Tau, sendo a análise proteómica destas proteínas de grande importância para o estudo da patologia em questão. A possibilidade de estudar a sinapse, assim como o seu conteúdo proteico através dos sinaptossomas constitui um modelo muito atrativo, uma vez que as suas características morfológicas e funcionais são preservadas após o isolamento. No presente estudo, foram testadas duas metodologias distintas para isolar sinaptossomas, o protocolo de gradiente de Percoll e o protocolo de gradiente de sacarose. Da análise bioquímica desses protocolos verificou-se que o protocolo de gradiente de sacarose é mais eficiente, tendo sido aplicado nos diferentes ensaios realizados. De modo a avaliar os efeitos do Abeta na fosforilação anormal de proteínas envolvidas na DA, neste estudo foram analisados os efeitos do Abeta na fosforilação da PPA e Tau, nos resíduos Thr_{668} e Ser_{262}, respectivamente. Verificou-se que nas fracções sinaptossomais de córtex e hipocampo o Abeta provoca um aumento da fosforilação da PPA e da Tau nos resíduos em estudo, principalmente nas concentrações mais elevadas. Adicionalmente, e sabendo que a DA pode resultar do mau funcionamento de proteínas cinases e fosfatases, que podem levar à desregulação de vias de transdução de sinal, é também importante determinar quais dessas cinases e fosfatases estão envolvidas na desfosforilação dos resíduos Thr_{668} na PPA e Ser_{262} na Tau. Neste estudo, através da utilização de inibidores de fosfatases, o ácido ocadeico (AO) e a cantaridina (CT), observou-se um envolvimento da PP1 na desfosforilação da PPA e da Tau. No seu conjunto, os resultados obtidos sugerem que o Abeta pode estar envolvido na alteração de vias de sinalização que culminam na Doença de Alzheimer.

keywords

Alzheimer´s disease, Abeta, Alzheimer´s Amyloid Precursor Protein (APP), APP phosphorylation, Tau, Tau phosphorylation, synaptosomes, protein phosphatases.

abstract

Alzheimer´s disease (AD) is a neurodegenerative disorder characterized by the presence of extracellular senile plaques (SP) mainly composed by beta-amyloid peptide (Abeta), intracellular neurofibrillary tangles (NFTs) comprising hyperphosphorylated Tau and by synaptic dysfunction. Thus AD involves altered expression of some proteins, like Alzheimer´s Amyloid Precursor Protein (APP) and Tau, and therefore proteomic studies are of paramount importance for AD pathology. The possibility to investigate the synapse and their proteomic content using synaptosomes is a very attractive model since they preserve morphological and functional characteristics of synapse. In the present study, were tested two different methodologies: Percoll gradient protocol and sucrose gradient protocol to isolate synaptosomes, and it was shown that sucrose gradient protocol is more effective, being this protocol chosen to perform the following experiments. Due to the key role played by Abeta and abnormal protein phosphorylation in AD, in this study we analyzed the Abeta effects on APP and Tau phosphorylation, at Thr_{668} and Ser_{262} residues, respectively. We verified an increase in APP and Tau phosphorylation at these specific residues, for both cortical and hippocampal-synaptosomal enriched fractions, upon Abeta treatment, specially with higher concentrations. Additionally, and knowing that possibly AD is caused by protein kinases (PKs) and protein phosphatases (PPs) imbalance, which alters crucial signal transduction pathways, therefore is very important to establish the PPs involved in APP (Thr_{668}) and Tau (Ser_{262}) dephosphorylation. We observed an involvement of PP1 on APP and Tau dephosphorylation. Taken together, these findings suggest that Abeta could deregulate some signaling cascades leading to Alzheimer´s disease.

Abbreviations

Abeta	Amyloid β-peptide
AD	Alzheimer´s disease
ADAM	A Desintegrin And Metalloproteinase
ADP	Adenosine diphosphate
AICD	Amyloid precursor protein intracellular domain
AMPA	α-amino-3-hydroxy-5-methyl-4-isoxazole propionic acid receptor
AP	Amyloid plaque
Aph1	Anterior pharynx-defective 1
APLP1	APP Like Protein 1
APLP2	APP Like Protein 2
APOE	Apolipoprotein E
APP	Alzheimer´s amyloid precursor protein
APS	Ammonium persulfate
ATP	Adenosine triphosphate
BACE	Beta-APP cleaving enzyme
BCA	Bicinchoninic acid
BSA	Bovine serum albumin
CaMKII	Calcium/Calmodulin-dependent protein kinase
cAMP	Cyclic Adenosine Monophosphate
cdc2	Cyclin dependent protein kinase 2
cdc25	Cell division cycle 25
cdk5	Cyclin-dependent protein kinase 5
CKI	Casein Kinase I
CKII	Casein Kinase II
CNS	Central Nervous System
CSF	Cerebrospinal Fluid
CT	Computed Tomography
CT	Cantharidin
CTFα	Carboxyl-terminal fragment α
CTFβ	Carboxyl-terminal fragment β
DAG	Dyacilglycerol
DC	Dielectric constant
DSPases	Dual Specificity Protein phosphatases
DTT	Dithiothreitol
Dyrk1A	Dual-specific tyrosine (y) regulated kinase 1A

ECL	Enhanced chemiluminescence
EGTA	Ethylene glycol tetraacetic acid
EOAD	Early Onset Alzheimer´s Disease
ERK	Extracellular signal Regulated MAP Kinase
FAD	Familial Alzheimer´s Disease
FDG	18F-2-deoxy-2-fluoro-D-glucose
GKAP	Guanylate kinase-associated protein
GPCR	G-Protein Coupled Receptor
GSK3	Glycogen synthase kinase-3
HEPES	4-(2-hydroxyethyl)-1-piperazineethanesulfonic acid
I1	Inhibitor 1
I2	Inhibitor 2
imAPP	immature APP
IP3	Inositol triphosphate
IR	Insulin receptor
IRS	Insulin receptor substrate
JNK	Jun N-terminal kinase
KPI	Kunitz-type serine protease inhibitor
LB	Loading buffer
LGB	Lower gel buffer
LOAD	Late Onset Alzheimer´s Disease
MAP	Microtubule Associated Protein
MAPK	Mitogen-activated protein kinase
mAPP	mature APP
MAPT	Microtubule Associated Protein Tau
MARK	Microtubule affinity regulating kinase
Mint	Munc18-interacting protein
MRI	Magnetic Resonance Imaging
mRNA	Messenger RNA
MTT	3-(4,5-Dimethylthiazol-2-yl)-2,5-diphenyltetrazolium bromide
Munc13	Mammalian homologues of the C.elegans unc-13 gene
Munc18	Mammalian homologues of the C.elegans unc-18 gene
Nct	Nicastrin
NEP	Nerve ending particles
NFTs	Neurofibrillary tangles
NMDAR	N-methyl-D-aspartate Receptor
OA	Okadaic acid
ON	Overnight

P1	First pellet
P2	Second Pellet
PAGE	Polyacrylamide-gel electrophoresis
p-APP	Phosphorylated Alzheimer´s amyloid precursor protein
PDK1	Phosphoinositide dependent Kinase 1
Pen-2	Presenilin enhancer 2
PET	Positron Emission Tomography
PHF	Paired Helical Filaments
Pi	Inorganic phosphate
PI3K	Phosphoinositide 3 Kinase
PIB	Pittsburgh compound B
PIP2	Phosphatidylinositol (4,5) biphosphate
PIP3	Phosphatidylinositol (3,4,5) triphosphate
PK	Protein Kinase
PKA	Cyclin AMP-dependent protein kinase
PKB	Protein Kinase B
PKC	Protein kinase C
PLCβ	Phospholipase C-β
PNS	Peripheral Nervous System
PP	Protein Phosphatase
PP1	Protein Phosphatase 1
PP2A	Protein Phosphatase 2A
PP2B	Protein Phosphatase 2B
PP2C	Protein phosphatase 2C
PP5	Protein Phosphatase 5
PP6	Protein Phosphatase 6
PPM	Protein Phosphatase metal-dependent
PPP	Phosphoprotein Phosphatase
PS1	Presenilin-1
PS2	Presenilin-2
PSD	Post-synaptic density
PSD-93	Post-synaptic density of 93 kDa
PSD-95	Post-synaptic density of 95 kDa
PSEN1	Presenilin-1 gene
PSEN2	Presenilin-2 gene
p-Tau	Phosphorylated Tau protein
PTEN	Phosphatase and Tensin homolog
PTP	Protein Tyrosine Phosphatase

RIM	Rab3-interacting molecule
RNA	Ribonucleic Acid
ROS	Reactive Oxygen Species
RT	Room temperature
S1	First supernatant
S2	Second supernatant
SAP90	Synapse Associated Protein of 90 kDa
sAPP	Secreted APP
sAPPα	Secreted APP α
sAPPβ	Secreted APP β
SCAMPs	Secretory carrier-associated membrane proteins
SDS	Sodium dodecyl sulfate
Ser	Serine
SHANK	SH3 domain and ankyrin repeat domain
SNAP-25	Synaptosome-associated protein of 25 kDa
SNARE	Soluble NSF attachment protein receptor
SP	Senile plaques
SPECT	Single Photon Emission Computed Tomography
SV	Synaptic Vesicles
Syn	Synaptosomes
TBS	Tris buffered saline
TBS-T	Tris buffered saline - tween
Thr	Threonine
Tris	Tris(hydroxymethyl)aminomethane
Tyr	Tyrosine
VAMPs	Vesicle-associated membrane polypeptides
UGB	Upper gel buffer
WR	Working reagent

Index

1 Introduction 9
1.1 Alzheimer´s Disease 10
1.1.1 Hallmarks of Alzheimer´s Disease 10
1.1.2 Classification of Alzheimer´s disease 12
1.1.2.1 Amyloid cascade hypothesis 15
1.1.3 Stages of Alzheimer´s Disease 16
1.1.4 Diagnosis and Treatment 17
1.2 Alzheimer´s Amyloid Precursor Protein (APP) gene family 18
1.2.1 APP isoforms 19
1.2.2 APP Processing 21
1.2.3 Abeta peptide 22
1.3 Tau biology and function 23
1.3.1 Tau isoforms 23
1.4 Protein Phosphorylation 25
1.4.1 APP Phosphorylation 28
1.4.2 Tau Phosphorylation 30
1.4.3 Influence of Abeta Peptide on APP and Tau phosphorylation 34
1.5 Synaptic Transmission 36
1.6 Synaptosomes 39
2 Aims of the Dissertation 43
3 Materials and Methods 45
3.1 Antibodies 46
3.2 Preparation of biological material 47
3.2.1 Brain dissection and cortical and hippocampal homogenate preparation 47
3.2.2 Obtention of synaptosomal fraction 48

3.2.2.1 Percoll gradient protocol 48
3.2.2.2 Sucrose gradient protocol 48
3.3 Acetone protein precipitation 50
3.4 Treatment of synaptosomes with Abeta 50
3.5 Treatment of cortical synaptosomes with protein phosphatase inhibitors 51
3.6 MTT assay 51
3.7 BCA protein quantification assay 52
3.8 Sodium dodecyl sulfate - polyacrylamide gel electrophoresis (SDS-PAGE) and Electrotransference 53
3.9 Immunoblotting 54
3.10 Quantification and statistical analysis 56
4 Results 57
4.1 Comparison of two methodologies to isolate synaptosomes: Percoll gradient protocol versus Sucrose gradient protocol 58
4.1.1 Isolation of cortical synaptosome-enriched fractions 59
4.1.2 Isolation of hippocampal synaptosome-enriched fractions 61
4.2 Effect of $Abeta_{1-42}$ treatment on synaptosome viability 63
4.2.1 MTT assay of cortical synaptosome-enriched fractions 63
4.2.2 MTT assay of hippocampal synaptosome-enriched fractions 64
4.3 Role of Abeta on APP and Tau phosphorylation 65
4.3.1 Cortical synaptosome-enriched fractions 65
4.3.1.1 APP phosphorylation in cortical synaptosome-enriched fractions 66
4.3.1.2 Tau phosphorylation in cortical synaptosome-enriched fractions 67
4.3.2 Hippocampal synaptosome-enriched fractions 69
4.3.2.1 APP phosphorylation in hippocampal synaptosome-enriched fractions 69
4.3.2.2 Tau phosphorylation in hippocampal synaptosome-enriched fractions 70
4.4 Protein phosphatases involved on APP and Tau dephosphorylation 72

4.4.1 Effect of Okadaic acid and Cantharidin on APP phosphorylation 72

4.4.1.1 Okadaic acid and APP phosphorylation..... 72

4.4.1.2 Cantharidin and APP phosphorylation 74

4.4.2 Effect of Okadaic acid on Tau phosphorylation 75

5 Discussion..... 77

6 Concluding Remarks..... 85

7 References..... 87

8 Appendix 97

1 Introduction

1.1 Alzheimer´s Disease

In 1906, Alois Alzheimer, a German psychiatrist, identified and described a neuropsychiatric disorder that affect the elderly, which is known as Alzheimer´s disease (AD) (Irvine et al., 2008; Pleckaityte, 2010). AD is the most common form of dementia and is a chronic, irreversible and progressive neurodegenerative disorder. Clinically is characterized by deterioration of memory (inability to form new and to retrieve old ones), cognitive decline and behavioral changes resulting in dementia. This disease leads to death, usually within 7 to 10 years after diagnosis, but some patients live longer than 20 years (Masters et al., 2006; Irvine et al., 2008; Crewes and Mashliah, 2010).

Currently, AD affects more than 24 million people worldwide, with 4.6 million new cases each year. In Portugal, 90000 people are affected by AD (www.alzheimerportugal.org/). Due to increasing of elderly population, it is expected that in 2050, 100 million of patients will develop this neurodegenerative disease (Wimo and Prince, 2010). Age is the biggest known risk factor, with the incidence of the disease increasing from one in ten of those over 65 years-old to almost half of those over 85 years-old. Women are more affected by AD, for the simple reason that they live longer than men (Irvine et al., 2008).

1.1.1 Hallmarks of Alzheimer´s Disease

Histopathologically, brain tissues from individuals affected with AD are characterized by the presence of two insoluble protein aggregates: β-amyloid plaques (APs), also called senile plaques (SPs) (Figure 1A), and neurofibrillary tangles (NFTs) (Figure 1B). Additionally, neuronal and synaptic loss in distinct brain areas, including neocortex and hippocampus, which in turn impaired synaptic contacts, are also characteristics of AD brains (Figure2; DeKosky and Scheff, 1990; Katzam and Saitoh, 1991).

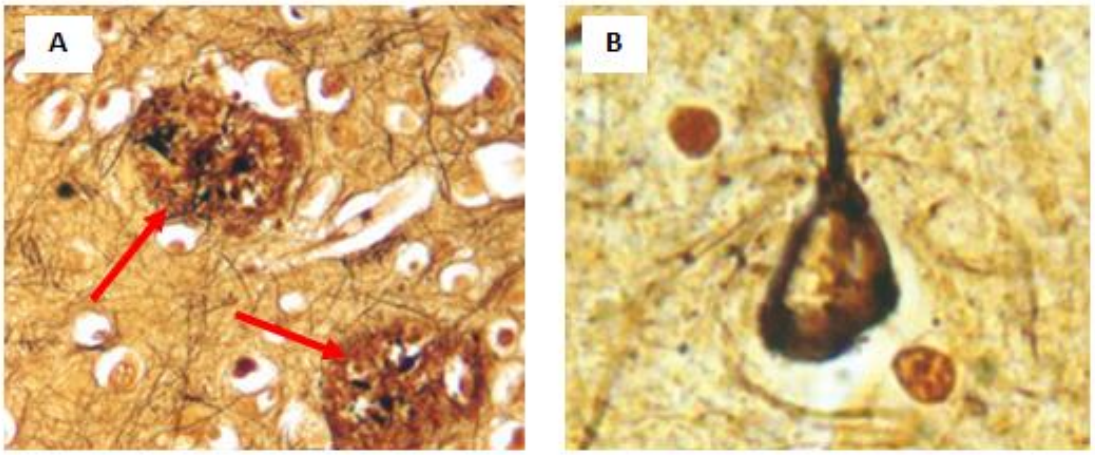

Figure 1: The two main histopathological hallmarks of AD. **A**) Senile plaques (SPs) mainly composed by Abeta peptide. **B**) Neurofibrillary tangles (NFTs), which are composed by hyperphosphorylated forms of microtubule-associated protein tau (MAPT). (Adapted from O´Brien and Wong, 2011).

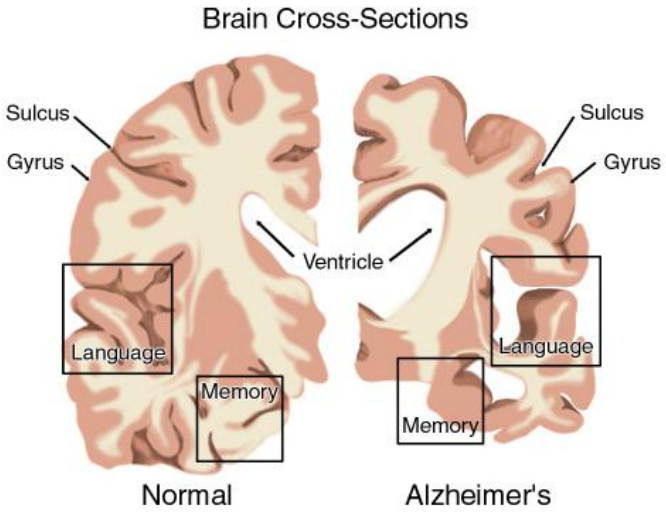

Figure 2: Normal brain and Alzheimer´s brain. (Taken from www.alzheimerportugal.org/)**.**

The SPs (Figure 1A) are largely insoluble spherical extracellular deposits, reaching up 200µm of diameter, and are prevalent throughout the cortex and hippocampus of affected brains (Glenner et al., 1984). These deposits are composed of proteinaceous deposits made mostly of Abeta peptide, predominantly the $Abeta_{1-42}$ form, which has more propensity to aggregate and form oligomers. These deposits are associated with

astrogliosis, microglia, and degenerating nerve terminals (dendrites and axons). Abeta peptide derives from proteolytic cleavage of Azheimer´s amyloid precursor protein (APP). In AD the accumulation of this peptide could result from an increased Abeta production and/or failure in clearance mechanisms (Pimplikar, 2009).

NFTs (Figure 1B) are intracellular aggregates of paired helical filaments (PHFs). PHFs are composed of abnormal hyperphosphorylated forms of microtubule-associated protein Tau (MAPT) mainly associated with smaller amounts of neurofilament protein, microtubule-associated proteins (MAPs), ubiquitin and APP (Yates and McLoughlin, 2007; Hooper et al., 2008).

Both SPs and NFTs are found only in the central nervous system (CNS) and they can be visualized in post-mortem brain analysis, specifically in the cerebral cortex and hippocampus (Katzam and Saitoh, 1991) . This evaluation is crucial for the confirmation of AD diagnosis (Irvine et al., 2008).

1.1.2 Classification of Alzheimer´s disease

Alzheimer´s disease is a multifactorial disease, being AD patients classified in two main groups: sporadic or non-familial form (more common) and genetic or familial form (rare). Only 5-10% of the AD patients have a familial Alzheimer´s disease (FAD) and 90-95% have a sporadic form of AD (Maccioni et al., 2001).

The causes of the sporadic cases are unknown, however some risk factors have been associated with AD. The age is thought to be the most predominant risk factor, which leads to synaptic failure and neuronal damage in cortical areas of the brain that are crucial for memory and mental functions (Masters et al., 2006) . The presence of a specific allele in the *APOE* gene that encodes apolipoprotein E, a protein involved in lipid transport and metabolism, is considered a risk factor for AD, more precisely in late onset AD cases. In fact this gene has 3 major alleles: ε2, ε3 and ε4. This last variant increases the risk to develop AD (Masters et al., 2006).

The gender, decreased mental activity, level of education, viral infections and head trauma history are other risk factors that are relevant for the developing of AD.

This type of disease could also be Late Onset Alzheimer´s Disease (LOAD), since it develops after the age of 65 years. LOAD does not show any overt pattern of familial segregation (Masters et al., 2006).

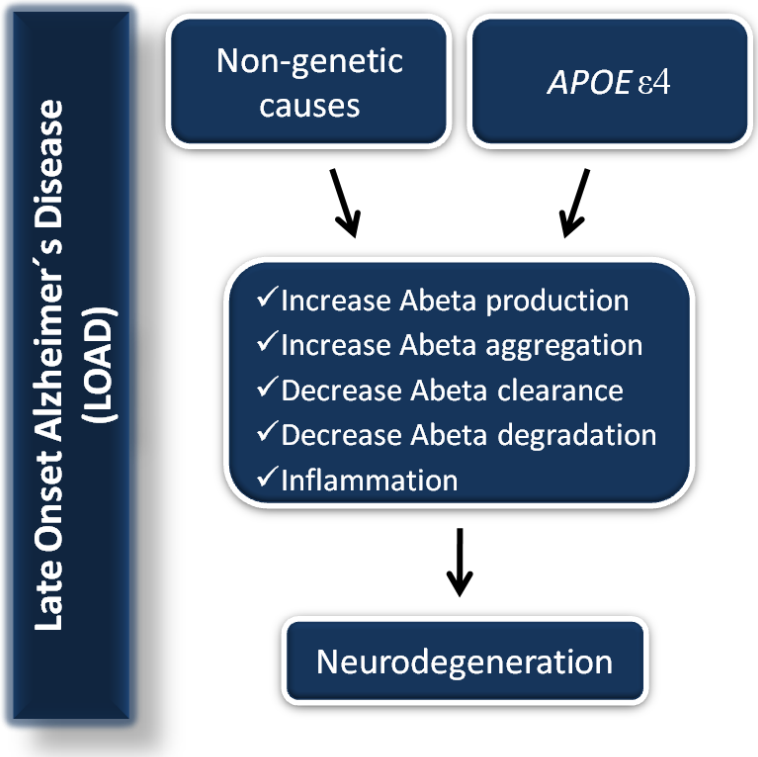

Figure 3: Schematic representation of principal causes of Late Onset Alzheimer´s Disease (LOAD). The non-genetic causes (age, gender, level of education, history of head trauma) and presence of APOEε4 allele, results in increased Abeta production or failure of clearance mechanisms that ultimately leads to neurodegeneration.

In familial cases, the major risk factors are mutations in at least three genes: amyloid precursor protein (*APP*) located on chromosome 21, presenilin-1 (*PSEN1*) located on chromosome 14 and presenilin-2 (*PSEN2*) on chromosome 1 (Figure 4). They encode APP, presenilin-1 (PS1) and presenilin-2 (PS2) proteins, respectively (Masters et al., 2006). Genetic cases are characteristic of Early Onset Alzheimer´s Disease (EOAD), which develops before the age of 65 years-old, with more than half of all such cases transmitted

as autosomal dominant trait. In the familial forms of EOAD (Figure 4), the mutations in *APP* or in *PSEN1* and *PSEN*2 genes, are related to an increased accumulation of Abeta which is directly correlated with AD pathogenesis (Maccioni et al., 2001).

However, besides these mutations and since mutations of *APP*, *PSEN*1 and 2 cannot explain all EOAD, is though that there are other undiscovered mutant genes that can be in the origin of some causes of AD.

Interestingly, the progression of AD is similar for both EOAD and LOAD (Sisodia and Tanzi, 2007; Irvine et al., 2008).

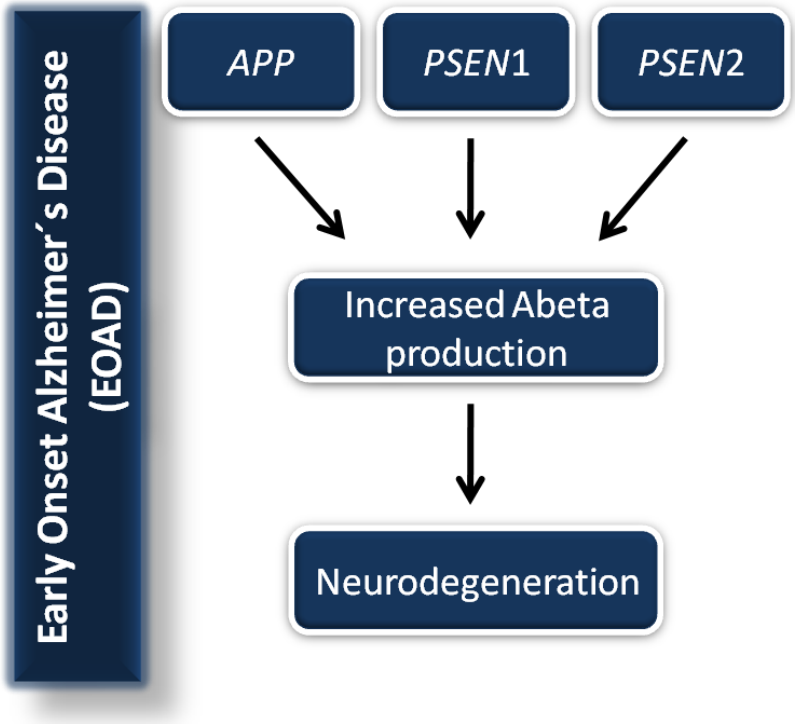

Figure 4: Schematic representation of principal causes of Early Onset Alzheimer´s Disease (EOAD). The later result is the increased Abeta production that will aggregate to form Senile Plaques that ultimately leads to neurodegeneration.

Genetic and sporadic causes of AD can interfere with signal transduction pathways leading to neurodegenerative conditions (Cong et al., 1993). However, other events could also be related with AD, resulting in abnormal protein processing, protein expression and subcellular localization. Abnormal phosphorylation of key control proteins has been

detected in many cases of AD and is thought to underlie the associated cellular dysfunctions that are characteristics of this disease (da Cruz e Silva and da Cruz e Silva, 2003) .

1.1.2.1 Amyloid cascade hypothesis

The amyloid cascade hypothesis defends that mismetabolism of APP, abnormal production, aggregation and deposition of Abeta are central mechanism to the AD pathogenesis, and that Abeta pathology, somehow leads to the Tau/NFT pathology (Figure 2 and 5; Karran et al., 2011).

As mentioned before the genetic mutations on *APP*, *PSEN1* and *PSEN2* genes, increases the risk to develop AD, since these mutations cause an increase of Abeta production (Levy-Lahad et al., 1995; Rogaev et al., 1995; Sherrington et al., 1995). Also, the localization of *APP* gene on chromosome 21 provides a connection of the development of AD pathology in patients with Down´s syndrome (Sisodia and Tanzi, 2007). These patients have an extra copy of chromosome 21 (trisomy) and therefore a third copy of *APP* gene, increasing the risk to develop AD because there is a higher Abeta production and deposition (Holtzman et al., 2000). Another aspect that supports this hypothesis is the *APOE* gene that increases the risk to develop LOAD. This gene is associated with Abeta clearance mechanism, and when deregulated, an increase of Abeta production is verified (Holtzman et al., 2000).

All this alterations cause Abeta accumulation, which results in neuronal death and, finally, in dementia (Karran et al., 2011).

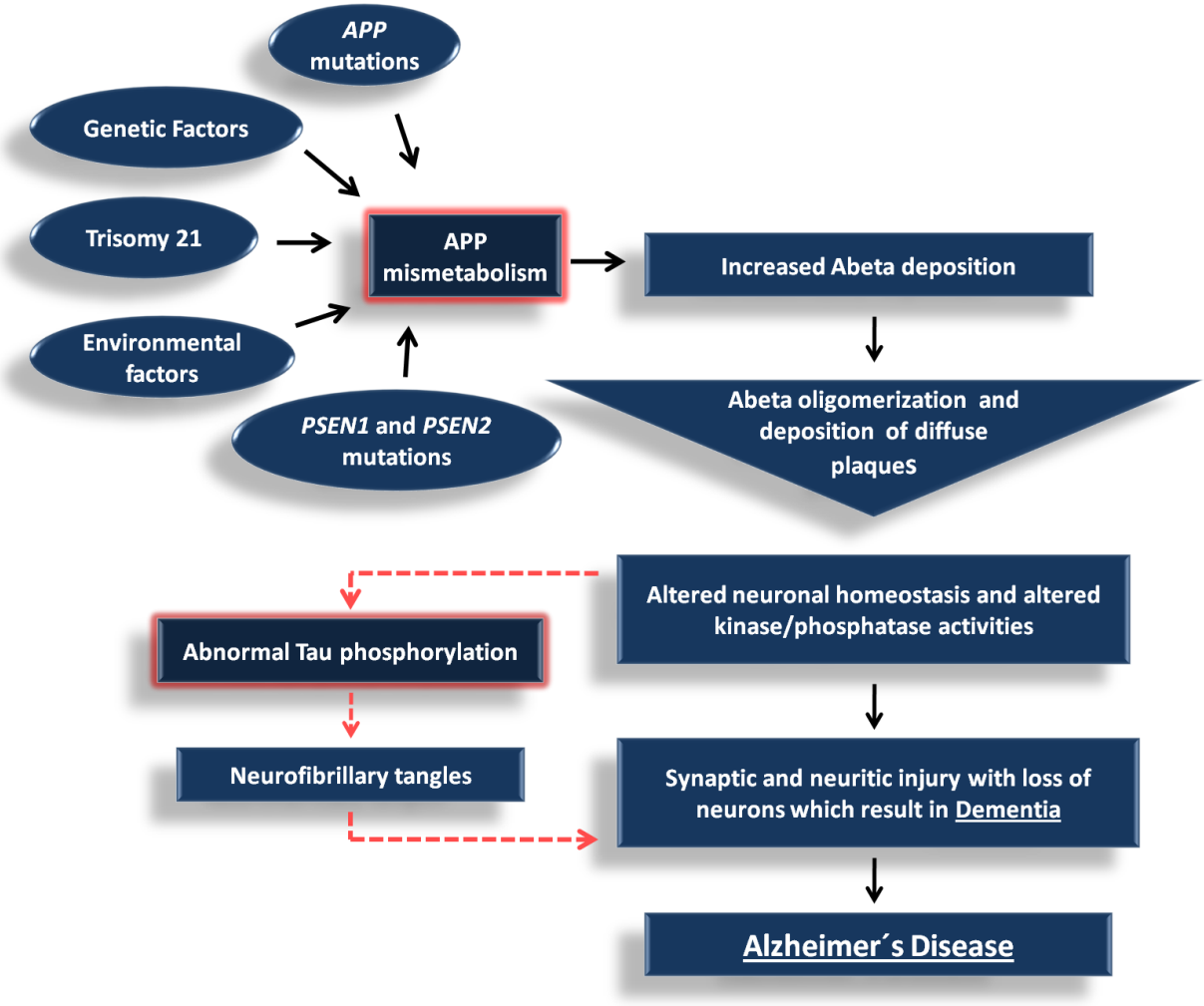

Figure 5: Amyloid cascade hypothesis. Mutations on *APP*, *PSEN1*, *PSEN2* and *APOE* genes are responsible for Abeta accumulation, which causes neuronal dysfunction and dementia (Adapted from Irvine et al., 2008; Karran et al., 2011).

1.1.3 Stages of Alzheimer´s Disease

During the progression of AD symptoms, three stages can be distinguished: mild, moderate and severe. In the first stage, patients manifest loss of memory, due to damage in hippocampal neurons (region of memory formation). In this stage, patients may forget words and names with increasing frequency and get lost even in familiar places. In the moderate stage, cortical regions, which are responsible for reasoning, are affected and AD patients may begin to lose their logical thinking and start to experience

some confusion. This stage is characterized by the difficulty of patients to recognize, identify family members and by changes in their personality. Finally, in the third stage, additional brain regions are damaged, resulting in loss of control of many normal physiological functions. AD patients are unable to take care of their daily living (feeding, hygiene, even walking) and lose their ability to speak coherently. Normally, the cause of death in AD cases result from deterioration of the brain's capacity to control vital physiological functions (Kelly, 2008).

1.1.4 Diagnosis and Treatment

AD is usually diagnosed clinically from the patient history, memory tests that can further characterize the state of the disease, clinical observations, based on the presence of characteristic neurological and neurophysiological features and by laboratory tests.

Currently, neuroimaging techniques are available to diagnose AD with high sensitivity and specificity. As imaging techniques can be referred Computed Tomography (CT), Magnetic Resonance Imaging (MRI), Single Photon Emission Computed Tomography (SPECT) and Positron Emission Tomography (PET) (Masters et al., 2006). All these techniques could be used to help in AD diagnose because they could exclude other cerebral pathologies. The detection of enlarged ventricular spaces is used to support the diagnosis of AD. For this purpose, MRI technique could be used to detect atrophy of specific brain regions that is a characteristic of AD patients (de Leon et al., 2004). PET exams allows for visualization of metabolism in various regions of the brain by using ^{18}F-2-deoxy-2-fluoro-D-glucose (FDG) as a surrogate marker of glucose metabolism. This is important because in patients with early AD, in some regions of brain, is detected a decreased metabolism of glucose (Masdeu et al., 2005). Recently, a new compound was discovered, called Pittsburgh compound B (PIB) and used in addition to PET in diagnosis. This compound is labeled with carbon-11 and has the capacity to cross the blood-brain barrier, binding to β-sheet-rich fibrils (amyloid deposits) in the brain parenchyma. Then

this marker could be detected by PET imaging. This is a promising *in vivo* technique that complements diagnosis of AD by detecting Abeta accumulation (Mathis et al., 2005).

Additionally, biochemical analysis of cerebrospinal fluid (CSF) are also available and the measurement of Abeta, total-Tau and p-Tau (phospho-Tau) in CSF, are some examples of methods that are being used as AD diagnosis tools (Irvine et al., 2008). However, full diagnosis is only confirmed after death.

Regarding to AD treatment, there is no effective treatment against progression of disease. The drugs available only delay worsening of symptoms. Different therapies are under development, including therapies that reduce Abeta and/or Tau deposition, therapies that improve memory by activating cholinergic neurotransmission and anti-oxidants.

1.2 Alzheimer´s Amyloid Precursor Protein (*APP*) gene family

The Alzheimer´s amyloid precursor protein (*APP*) gene was first identified in 1987. *APP* gene is located on chromosome 21 (21q21.2-3) in humans and encodes APP protein. This protein belongs to a protein family that includes APP like protein 1 (APLP1) and APP like protein 2 (APLP2) (Matsui et al., 2007). All are type I transmembrane proteins that are cleaved by a similar manner. However, only APP contain the sequence that encodes Abeta domain (Zhang et al., 2011). Therefore APLP1 and APLP2 are not Abeta precursors and their contribution to AD pathogenesis is by an indirect manner (Sisodia and Tanzi, 2007).

APP is ubiquitously expressed in several cell types, including Central Nervous System (CNS) cells, where is concentrated in neuronal synapses (Neve et al., 2000).

APP has a large hydrophilic aminoterminal domain projected toward the extracellular space, a single hydrophobic transmembrane domain consisting of 23 residues and a small carboxy-terminal cytoplasmic domain (Figure 6; Kang et al., 1987).

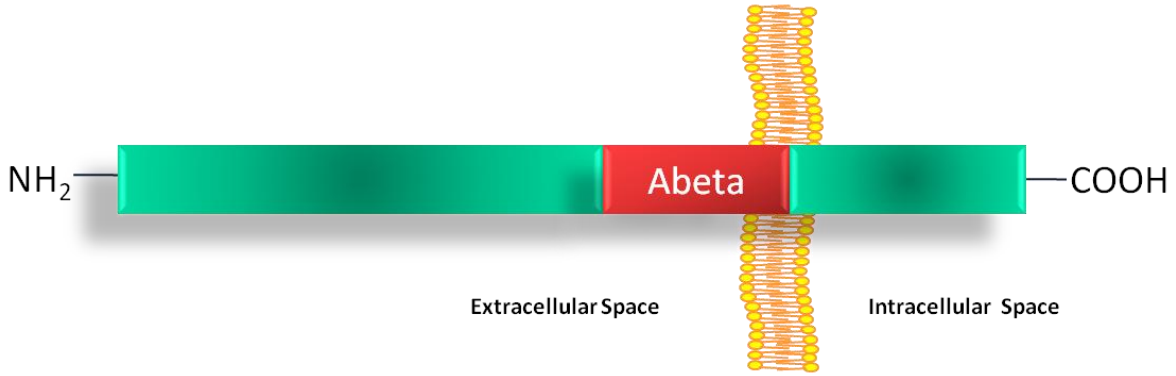

Figure 6: Representation of APP structure. APP has a large N-terminal ectodomain projected to extracellular space and a shorter C-terminal in cytoplasmatic domain. The region that will originate Abeta peptide is represented in red. (Adapted from Gandy, 2005).

1.2.1 APP isoforms

Alternative mRNA splicing of exons 7, 8 and 15 of *APP* gene result in at least 10 isoforms, ranging from 365 to 770 amino acids (da Cruz e Silva and da Cruz e Silva, 2003). However, the major isoforms, which predominate in most tissues, are APP_{695}, APP_{751} and APP_{770}, containing 695, 751, and 770 amino acids, respectively (Figure 7; da Cruz e Silva and da Cruz e Silva, 2003). The APP_{695} isoform is highly expressed in neurons, while APP_{751} and APP_{770} are highly expressed in non-neuronal cells (da Cruz e Silva and da Cruz e Silva, 2003). The isoforms are frequently divided into Kunitz-type protease inhibitor domain-containing isoform (APP-KPI^+) or Kunitz-type protease inhibitor domain-lacking isoforms (APP-KPI^-), which are generated by the alternative splicing of exon 7 (da Cruz e Silva and da Cruz e Silva, 2003). APP-KPI^+ isoforms, including APP_{751} and APP_{770}, have KPI domain and are the predominant isoforms expressed in non-neuronal cells under normal conditions (Tanzi et al., 1988) and APP-KPI^- isoform, like APP_{695}, has not KPI domain and is the predominant form produced by neurons and neuronal cells (Matsui et al., 2007).

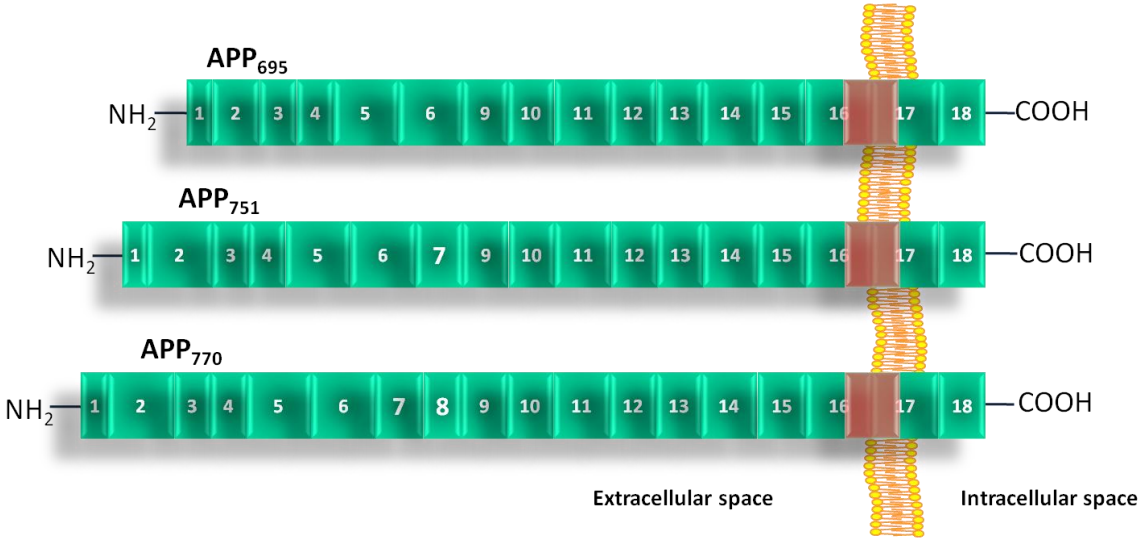

Figure 7: Schematic representation of the predominant APP isoforms. Boxes with respective number are representative of the exons. The most abundant neuronal isoform is APP_{695}, and differs from APP_{751} and APP_{770} isoforms since it lacks the exons 7 and 8. The red region represents the Abeta peptide sequence encoded by the exons 16 and 17. (Adapted from da Cruz e Silva and da Cruz e Silva, 2003) .

APP-KPI^- isoforms are enriched in AD brain, and for this reason, they are considered more amyloidogenic (Moir et al., 1998). The three main isoforms present in neuronal like cells (such as PC12 cells) are APP_{695}, APP_{751} and APP_{770} in both mature and immature forms. The sizes of these isoforms are in between 100-140 KDa (Figure 8).

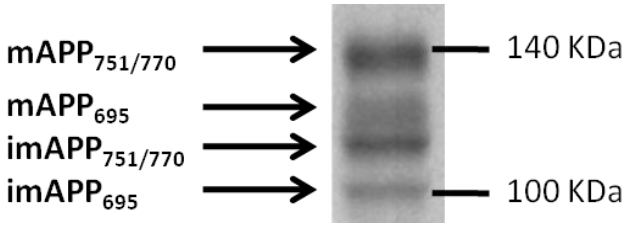

Figure 8: Intracellular expression of APP isoforms in PC12 cells. imAPP, immature APP; mAPP, mature APP. (Adapted from da Cruz e Silva and da Cruz e Silva, 2003).

Despite the enormous efforts to determine APP functions they still unclear. However several functions have been described to APP that includes functions as a receptor, involvement in synaptogenesis process and cell adhesion, iron export, synapse formation

and neural plasticity. APP could also have neurotrophic and neuroprotective properties (Maccioni et al., 2001; Priller et al., 2006; Schmidt et al., 2008).

1.2.2 APP Processing

During APP processing, a set of proteases called α-, β- and γ-secretases are involved, and depending on the enzyme that is acting and the final products, two major pathways can be distinguished: non-amyloidogenic pathway and amyloidogenic pathway (Maccioni et al., 2001; Yates and McLoughlin, 2007). In non-amyloidogenic pathway there is no Abeta production. In this case, α-secretase cleaves within the Abeta sequence releasing the soluble extracellular APP domain (sAPPα) while the α-C-terminal fragment (CTFα), also known as C83, is kept attached to the membrane and is further cleaved by γ-secretase complex generating the APP intracellular domain (AICD) and the p3 fragment (Figure 9). In this case, α-secretase has a neuroprotective action, because cleaves APP in position that prevents Abeta formation (Yates and McLoughlin, 2007). In amyloidogenic pathway, Abeta is produced by the action of β- and γ-secretases. Therefore, APP is first cleaved by the β-secretase, releasing a shorter variant of the soluble extracellular domain, sAPPβ and a CTFβ (C99) that is further cleaved by γ-secretase complex to produce AICD and Abeta (Figure 9; Yates and McLoughlin, 2007). Abeta production leads to Abeta monomer formation that will associate to form small oligomers that increase in size, leading to fibril formation, which culminates with SP formation (Irvine et al., 2008).

APP processing is regulated by three proteases: α-, β- and γ-secretases. α-secretase is a member of ADAM (a desintegrin and metalloproteinase) family of proteinases (Yates and McLoughlin, 2007); β-secretase has been identified as the aspartic protease BACE1 (β-APP cleaving enzyme) with a close homolog termed BACE2 (Yates and McLoughlin, 2007); and finally, γ-secretase is a multiprotein complex comprising at least four proteins: PS1 or PS2 (the catalytic component); nicastrin (Nct), a type I transmembrane glycoprotein; and Pen-2 and Aph-1, two transmembrane proteins (Yates and McLoughlin, 2007; Bergmans and De Strooper, 2010).

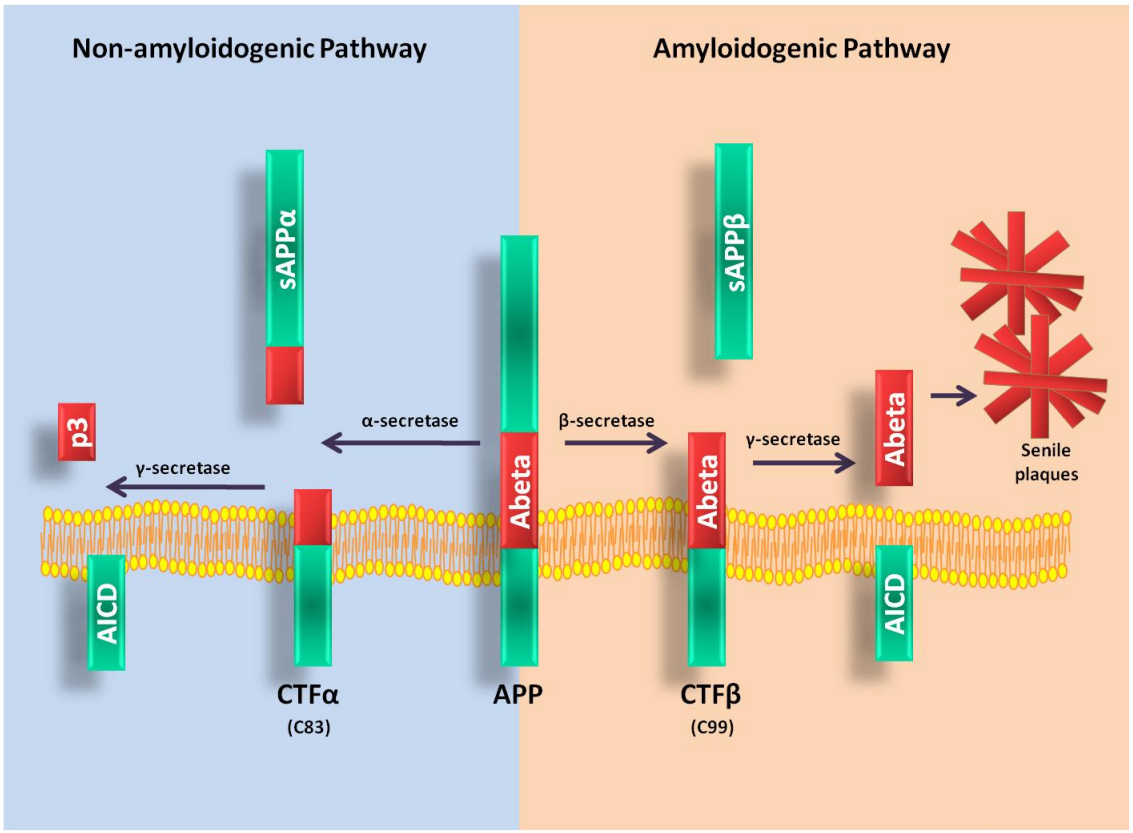

Figure 9: Schematic representation of APP processing. Non-amyloidogenic pathway involves the action of both α- and γ-secretases, resulting in generation of sAPPα, AICD and p3 fragments. Amyloidogenic pathway involves the activity of both β and γ-secretases and results in generation of sAPPβ, AICD and Abeta fragments. These fragments can self-aggregate to form Senile plaques. The different parts of APP are represented.

1.2.3 Abeta peptide

Abeta is produced during normal cellular metabolism and depending on the site of γ-secretase cleavage several species could be produced varying between 38 and 43 amino acids. These species have in overall around 4KDa (Haass et al., 1992). The two main forms of Abeta are composed by 40 amino acid residues ($Abeta_{1-40}$) and 42 amino acid residues ($Abeta_{1-42}$). The longer form of Abeta is more insoluble and increases the capacity to generate fibrils, self-aggregate and incorporate into SPs. For this reason, $Abeta_{1-42}$ has a greater tendency to aggregate compared with $Abeta_{1-40}$ and increased neurotoxicity in neuronal cells (Citron et al., 1996; Yates and McLoughlin, 2007). Neurotoxicity is the result of an imbalance between the production and clearance of Abeta, leading to progressive

accumulation of Abeta oligomers in the nerve terminal, which trigger a series of reactions like production of Reactive Oxygen Species (ROS), excitotoxicity mediated through elevated intracellular calcium (Ca^{2+}), altered energy metabolism due to damaged mitochondria and inflammatory responses. These mechanisms may lead to oxidative stress, synaptic dysfunction, microgliosis and loss of specific neuronal cell populations either via activation of necrotic or apoptotic pathways (Masters et al., 2006).

1.3 Tau biology and function

Tau is a low molecular and multifunctional microtubule-associated protein (MAP). In humans, Tau protein is predominantly expressed in neurons of both peripheral (PNS) and central nervous system (CNS). At normal conditions, it bounds to microtubules (components of neuronal cytoskeleton), stabilizing their structure and maintaining internal architecture (Yates and McLoughlin, 2007).

1.3.1 Tau isoforms

Human Tau proteins are encoded by a single gene, microtubule-associated protein Tau (*MAPT)* gene, located on locus 17q21-22 at chromosome 17, which consists of 16 exons. Tau is a family of six isoforms, ranging in length from 352 to 441 amino acids generated by alternative mRNA splicing of exons 2, 3 and 10 (Alonso et al., 2001). Tau isoforms can be distinguished by their composition of microtubule-binding domain and projection domain (Buee et al., 2000). Tau contains three or four C-terminal repeat domains (R1, R2, R3 and R4), encoded by exons 9, 10, 11 and 12, respectively. Each repeat domain consists of 18 amino acid sequence separated by less conserved 13 or 14 amino acid sequences. The sequence of 18 amino acids is responsible for binding to microtubules, promoting microtubule polymerization and stabilization. For this reason Tau isoforms with 4R (R1, R2, R3, R4) binds more efficiently to microtubules than the isoforms with 3R (R1, R3, R4) (Figure 10; Buee et al., 2000; Alonso et al., 2001).

Projection domain consists of the N-terminal part of protein Tau and is composed by none (0N), 29 (1N) or 58 (2N) amino acid sequences resulted from alternative splicing of exon 2 and exon 3, respectively (Figure 10). This domain projects from the microtubules and interacts with other cytoskeletal elements and plasma membrane (Buee et al., 2000). Tau proteins bind to spectrin and actin filaments and through these interactions, may allow microtubules to interconnect with other cytoskeletal components such as neurofilaments, which restrict the flexibility of the microtubules. (Buee et al., 2000; Alonso et al., 2001; Johnson and Stoothoff, 2004).

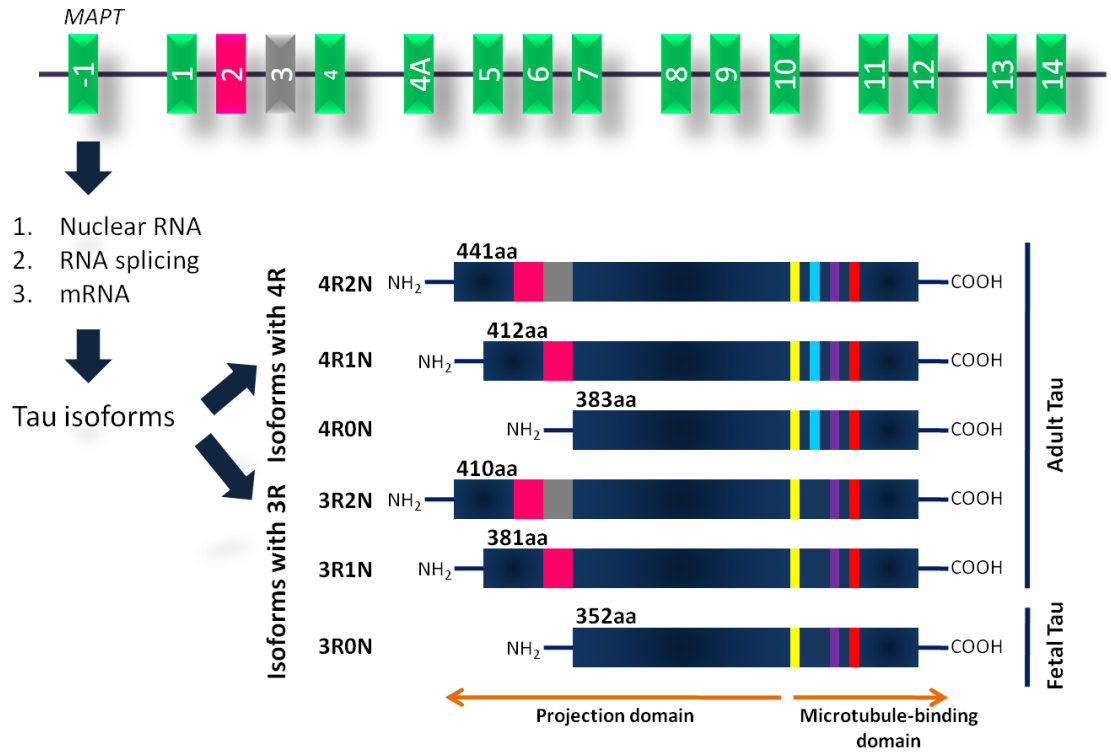

Figure 10: *MAPT* gene and its isoforms. *MAPT* gene located on the human chromosome 17 is transcribed into the corresponding nuclear RNA that after alternative splicing yields several Tau mRNAs. These mRNAs are translated and can originate 6 different Tau isoforms. These isoforms differ by the absence or presence of 29 (1N) or 58 (2N) amino acids inserts encoded by exon 2 (pink) and 3 (gray) in the amino terminal part, in combination with either three or four repeat regions in the carboxyl-terminal part. R1 (yellow), R2 (blue), R3 (purple) and R4 (red). (Adapted from Avila et al., 2004).

As shown in the Figure 10, the different Tau isoforms are 4R2N, 4R1N, 4R0N, 3R2N, 3R1N and 3R0N. The longest isoform has four repeats, two inserts and 441 residues. The shortest isoform is composed by three repeats, no inserts and possess 352 residues

(Johnson and Stoothoff, 2004). The later smallest isoform is called fetal Tau and is found in fetal human brain. However, all isoforms are found in adult human brain.

The six isoforms expressed in neurons are presented in Figure 11 and have molecular weight in between 50 and 75 KDa.

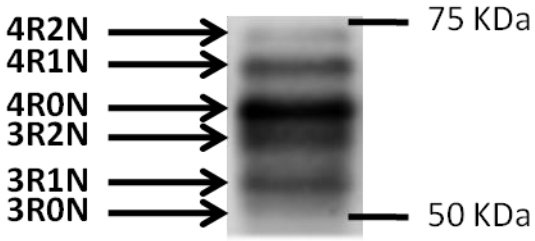

Figure 11: Intracellular expression of the six Tau isoforms in normal adult human brain.
(Adapted from Billingsley and Kincaid, 1997; Deshpande et al., 2008).

1.4 Protein Phosphorylation

Protein phosphorylation is an important reversible post-translational modification that regulates the structural and functional properties of proteins, and consequently, regulates protein activity, cell cycle, gene regulation, learning and memory (Johnson and Barford, 1993; Hunter, 1995). This modification is characterized by the addition of a phosphate group, provided by ATP, to a specific hydroxyl group of a serine, tyrosine or threonine residue of the protein. This reaction is catalyzed by protein kinases (PKs) and the addition of a phosphate group is responsible for a structural change because of its negative charge. Therefore the phosphorylation reaction can be reversed by a protein phosphatase (PP) that removes the phosphate from the protein (Figure 12).

The level of protein phosphorylation is controlled by the opposing actions of PKs and PPs. Abnormal function of these proteins can cause several diseases by altering the phosphorylation of critical proteins in normal and abnormal cellular processes (Hunter, 1995; Chung, 2009).

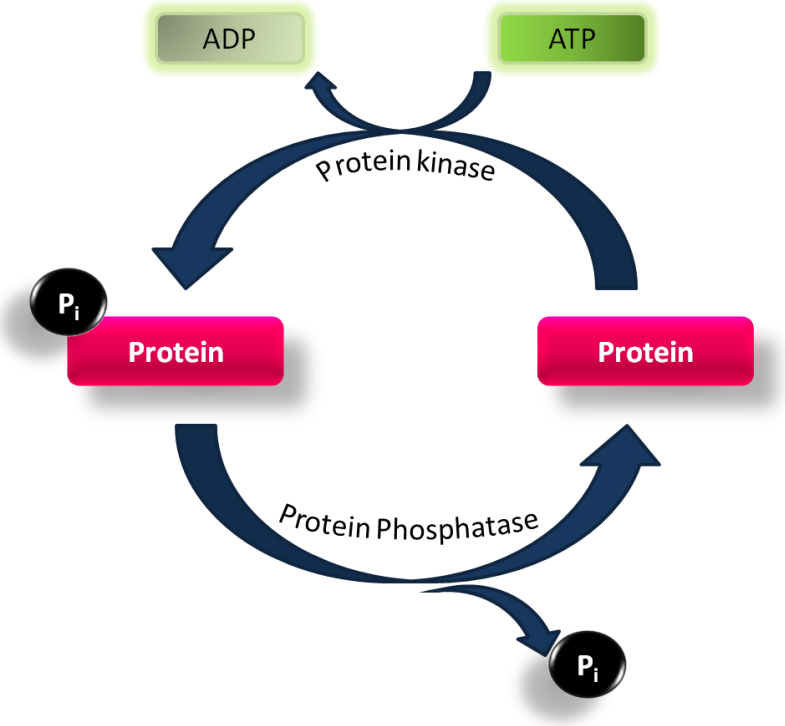

Figure 12: Protein phosphorylation. Proteins are phosphorylated by protein kinases which remove a phosphate from ATP to a donor, whereas protein phosphatases remove the phosphate group from a protein resulting in dephosphorylation of that protein.

Abnormal protein phosphorylation has been associated with several pathologies including AD, since it modifies substrates in various functions such as interaction with other proteins, subcellular localization, enzymatic activity, ligand binding, and other properties (Chung, 2009). In Table 1 are summarized the PKs and PPs that are thought to be involved in AD.

Table 1: Protein kinases (PKs) and Protein phosphatases (PPs) with altered expression and/or activity in AD. (↑ increased, ↓ decreased) (Adapted from Chung, 2009).

PKs	↑ Glycogen synthase kinase 3 (GSK3)
	↑ Cyclin-dependent kinases (Cdc2 and cdk5)
	↑ Dual-specific tyrosine (Y) Regulated Kinase 1A (Dyrk1A)
	↑ Ca^{2+}/Calmodulin-dependent protein kinase (CaMKII)
	↑ Casein Kinase I and II (CKI and CKII)
	↓ Cyclic-AMP-dependent kinase (PKA)
	↓ Protein Kinase C (PKC)
	↑ Protein kinase B (PKB or Akt)
	↑ Mitogen-activated protein kinases (MAPKs)
PPs	↓ Protein Phosphatase 1 (PP1)
	↓ Protein Phosphatase 2A (PP2A)
	↑ Protein Phosphatase 2B (PP2B or Calcineurin)
	↓ Protein Phosphatase 5 (PP5)
	↑ Cell division cycle 25A and 25B (cdc25A and cdc25B)
	↓ Phosphatase and Tensin Homolog (PTEN)

Protein kinases such as Glycogen synthase kinase 3 (GSK3α and β), Cyclin-dependent kinase 5 (Cdk5), Dual-specific tyrosine (Y) Regulated Kinase 1A (Dyrk1A) and Mitogen-Activated Protein Kinases (MAPKs), like c-Jun-N-terminal kinase (JNK), extracellular signal regulated MAP Kinase (ERK) and p38 are up regulated in their expression and activity in AD patients (Chung, 2009).

Relatively to protein phosphatases they can be classified into three main classes based on sequence, structure and catalytic site: phosphoprotein phosphatase (PPP) and protein phosphatase metal-dependent (PPM) families which are both Serine/Threonine protein phosphatases, and the protein tyrosine phosphatase (PTP) superfamily. The largest class of PPs is the PPP family and includes PP1, PP2A, PP2B, PP4, PP5 and PP7 whereas the PPM family comprises Mg^{2+}-dependent enzymes such as PP2C and mitochondrial protein phosphatases. Members of the PTP superfamily are categorized as either classical PTPs or dual specificity protein phosphatases (DSPases). DSPases dephosphorylate the serines, threonines and tyrosines of a particular substrate and consist of cdc25 and phosphatase and tensin homolog (PTEN) (Tian and Wang, 2002; Chung, 2009).

In order to determine which protein phosphatases are involved in dephosphorylation of proteins, some synthetic inhibitors commercially available could be used, as okadaic acid (OA) and cantharidin (CT), among others. OA and CT are both used to inhibit PP-family Serine/Threonine protein phosphatases like PP1 and PP2A. OA is the most widely used inhibitor to study PP1 and PP2A, being able to inhibit other PPs as PP4, PP5 and PP6. Cantharidin could also be used to inhibit PP1 and PP2A, being a weak inhibitor of PP2B (Swingle et al., 2007).

1.4.1 APP Phosphorylation

APP contains several residues that can be phosphorylated in its cytoplasmic and ectoplasmic domains (Gandy et al., 1988; Knops et al., 1993). The following phosphorylation sites were recently shown to be phosphorylated in AD brains: Ser_{198}, Ser_{206}, Tyr_{653}, Thr_{654}, Ser_{655}, Thr_{668}, Ser_{675}, Tyr_{682}, Thr_{686} and Tyr_{687} (Figure 13; Lee et al., 2003; Chung, 2009).

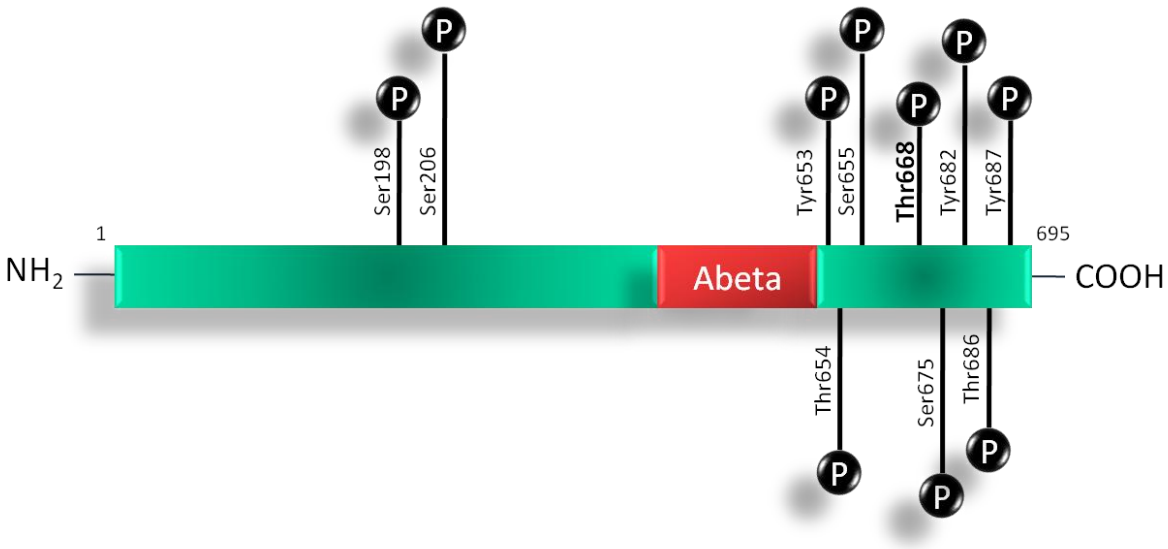

Figure 13: Phosphorylation sites on APP cytoplasmic and ectoplasmic domains. (Adapted from Slomnicki and Lesniak, 2008).

A summary of the kinases responsible for APP phosphorylation are presented in Table 2. However, the phosphorylation of some residues still unknown. Also, relative to APP dephosphorylation, there are no conclusive studies regarding the protein phosphatases involved.

Table 2: APP phosphorylatable residues. The protein kinases (PKs) involved are also indicated (Tian and Wang, 2002; da Cruz e Silva and da Cruz e Silva, 2003; da Cruz e Silva et al., 2004; Chung, 2009).

PKs	APP Residues
PKC, CaMKII	Thr_{654}, Ser_{655}
GSK3β, Cdk5, JNK3, Dyrk1A, Cdc2	Thr_{668}
CKII	Ser_{198}
CKI	Ser_{206}
Abl, Trka	Tyr_{682}

Phosphorylation of APP on Thr_{654} and Ser_{655} residues by PKC has a protective role against AD, by favoring the non-amyloidogenic pathway. The reduction of PKC activity in the brains of AD patients leads to amyloidogenic pathway, and for this reason, more Abeta is produced (Gandy et al., 1993). Another residue that has an important role in APP processing is Tyr_{682}. This residue is necessary for interaction between APP and its binding partners, like Fe65, that are important to regulate APP metabolism. (Barbagallo et al., 2010). The Thr_{668} residue of APP has also an important role in AD. This residue is localized in APP cytoplasmic domain and could be phosphorylated by various proline-directed protein kinases that are upregulated in AD, including Cdk5, GSK3β, JNK3 and Dyrk1A (Lee et al., 2003). Thr_{668} phosphorylation seemed to cause a conformational change in the APP backbone such that the interaction of APP with its binding partners is affected. Studies suggests that phosphorylation on Thr_{668} residue is elevated in AD brains, which is thought to cause an increase of Abeta peptide production, resulting in SP formation (Lee et al., 2003). This residue is going to be object of study in this work.

1.4.2 Tau Phosphorylation

In AD, Tau phosphorylation can occur in high degree. An imbalance between the activity of PKs and PPs can cause Tau hyperphosphorylation, which results in its dissociation of microtubules and disruption of axonal transport. The major kinases that phosphorylate Tau are GSK3 (GSK3α and GSK3β), Cdk5, Dyrk1A, CaMKII, PKA, PKC and microtubule-affinity-regulating kinase (MARK) (Johnson, 2006; Ryoo et al., 2007). To date, more than 39 phosphorylation sites have been identified in PFH-Tau, including serine and threonine residues (Figure 14; Kopke et al., 1993; Giese, 2009).

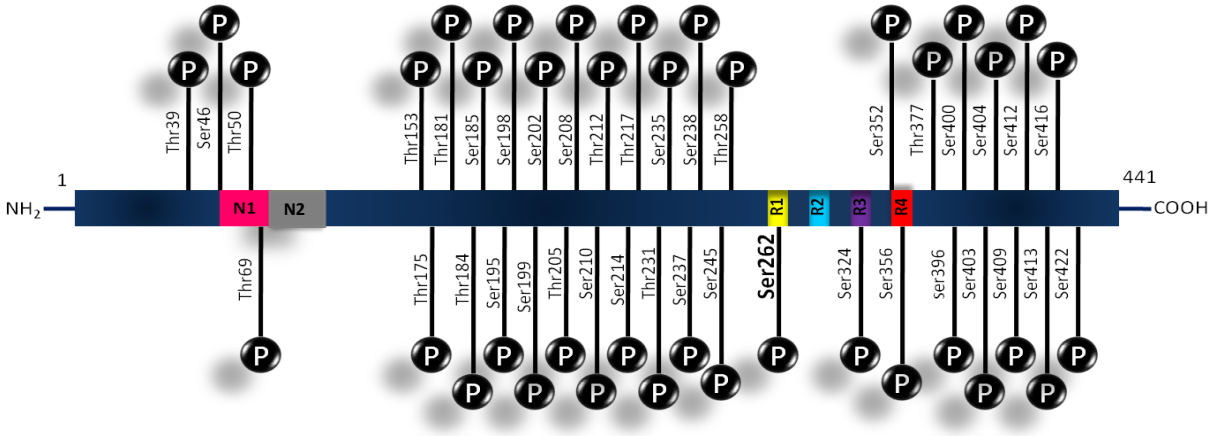

Figure 14: Tau phosphorylated residues already described on the longest Tau isoform. (Billingsley and Kincaid, 1997; Pevalova et al., 2006).

Studies demonstrated that Tau hyperphosphorylation negatively regulates its ability to stimulate microtubule assembly, being for that reason, responsible for the loss of its biological function, gain on toxicity and aggregation into PHFs, which form NFTs (Liu et al., 2005). In this work, Ser_{262} residue is going to be object of study. This residue is present in microtubule binding domain being important to maintain microtubule assembly. Hyperphosphorylation of Ser_{262} is responsible for disruption of microtubule assembly and self assembly of Tau into PHF, which can lead to AD.

As mentioned before, up-regulation of Tau kinases or down-regulation of Tau phosphatases result in Tau hyperphosphorylation in the brain. To elucidate the mechanisms of abnormal hyperphosphorylation, some studies have been performed, and allowed the identification of several kinases like GSK3, Cdk5, PKA and PKC as being responsible for Tau phosphorylation. These kinases modulate the proline-rich regions of Tau *in vivo*, either directly or indirectly (Johnson, 2006; Ryoo et al., 2007). Among these Tau kinase candidates, GSK-3β, Cdk5 and PKA have been most implicated in Tau phosphorylation, and consequently, in AD (Liu et al., 2006).

The following table summarizes the Tau phosphorylation residues as well as the Kinases and Phosphatases involved.

Table 3: Tau phosphorylatable residues. The protein kinases (PKs) and protein phosphatases (PPs) involved are also indicated. (Billingsley and Kincaid, 1997; Liu et al., 2005; Pevalova et al., 2006).

		Tau Residues
PKs	GSK3α	Ser_{199}, Ser_{202}, Thr_{212}, Thr_{231}, Ser_{235}, Ser_{262}, Ser_{324}, Ser_{356}, Ser_{396}, Ser_{404}
	GSK3β	Thr_{181}, Ser_{199}, Thr_{205}, Ser_{214}, Thr_{231}, Ser_{262}, Ser_{369}, Ser_{413}
	Cdk5	Ser_{195}, Ser_{202}, Thr_{205}, Thr_{212}, Thr_{217}, Thr_{231}, Ser_{235}, Ser_{396}, Ser_{404}
	PKA	Ser_{214}, Ser_{262}, Ser_{324}, Ser_{356}, $Ser_{396/404}$, Ser_{409}, Ser_{416}
	PKC	Ser_{324}
	CaMKII	Ser_{262}, Ser_{356}, Ser_{409}, Ser_{416}
	MARK	Ser_{262}
	JNK	Thr_{181}, Ser_{199}, Thr_{205}, Ser_{214}, Thr_{231}, Ser_{262}
	Dyrk1A	Thr_{181}, Ser_{199}, Thr_{205}, Ser_{214}, Thr_{231}, Ser_{262}
PPs	PP1	Ser_{199}, Ser_{202}, Thr_{231}, Ser_{235}, Ser_{262}, $Ser_{393,}$ Ser_{404}
	PP2A	Ser_{46}, Ser_{199}, Ser_{202}, Thr_{205}, Ser_{214}, Ser_{235}, Ser_{262}, Ser_{396}, Ser_{404}
	PP2B	Ser_{202}, Thr_{205}, Thr_{181}, Thr_{231}, Ser_{235}, Ser_{262}

GSK3β (also called Tau kinase I) is a multifunctional Serine/Threonine kinase expressed in brain at high levels, and it is localized in neurons where is also present the Tau protein. This kinase is involved in many cellular processes, including signaling pathways, metabolic control, apoptosis/cell survival, oncogenesis, memory impairment, increased production of Abeta, inflammatory response and in a wide range of diseases such as AD (Balaraman et al., 2006; Hooper et al., 2008). The activation of GSK3β depends on Tyrosine (Tyr)

phosphorylation at residue 216 which increases GSK3 activity (Hooper et al., 2008). However, GSK3 phosphorylation at Ser_9 and Ser_{389} residues by Akt, also known as protein kinase B (PKB), inhibits its activity (Grimes and Jope, 2001). GSK3β is associated with microtubules and when is overexpressed in cells, Tau phosphorylation state increases dramatically. Immunoblotting analysis revealed that this kinase is overexpressed in AD brains, resulting in hyperphosphorylation of Tau. Biological function of this protein could be lost, improving Tau filaments formation and aggregation into PHFs that are the main constituent of NFTs. This increases the toxicity and cell death (Figure 15; Lucas et al., 2001; Johnson and Stoothoff, 2004).

Cdk5 (Tau kinase II) is the predominant Cdk in the brain. Is highly expressed in neurons and is important to synaptic plasticity and neuronal development (Cicero and Herrup, 2005). Cdk5 is responsible for the regulation of neurogenesis during neurodevelopment. This kinase is also important in a variety of cellular functions such as actin dynamics, microtubule stability, axon guidance, membrane transport and dopamine signaling (Dhavan and Tsai, 2001). Upon activation, Cdk5 can phosphorylate several proteins (Dhavan and Tsai, 2001). Under neurotoxic conditions, p35 is proteolytic cleaved by calpain to generate p25, which causes aberrant Cdk5 activation and leads to abnormal phosphorylation of its substrates, such as Tau (Ahlijanian et al., 2000; Lee et al., 2000). In human AD brains, p25 expression and Cdk5 activity are increased compared with age-matched control brains. Studies using transgenic mice overexpressing p25, demonstrate Tau hyperphosphorylation, neurofibrillary pathology, increased Abeta levels and neurodegeneration, most likely due to Cdk5-mediated phosphorylation of Tau (Cruz et al., 2003).

Finally, PKA is regulated by intracellular concentrations of cAMP levels. When cAMP binds to PKA, this kinase is activated and can modulate Tau phosphorylation (Billingsley and Kincaid, 1997) .

Relatively to protein phosphatases, some of them are associated with hyperphosphorylation levels of Tau. Protein phosphatases responsible for Tau dephosphorylation are PP1, PP2A and PP2B (Avila et al., 2004). However, the major Tau phosphatases are PP1 and PP2A (Rahman et al., 2005). PP1 is a Serine/Threonine-specific

phosphatase that is highly enriched in dendritic spines. This phosphatase can be activated when Inhibitor 1 (I1) is dephosphorylated by PP2B. Altered PP1 activity may contribute to Tau hyperphosphorylation. PP2A is localized on microtubules and binds directly to Tau, being downregulated in AD brain, underlying hyperphosphorylation of Tau (Pevalova et al., 2006). The downregulation of this phosphatase can be the result of up-regulation of two PP2A inhibitors, I1 and I2 (Liu et al., 2005; Tanimukai et al., 2005; Gong and Iqbal, 2008). Relatively to PP2B, this phosphatase is important to microtubules and microfilaments developing. An inhibition of this phosphatase causes a hyperphosphorylation of Tau. These phosphatases are able to dephosphorylate Ser_{262}, which is a phospho site specific to AD and also is an important site for the binding of Tau protein to microtubules, and therefore of extreme relevance for AD pathology. (Pevalova et al., 2006).

Tau phosphorylation has a physiological role and is important for neurite outgrowth, axonal transport and microtubule stability. However, when there is an imbalance between phosphorylation and dephosphorylation its biological function is affected, resulting in pathological role in the cell. Tau suffers conformational changes from its less phosphorylated (microtubule-bound form) to its hyperphosphorylated form (self-aggregated form) that is more pathogenic. This in turn, causes pathological Tau filaments formation, microtubule dysfunction and cell death (Figure 15; Ahlijanian et al., 2000; Maccioni et al., 2001; Bielska and Zondlo, 2006; Gong et al., 2006).

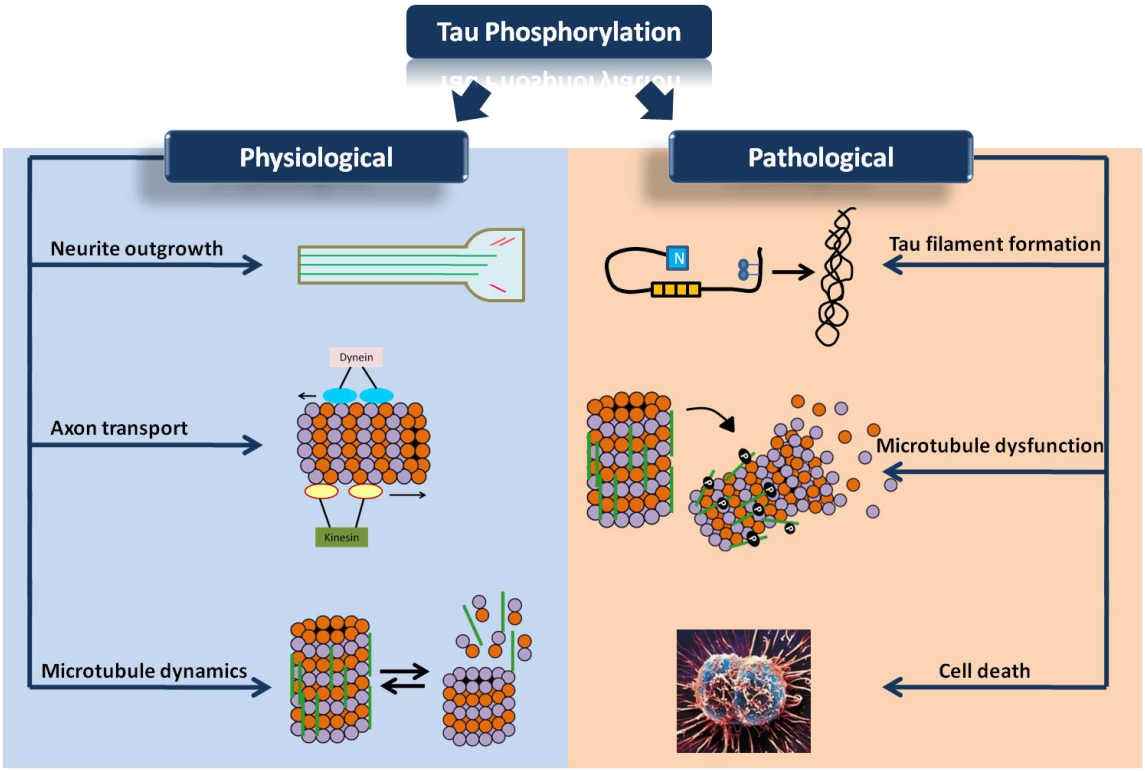

Figure 15: Tau phosphorylation plays both physiological and pathological roles in the cell. When the phosphorylation state of Tau (green lines) is appropriately coordinated, it regulates neurite outgrowth, axonal transport, microtubule stability and dynamics. In pathological conditions, there is an imbalance between phosphorylation/dephosphorylation of Tau. Aberrant Tau phosphorylation can cause Tau filament formation, disrupt microtubule-based processes owing to decreased microtubule binding and ultimately leads to cell death (Adapted from Maccioni et al., 2001).

1.4.3 Influence of Abeta Peptide on APP and Tau phosphorylation

During APP processing multiple Abeta species could be produced, including soluble monomeric peptides (40 amino acids) and more insoluble peptides (42 amino acids). These last ones have more ability to aggregate into oligomeric form, stimulating the production of ROS, being more toxic (Lublin and Gandy, 2010). Some studies have already been done in order to identify the effect of Abeta on protein phosphorylation. However, understanding the mechanisms whereby Abeta oligomers impair synaptic function remains elusive. According to amyloid cascade hypothesis, Tau hyperphosphorylation could be caused by toxic oligomers constituted by aggregated Abeta peptide (Karran et al., 2011). Studies performed by Takashima et al. (1993) reported that Abeta and Tau

phosphorylation are related. In these experiments, primary cultures of embryonic rat hippocampus were treated with 20μM of $Abeta_{1-43}$ peptide, and after 24 hours they observed an increase of 1.6 times in Tau phosphorylation compared to control cultures. (Takashima et al., 1993). If Abeta really promotes Tau phosphorylation, and in accordance with amyloid cascade hypothesis, extracellular Abeta may act through a transduction pathway to exert an effect on Tau protein and consequently lead to a loss of microtubule binding, destabilizing the cytoskeleton and affecting the entire neuron as a final result (Anoop et al., 2010). Another study, performed by Busciglio group in 1995 also showed a relation between Abeta and Tau phosphorylation. In this case, they used primary cultures of fetal rat hippocampal neurons and primary cultures of fetal human cortical neurons. The exposure of these cultures to $Abeta_{1-42}$ at a final concentration of 20μM resulted in increased levels of Tau phosphorylation at Ser_{202} and Ser_{396}/Ser_{404} residues. They also verified an increase in phosphorylated Tau in the somatodendritic compartment which indicates that normal axonal localization of Tau is altered after Abeta exposure. Finally, Busciglio et al. (1995) also saw incapacity of phosphorylated Tau to bind to microtubules (Busciglio et al., 1995).

In relation to APP is known that the level of phosphorylation is increased in AD brains. So, possibly Abeta may also be involved in APP phosphorylation, however there are no studies regarding this subject. A possible explanation is the fact that Abeta may promote the deregulation of some signaling cascades. Indeed, He et al. (2011), showed that the formation of SPs, could disturb intracellular calcium ions, affecting the signaling cascades that involve Ca^{2+} as a second messenger (He et al., 2011). Possibly, these changes in second messenger activity could affect protein phosphatases and kinases activity, which in turn could modulate the phosphorylation of APP (Gandy et al., 1993). Also, a study performed by Vintem et al. (2009) indicates that Abeta could inhibit PPs activity. Possibly, this inhibition may lead to an increase in phosphorylation of certain proteins, like APP.

So, whereas the influence of Abeta on APP phosphorylation remains an unknown field, some findings support a possible involvement of Abeta in Tau phosphorylation.

1.5 Synaptic Transmission

Brain tissues are composed by two main cells types: neurons, which produce and conduct electrochemical impulses and supporting cells - glial cells, which assists the functions of neurons and are more abundant (Williams and Herrup, 1988; Fox, 2010). Human brain is composed of an estimated 10^{12} heterogeneous neurons that communicate through synapses (Pocklington et al., 2006). These communicative contacts between neurons can be electrical or chemical.

In electrical synapses, adjacent cells are electrically coupled and join together by gap junctions, enabling the propagation of electrical impulses from one cell to another via direct and physical contact. These synapses are characterized by a relatively simple organization of membrane structure, presence of associated organelles, are less mutable (in terms of their function and molecular characteristics), and exhibit a decreased plasticity that typifies the chemical synapse (Zoidl and Dermietzel, 2002).

Chemical synapses provide the transmission across the majority of synapses in the nervous system and they are characterized by the release of chemical neurotransmitters and neuropeptides from pre-synaptic terminals. Cell-cell communications that occurs by chemical transmission is characterized by complex protein-driven molecular mechanisms of synthesis, delivery, storage, docking, fusion, neurotransmitter release and reuptake (Dale Purves, 2004). In general, synapses are composed of three main components: a pre-synaptic component (pre-synaptic ending, axon terminal), a synaptic cleft (20-30nM wide), and a post-synaptic component (dendritic spine). Pre and post-synaptic membranes are uniquely distinguishable by visible densities along their corresponding plasma membranes (Figure 16; Palay, 1958).

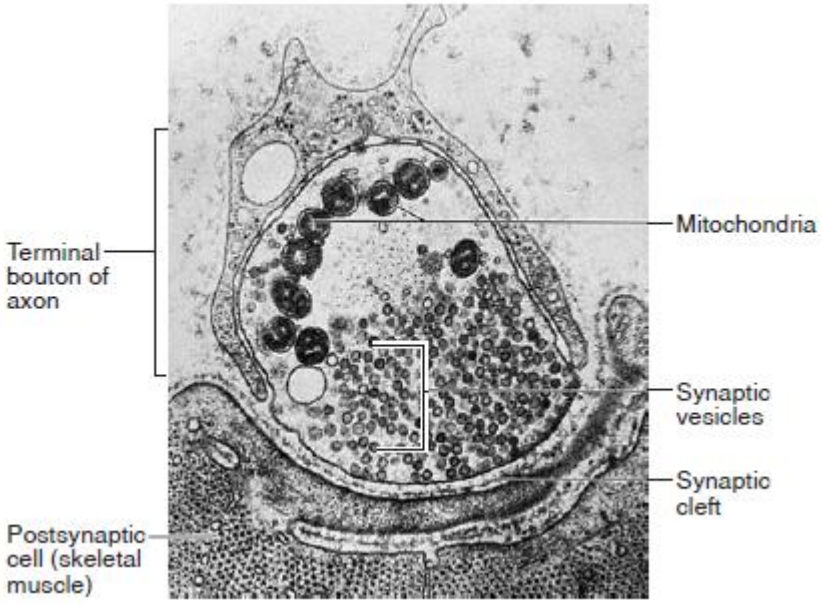

Figure 16: **Electron micrograph of a chemical synapse.** This image shows the synaptic vesicles at the end of the axon and the synaptic cleft. The synaptic vesicles contain the chemical neurotransmitter. The post-synaptic cell is also presented. (Taken from Fox, 2010) .

Typically, pre-synaptic ending is further distinguished from the post-synaptic component by the presence of neurotransmitter-filled synaptic vesicles. In response to pre-synaptic membrane depolarization, vesicles release their contents into the cleft through membrane-trafficking events. The pre-synaptic axon terminal, also called bouton, also contains other organelles such as mitochondria, smooth endoplasmic reticulum, microtubules and neurofilaments. The pre-synaptic membrane is variably populated by docking/fusion apparatus, ion channels, and other protein constituints (Palay, 1958). The major proteins that are in pre-synaptic ending are trafficking proteins, which include synaptobrevin (also called vesicle-associated membrane protein - VAMP) and synaptotagmin. A group of proteins are included in synaptic vesicle (SV), like synaptophysin, synaptogyrin and SCAMPs (secretory carrier-associated membrane proteins). SNARE complexes are also important because they are involved in membrane fusion and consequently in vesicles exocytose process. SNAPs (Soluble NSF Attachment Protein) are also present in pre-synaptic membranes. Another proteins present in pre-synaptic terminal, that have a role in the recruit of SV to pre-synaptic membrane, are

mammalian Unc-13 homolog (Munc13), Rab3 and Rab3-interacting molecule (RIM) (Figure 17; Chua et al., 2010).

The post-synaptic membrane, particularly at the dendritic spine, is recognizable by a collection of dense material visible by electron microscopy on its cytoplasmic surface. This so-called post-synaptic density (PSD) is a specialization of the nerve cell sub-membrane cytoskeleton composed of granular/filamentous material. A subcellular fraction enriched in structures with PSD-like morphology has been shown to contain signal-transduction molecules though to regulate receptor localization and function in the CNS (Palay, 1958; Kennedy, 1993). In this case, the major proteins in synaptic transmission are proteins found in the core of the PSD, such as members of the PSD-95 (Post-synaptic density-95), SAP90 (synapse-associated protein of 90 KDa), GKAP (Guanylate kinase-associated protein, which is formed by SAP90/PSD-95) and SHANK (SH3 domain and ankyrin repeat domain) (Figure 17; Chua et al., 2010).

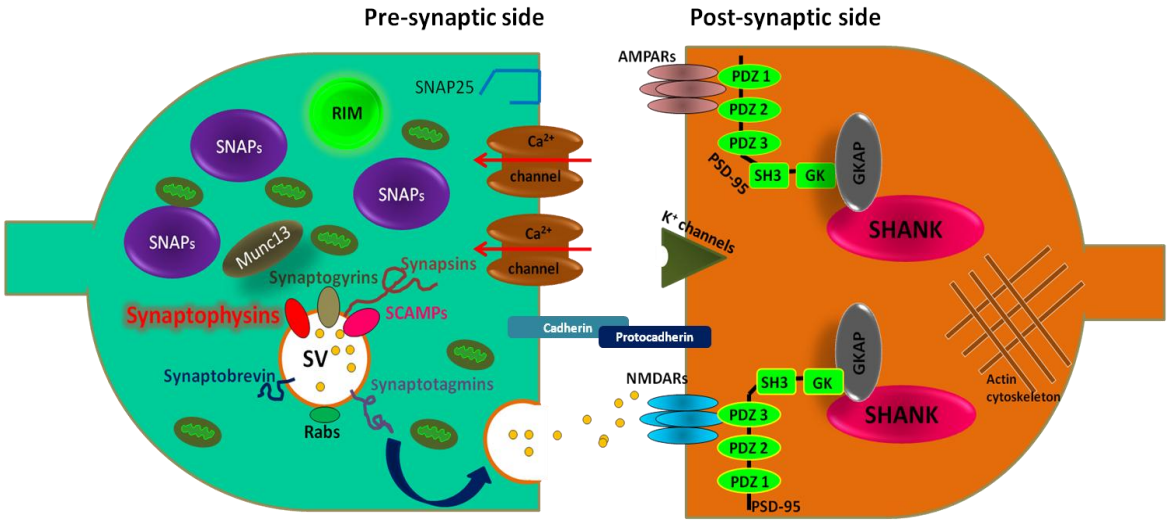

Figure 17: The architecture of a synapse. The functioning of the excitatory synapse is regulated by protein-protein interactions. On the pre-synaptic side, synaptic vesicles are filled with neurotransmitters (NT) which are released to the synaptic cleft, and bind to NT receptors on post-synaptic side. This results in a different membrane potential and trigger a signal transduction cascade. In this schematic diagram is also represented, the principal proteins of pre and post-synaptic terminals (Adapted from Staple et al., 2000; Chua et al., 2010).

1.6 Synaptosomes

The term “synaptosome” was first mentioned by Whittaker´s group in 1964 (Bai and Witzmann, 2007). Synaptosomes are membranous sacs that are obtained by subcellular fractionation techniques applied on homogenized nerve tissue. They contain the complete pre-synaptic terminal, including mitochondria and synaptic vesicles, along with the post-synaptic membrane and PSD. All the components involved in the formation and consolidation of synaptic contacts remain intact. For this reason, they are seen as an *in vitro* model to study synaptic transmission (Whittaker, 1993).

Through proteomics analysis of synaptosomes, molecular markers and the molecular mechanisms underlying synaptic neurotransmission could be studied. Therefore, synaptosomes could be important to understand some neurodegenerative disorders, including Alzheimer´s disease (Whittaker and Gray, 1962; Whittaker, 1993).

Nerve terminals differ in their shape and size, in their content of vesicles, mitochondria and cytoskeletal elements, in the number and nature of connections to post-synaptic cells, and also, in their content of neurotransmitters (Whittaker, 1993). The pre-synaptic side contains specialized secretion machinery for activity-dependent release of neurotransmitters into the synaptic cleft. At the post-synapse neurotransmitter, receptors and the downstream signal apparatus are organized mainly by the PSD (Schrimpf and Meskenaite, 2005).

For synaptosomes isolation, first the region of interest is dissected out from the brain and then is homogenized using an appropriate buffer and applying an appropriate mechanical force. This causes the nerve terminals, or boutons, to be torn away from their axons, post-synaptic and glial cells to which they were connected. The pre-synaptic membranes then reseal, and enclose the nerve terminal contents (cytoplasm, synaptic vesicles, mitochondria and cytoskeleton), within a membranous sac (Figure 18). After the isolation of synaptosomes the molecular machinery for the release, uptake and storage of neurotransmitters remain intact. Frequently, a part of the post-synaptic membrane and its post-synaptic density will remain attached to the pre-synaptic nerve terminal. During the homogenization, some nerve terminals can be destroyed, either because of their

shape and/or size, or because some or all of their contents will be lost before the pre-synaptic membrane reseals. However, most of them remain with a form and with functions that closely mimic nerve terminals in vivo (Whittaker, 1993; Dunkley et al., 2008).

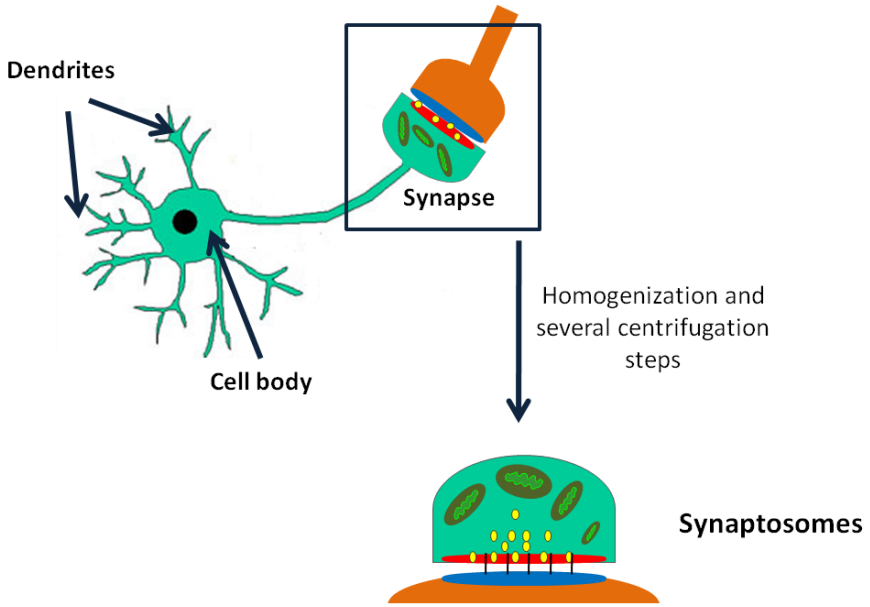

Figure 18: Isolation of synaptosomes. After isolation of synaptosomes the molecular machinery for the release, uptake and storage of neurotransmitters remains intact. (Adapted from Smalla et al., 2004).

Synaptosomes can be morphologically and functionally characterized. Morphologically they are characterized by the presence of one or more small mitochondria, presence of synaptic vesicles, and presence of lengths of characteristically electron-dense membrane resembling post-synaptic membranes (Whittaker, 1993). The morphology of synaptosomes can be observed via electron microscopy (Figure 19).

Figure 19: **Morphology of synaptosomes via electron microscopy**. (Taken from Smalla et al., 2004).

Functionally, synaptosomes are characterized by their capacity to produce ATP; presence on their plasma membranes of functional ion channels, carriers and receptors which allow them to maintain membrane potentials and ion homeostasis; by the capacity of their synaptic vesicles to take up and release neurotransmitters; recycling process of their membranes by endocytosis; and by the presence of functional enzymes and proteins normally present within nerve terminals. However, synaptosomes do not contain the machinery to make new proteins (except within their mitochondria) and their capacity for repair is therefore limited to a few respiratory complex proteins. For this reason, synaptosomes cannot be used for RNA_i experiments or DNA transfection (Dunkley et al., 2008).

After the isolation of synaptosomes, if they are kept at 4^oC and are provided with appropriate nutrients they can retain their function for many hours. If not appropriate mantained, they lose ATP rapidly (at 37^oC), and lose their functions (Dunkley and Robinson, 1986; Whittaker, 1993).

2 Aims of the Dissertation

AD is a neurodegenerative disease that involves altered expression of some proteins at synapse, like APP and Tau. The possibility to investigate the synapse and their proteomic content using synaptosomes is a very attractive model since these membranous sacs allow a direct study without the complications inherent of studying this *in situ*. For this reason this model was used in this work. However, to enable more efficient proteomic analysis using synaptosomes some techniques have been developed for the isolation of relative pure synaptosomes from rat brain. Using this proteomic approaches, the molecular causes of the two main hallmarks of AD, SPs and NFTs, could be investigated.

The mechanism whereby Abeta induces synaptic dysfunction is not clearly known yet, and also the relationship between Abeta and Tau phosphorylation.

Despite normal production of Abeta during APP processing, when neuronal machinery is exposed to high concentrations of Abeta during long periods of time, neurotoxicity is induced. So, the understanding of the main processes that are responsible for this neurotoxicity could be used to devise efficacious interventions, like in therapeutically field.

In this thesis, firstly, were tested and compared two different methodologies to isolate and purify synaptosomes: Percoll gradient protocol and sucrose gradient protocol. The method with better results in the enrichment of synaptosomal fraction was chosen to perform the following experiments. After that, was evaluated the effect of Abeta on APP and Tau phosphorylation, and also the protein phosphatases involved on APP and Tau dephosphorylation.

Thus the specific aims of this dissertation are:

- Compare two methodologies to isolate synaptosomes;
- Determine the role of Abeta on APP and Tau phosphorylation;
- Establish the protein phosphatases involved in APP and Tau dephosphorylation;

3 Materials and Methods

3.1 Antibodies

The following primary antibodies were used: mouse monoclonal synaptophysin antibody (Synaptic Systems) directed against synaptophysin, a pre-synaptic marker; mouse monoclonal PSD-95 antibody (Millipore) a post-synaptic marker; mouse monoclonal ATP synthase α (BD Biosciences Pharmingen) which specifically acts as mitochondrial marker; rabbit polyclonal p-APP Thr_{668} antibody (Cell Signalling), which detects APP phosphorylated at Thr_{668} residue; rabbit polyclonal p-Tau Ser_{262} antibody (Santa Cruz Biotechnology, Inc) directed against the phosphorylated Tau at Ser_{262} residue; mouse monoclonal Tau-5 antibody (Millipore) to detect all phosphorylated and non phosphorylated isoforms of Tau (total-Tau), rabbit polyclonal C-TERM antibody (Invitrogen), which detects all APP isoforms (holo-APP) and mouse monoclonal antibody (Invitrogen) against β-Tubulin. The primary antibodies are summarized in Table 4.

For immunoblotting were used as secondary antibody, Horseradish peroxidase anti-mouse and anti-rabbit (GE Healthcare), both used with a dilution of 1:5000.

Table 4: Summary of primary antibodies used, as well, the respective target, isotype, dilution and the expected band size.

Antibody	Target	Isotype	Dilution	Expected band size (KDa)
Synaptophysin	Synaptophysin (pre-synaptic protein)	Mouse (monoclonal)	1:5000	37
C-TERM	holo-APP	Rabbit (polyclonal)	1:500	100-140
PSD-95	PSD-95 (pos-synaptic protein)	Mouse(monoclonal)	1:500	95-100
ATP synthase α	Mitochondria	Mouse (monoclonal)	1:10000	55
Tau 5	total-Tau	Mouse (monoclonal)	1:500	46-68
p-Tau Ser_{262}	p-Tau at Ser_{262}	Rabbit (polyclonal)	1:500	46-68
p-APP Thr_{668}	p-APP at Thr_{668}	Rabbit (polyclonal)	1:1000	100-140
β-Tubulin	β-Tubulin	Mouse (monoclonal)	1:1000	50

3.2 Preparation of biological material

In this work synaptosomes were used as a model to perform the different experiments. Synaptosomal fractions were isolated from the homogenate of both rat cortex (cortical synaptosomes) and hippocampus (hippocampal synaptosomes). The homogenates were then subjected to a differential centrifugation and after to a gradient density centrifugation, obtaining the synaptosomal fraction. Two different gradient density methodologies to obtain synaptosomal fractions were tested: Percoll gradient protocol and discontinuous sucrose gradient protocol. After comparison the one with higher efficiency was selected to perform the following sets of experiments.

3.2.1 Brain dissection and cortical and hippocampal homogenate preparation

Cortex and hippocampus were obtained from Wistar female rats brains (9-15 weeks). These animals were obtained from IBMC (Instituto de Biologia Molecular e Celular - Porto) and Harlan. Animals were housed under controlled environment, 26ºC under a 12 hour light/dark cycle, with food and water available *ad libitum*.

These animals were sacrificed by rapid cervical dislocation followed by decapitation. After this step, cortex and hippocampus were quickly dissected out and placed in previous identified petri dishes with homogenizer buffer (0.32M sucrose, 0.05M Tris, 0.002M EGTA, 0.001M DTT, pH 7.6, in Percoll gradient protocol and 0.32M sucrose, 0.02M HEPES, 0.001M DTT, pH 7.4 and proper protease inhibitor, in sucrose gradient protocol). After cortex and hippocampus dissection, they were weighted and added to 10 volumes (1g of tissue to 9 ml) of respective homogenizer buffer. Tissues were then divided into small portions with a scissor and then homogenized with a Potter-Elvehjem tissue homogenizer with 10-15 strokes at 500-800 rpm. Each homogenate was then transferred to the respective tube (falcons of 15 ml) to be further used in Percoll or sucrose gradient protocols (described below). At same time, an aliquot of each homogenate was collected to be further analyzed.

3.2.2 Obtention of synaptosomal fraction

3.2.2.1 Percoll gradient protocol

After preparation of cortex and hippocampus homogenates, these were centrifugated at 3000xg during 10 minutes at 4ºC (Figure 20). The pellets (P1), contaminated by mitochondria and nucleus were discarded and the supernatants (S1) where the axonal terminals are present were collected to new tubes (falcons of 15 ml) and then centrifugated for 14000xg during 20 minutes at 4ºC. At the end of centrifugation, supernatants (S2) were collected and stored at 4ºC for further analysis, and the pellets collected (P2) were ressuspended in 1 ml of Percoll®45% (v/v) solution, prepared in Krebs buffer (0.14M NaCl, 0.005M KCl, 0.025M HEPES, 0.001M EDTA and 0.01M Glucose, pH 7.4). The ressuspended pellet was then centrifugated at 14000xg during 2 minutes at 4^{O}C (Figure 20). After centrifugation, the top layer that contains the synaptosomal fraction was collected with a Pasteur pipette to new tubes and the remaining fraction was collected to further analysis (S3). Then, the top layer collected was washed in 1 ml of Krebs buffer by centrifugation at 14000xg during 2 minutes at 4 ºC. This washing step was repeated twice (Protocol adapted from Rebola et al., 2005).

3.2.2.2 Sucrose gradient protocol

As in the previous protocol, after preparation of cortical and hippocampal homogenates they were centrifugated at 1000xg during 10 minutes at 4^{O}C (Figure 20). With a Pasteur pipette, supernatants (S1) were then collected to new tubes (falcons of 15 ml) and centrifugated for 15000xg during 22 minutes at 4ºC, while pellet (P1) was discarded (contaminated with mitochondria and nucleus). At the end of centrifugation, supernatants (S2) were collected and stored at 4ºC for further analysis, and pellets (P2) were ressuspended in Krebs buffer (0.14M NaCl, 0.005M KCl, 0.025M HEPES, 0.001M EDTA and 0.01M Glucose, pH 7.4) until make up 3,4 ml. With a Pasteur pipette, the pellets were then put on top of a discontinuous sucrose gradient (3.4 ml of 1.2M sucrose

on the lower layer, 3.4 ml of 0.8M sucrose on the intermediate layer and finally, 3.4 ml of synaptosomes ressuspended in Krebs buffer). Then, the pellets on top of sucrose gradient were centrifugated at 100000xg (32600 rpm) during 2 hours and 15 minutes at 4°C. After centrifugation, the synaptosomes were collected from the interface of the two densities (Figure 20), using a Pasteur pipette and transferred to new identified tubes (Protocol adapted from Bai and Witzmann, 2007).

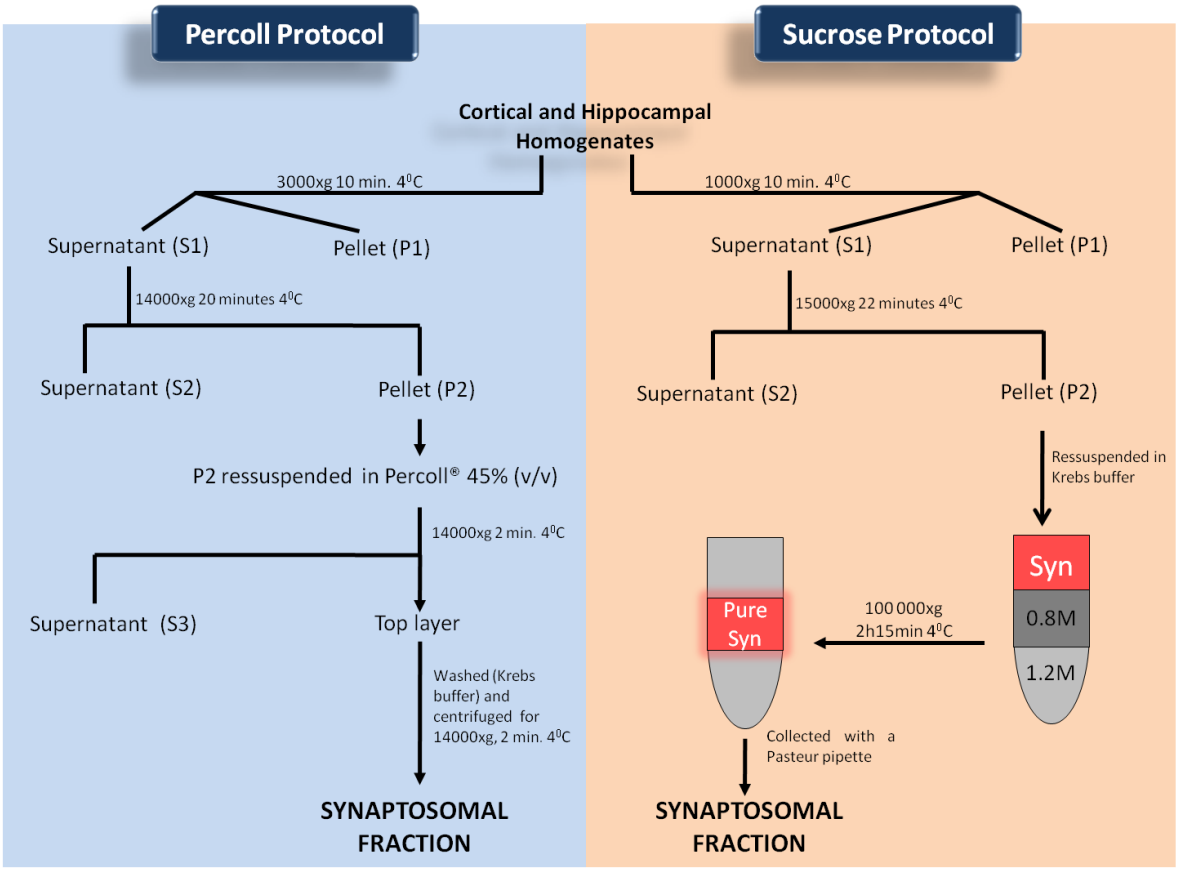

Figure 20: Summary of the main steps of Percoll gradient protocol and Sucrose gradient protocol. Syn: Synaptosomal fraction; P1: Pellet of first centrifugation; P2: Pellet of second centrifugation; S1: Supernatant of first centrifugation; S2: Supernatant of second centrifugation and S3: Supernatant of third centrifugation.

3.3 Acetone protein precipitation

This methodology consists in addition of acetone to the sample which results in a decrease of dielectric constant (DC). Consequently the interaction between proteins increase, which allow them to precipitate. The acetone is used to purify proteins in a sample. Briefly, cold (-20^{o}C) acetone was added to samples in four times the sample volume. They were vortexed and incubated ON at -20^{o}C. The samples were then centrifugated at 14000xg during 10 minutes at 4^{o}C. Supernatants were discarded carefully to avoid dislodgement of the protein pellet. The tubes were placed on a paper to allow the acetone to evaporate, during 30 minutes at room temperature. The pellets were further ressuspended on boiling 1% SDS and transferred to new 2 ml microtubes. They were boiled during 10 minutes and then stored at -20^{o}C. Their protein content was determined using BCA assay (as described below).

3.4 Treatment of synaptosomes with Abeta

To evaluate the effects of Abeta$_{1-42}$ on APP and Tau phosphorylation, approximately 2µg/µl of cortical and hippocampal synaptosomes were incubated with different concentrations of Abeta$_{1-42}$ peptide: 0.25µM, 0.5µM and 2µM Abeta$_{1-42}$. The experiments were always conducted in duplicate. To evaluate the test validity we added an extra condition (positive control), which consisted in a scrambled Abeta$_{1-42}$ at 2µM. Abeta$_{1-42}$ stocks and scrambled Abeta$_{1-42}$ were first prepared and used at 100µM. After Abeta$_{1-42}$ addition, synaptosomes were incubated at 37^{o}C for 3 hours. After that period loading buffer (LB) was added to each tube. After mixing the samples they were boiled for 10 minutes. Subsequently, the samples were analyzed by SDS-Polyacrylamide Gel Electrophoresis (SDS-PAGE).

3.5 Treatment of cortical synaptosomes with protein phosphatase inhibitors

In order to establish the protein phosphatases (PPs) involved on APP and Tau dephosphorylation, synaptosomes were incubated with okadaic acid (OA) and cantharidin (CT), two well known PPs inhibitors (Table 5; Swingle et al., 2007).

Table 5: Range of IC_{50} values of protein phosphatase inhibition. All values are expressed as nanomolar (nM). PP, Protein phosphatase; IC_{50}, 50% inhibition concentration. (Adapted from Swingle et al., 2007).

	Inhibition of Ser/Thr Protein Phosphatase activity (IC_{50})					
Compound	**PP1**	**PP2A**	**PP2B**	**PP4**	**PP5**	**PP7**
Okadaic acid (OA)	15-50	0.1-0.3	4000	0.1	3.5	>1000
Cantharidin (CT)	1100	194	>10000	50	600	nd

Different stock solutions of OA (0.1µM, 10µM and 100µM) and CT (100µM) were prepared and different concentrations were tested: 0.1nM, 0.25nM, 50nM, 500nM and 5000nM for OA and 100nM, 250nM, 500nM, 1000nM and 10000nM for CT.

Cortical synaptosomes were incubated with several OA and CT concentrations for 30 minutes and 3 hours, at 37^{o}C. Each 30 minutes the samples were mixed to avoid the formation of precipitate. After these periods of time, LB was added to each tube and a spin down was done. After mixing the samples they were boiled and stored at -20^{o}C until further analysis by SDS-PAGE (as described below).

3.6 MTT assay

MTT assay is a colorimetric assay used to evaluate cell viability. This methodology measures the activity of succinate dehydrogenase on the reduction of the yellow compound 3-(4,5-Dimethylthiazol-2-yl)-2,5-diphenyltetrazolium bromide (MTT) to

insoluble purple formazan. This is then solubilized with an organic solvent (isopropanol) to dissolve the insoluble purple formazan product. Then the absorbance was quantified by a spectrophotometer. The reduction of MTT only occur in metabolically active cells, and for this reason, the level of formazan formation is an indirect measure of cell viability.

For this assay cortical and hippocampal synaptosome-enriched fractions were used and was evaluated the effect of $Abeta_{1-42}$ treatment on synaptosomal viability. The same $Abeta_{1-42}$ concentrations were used as described above (0.25µM, 0.5µM and 2µM) and scrambled $Abeta_{1-42}$ (2µM) was also used. The tubes were then incubated during 2 hours at 37^{o}C. After this time, MTT 5mg/ml was added to each tube for a final concentration of 0.5mg/ml, and further incubated for 1 hour at 37^{o}C. Then, 0.04M HCl/isopropanol (4 ml of HCl in 100 ml of final volume of solution) was added in a 1:1 proportion to MTT. Formazan crystals were ressuspended until these crystals were completely dissolved and then, the tubes were centrifugated at 13000xg during 2 minutes. The supernatants were transferred to cuvetes, wrapped with parafilm and homogenized to be quantified on spectrophotometer at 570 nm.

3.7 BCA protein quantification assay

The bicinchoninic acid (BCA) assay (Pierce) is a biochemical assay used to determine total protein content in a test sample. This method consists in a color change of the sample solution from green to purple in proportion to protein concentration. This assay is performed in two reactions. Firstly, Cu^{2+} is reduced to Cu^{+} by protein in an alkaline medium, which results in a light blue complex - biuret reaction (temperature dependent reaction). This reaction occurs with high sensitivity. Then, the colorimetric detection is allowed through the colorimetric detection of Cu^{+} cation, that was formed in step one, by BCA. More precisely, the reaction of two molecules of BCA with one Cu^{+} ion, results in an intense purple-colored reaction product. The BCA/Cu^{+} complex is water-soluble and exhibits a strong linear absorbance at 562nm with increasing protein concentrations (over a working range between 20µg/ml to 2000 µg/ml).

The standards were prepared in duplicate as described in Table 6. The final volume for each standard and sample was equal to 50 µl.

Table 6: Summary of BCA standards preparation. BSA, bovine serum albumin; WR, working reagent; SDS, Sodium Dodecyl Sulfate.

Standards	BSA (µl)	10% SDS (µl)	H_2O (µl)	Protein mass (µg)	WR (ml)
P0	0	5	45	0	1
P1	1	5	44	2	1
P2	2	5	43	4	1
P3	5	5	40	10	1
P4	10	5	35	20	1
P5	20	5	25	40	1
P6	40	5	5	80	1

After prepare BCA standards, the samples were prepared also in duplicate, using 5 µl of synaptosomes and 45 µl of 1% SDS (final volume of 50µl). Then, 1 ml of Working (WR) reagent was added to both standards and samples. WR was prepared adding 50 parts of reagent A to 1 part of reagent B. After that, all the tubes were vortexed and incubated at 37ºC during 30 minutes. Then, the tubes were cooled at room temperature during 2/3 minutes and the absorbances were measured at 562 nm using a spectrophotometer. A standard curve was prepared by plotting the optical density (OD) value for each BCA standard against its concentration. This standard curve allowed the determination of protein concentration of each sample.

3.8 Sodium dodecyl sulfate - polyacrylamide gel electrophoresis (SDS-PAGE) and Electrotransference

SDS-PAGE is a technique commonly used to separate proteins based on their molecular weight. This method uses a discontinuous polyacrylamide gel as a support medium and Sodium Dodecyl Sulfate (SDS) to denature proteins. SDS is an anionic detergent that denatures proteins by wrapping around the polypeptide backbone, which

results in an unfolding and individual polypeptide. Therefore the SDS confers a net negative charge to the polypeptide in proportion to its length. This reaction occurs in presence of SDS when the samples are heated to 100^{o}C. SDS-PAGE can thus be used to estimate relative molecular mass, to determine the relative abundance of major proteins in a sample and to determine the distribution of proteins among fractions. The migration of heavy molecules is slower, while the migration of light molecules is fast.

After preparing the samples, they were subjected to a 5%-20% gradient SDS-PAGE. First, gradient gels were prepared and then loaded between two glasses plates. These gels polymerized during 45 minutes at room temperature. Then, the stacking gel solution was prepared and loaded on the top of gradient gel. Subsequently, a comb was inserted into each “sandwich” and the gel was allowed to sit for at least 30 minutes at RT.

During the polymerization time, the samples were prepared by adding Loading Buffer (LB) to each tube. Then they were boiled for 5 minutes. After this, a spin down was done to each sample and then the samples were loaded into the wells. A molecular weight marker was also loaded (Precision Plus Protein^{TM}, Bio-Rad). Gels were run at 90 mA during approximately 3 hours. After running the proteins, they were electrotransferred to a solid support (nitrocellulose) for 18 hours at 200mA. After electrotransference the detection of the protein of interest was carried out by immunoblotting (as described below).

3.9 Immunoblotting

Immunoblotting is a technique in which proteins are transferred from an electrophoresis gel to a support membrane (nitrocellulose sheets) and then probed with antibodies. In this process, transferred proteins become immobilized on the surface of the membrane in a pattern that is an exact replica of the gel. After electrotransference the detection of proteins is carried out using specific antibodies against the proteins of interest. The general protocol is similar to each antibody however some antibodies have specific recommendations (Table 7).

Table 7: General immunoblotting protocol used for each antibody. ON, overnight; RT, Room Temperature;min, minutes; h, hours.

	Blocking Agent	Primary Antibody	Washings	Secondary Antibody	Washings	Detection method
ATP-Synthase α	- 5% low fat milk in 1x TBS-T;- -4h at RT.	-3% low fat dry milk in 1x TBS-T; -4h at RT + ON at 4°C.	-1x TBS-T; -3 times; -10 min each.	-3% low fat dry milk in 1x TBS-T; -2 h at RT.	-1x TBS-T; -3 times; -10 min each.	ECL
C-Terminal	- 5% low fat milk in 1x TBS-T; -4h at RT.	-3% BSA in 1x TBS-T; -4h at RT + ON at 4°C.	-1x TBS-T; -3 times; -10 min each.	-3% BSA in 1x TBS-T; -2 h at RT.	-1x TBS-T; -3 times; -10 min each.	ECL Plus
p-APP Thr_{668}	-5% BSA in 1x TBS-T; -4h at RT.	-3% BSA in 1x TBS-T; -4h at RT + ON at 4°C.	-1x TBS-T; -3 times; -10 min each.	-3% BSA in 1x TBS-T; -2 h at RT.	-1x TBS-T; -3 times; -10 min each.	ECL
PSD-95	- 5% low fat milk in 1x TBS-T; -4h at RT.	-3% low fat dry milk in 1x TBS-T; -4h at RT + ON at 4°C.	-1x TBS-T; -3 times; -10 min each.	-3% low fat dry milk in 1x TBS-T; -2 h at RT.	-1x TBS-T; -3 times; -10 min each.	ECL
p-Tau Ser_{262}	-5% BSA in 1x TBS-T; -4h at RT.	-3% BSA in 1x TBS-T; -4h at RT	-1x TBS-T; -3 times; -10 min each.	-3% BSA in 1x TBS-T; -2 h at RT.	-1x TBS-T; -3 times; -10 min each.	ECL Plus
Synaptophysin	- 5% low fat milk in 1x TBS-T; -4h at RT.	-3% low fat dry milk in 1x TBS-T; -4h at RT + ON at 4°C.	-1x TBS-T; -3 times; -10 min each.	-3% low fat dry milk in 1x TBS-T; -2 h at RT.	-1x TBS-T; -3 times; -10 min each.	ECL
Tau 5	-5% BSA in 1x TBS-T; -2h at RT.	-3% BSA in 1x TBS-T; -2h at RT.	-1x TBS-T; -3 times; -10 min each.	-3% BSA in 1x TBS-T; -2 h at RT.	-1x TBS-T; -3 times; -10 min each.	ECL
β-Tubulin	- 5% low fat milk in 1x TBS-T; -2h at RT.	-3% low fat dry milk in 1x TBS-T; -2h at RT.	-1x TBS-T; -3 times; -10 min each.	-3% low fat dry milk in 1x TBS-T; -2 h at RT.	1x TBS-T; -3 times; -10 min each.	ECL

First, the membranes were rehydrated in 1x TBS during 10 minutes. After this, the membranes were blocked with 5% non-fat dry milk in 1x TBS-T or 5% BSA in 1x TBS-T (blocking solution) usually during 4 hours. This step allows that unoccupied protein-

binding sites on the membrane are saturated to prevent non-specific binding of antibodies. Then, the membranes were probed for the protein of interest with a specific primary antibody, usually during 4 hours with agitation and then sit overnight (Table 7). The primary antibody solution is appropriated prepared according to respective dilution, Table 4. After the incubation period with primary antibody, membranes were washed three times, each one during 10 minutes with 1x TBS-T, and then were probed a second time with secondary antibody during 2 hours under agitation. The secondary antibody solution was used at 1:5000 and is diluted in 3% non-fat dry milk in 1x TBS-T or 3% BSA in 1x TBS-T. This antibody was specific for the primary antibody. Membranes were then washed three times with 1x TBS-T, each during 10 minutes.

After this, the membranes were incubated 1 minute with ECL detection kit or 5 minutes with ECL plus detection kit in a dark room. Then, the nitrocellulose sheets incubated with ECL were placed on an x-ray film cassette with a sheet of film on top of it. The cassette was closed during an appropriate time to obtain signal and then the film was developed and fixed with appropriate solutions. Films were dried and quantified subsequently.

3.10 Quantification and statistical analysis

Quantitative analysis of immunoblots was performed using the Quantity One GS-800 densitometry software (Bio-Rad). This software allows the quantifications of band intensity and correlates it to protein levels. Data are expressed as means±SEM of triplicate determinations, from at least three independent experiments.

4 Results

4.1 Comparison of two methodologies to isolate synaptosomes: Percoll gradient protocol versus Sucrose gradient protocol

The knowledge of the synaptic proteome is a field in rapid expansion. The study of various subproteomes from the synapse, using synaptosomes as a model of study, holds great promise for improving our understanding of the processes that control synaptic proteins in both normal and disease states. For this reason, altered expression of multiple proteins in AD makes this disease a good candidate for proteomic analysis.

The use of synaptosomes as an *in vitro* model to study the expression of some proteins that are altered in some disorders, such as in AD, has been improved by the development of procedures to isolate and purify nerve terminals from the brain. In this thesis we compared two different procedures for this purpose. Both start with differential centrifugation of the brain homogenate to isolate synaptosomes and after this step, synaptosomes were collected and subjected to two different purification procedures: Percoll gradient and to a discontinuous sucrose gradient. These two protocols were detailed previously on section 3.2.2.1 and 3.2.2.2, respectively.

During the isolation procedure using Percoll gradient protocol were taken seven aliquots (Hm, S1, S2, S3, S4, S5 and Syn) for being further analyzed and using sucrose gradient protocol were taken four aliquots (Hm, S1, S2 and Syn) for further analysis. After the isolation, all samples were precipitated with acetone, ressuspended in 1% boiling SDS and the protein content determined using the BCA method. The samples were further subjected to SDS-PAGE and then, the expression of various markers was evaluated by immunoblotting, using specific antibodies against pre and post-synaptic region and also mitochondria. The comparison between these two protocols was performed by analyzing in each fraction a pre-synaptic protein (Synaptophysin), a post-synaptic protein (PSD-95) and also the presence of mitochondria, using for this purpose ATP-Synthase α antibody (ATP-S α). All fractions were compared with the homogenate fraction (Hm) to which was attributed the relative value of 100% to each specific marker. The homogenate fraction is particularly interesting since give us the idea of the initial amount of each protein (before

the isolation procedure), while the other fractions give information regarding the isolation procedure.

4.1.1 Isolation of cortical synaptosome-enriched fractions

Essentially, we summarize the main differences between these two protocols, through observation of the enrichment of some markers in different fractions collected during the isolation procedure and the results are presented in Figure 21.

For Percoll gradient protocol there is a decrease in synaptophysin (Synapt.) levels on synaptosomal fraction, when compared with the homogenate fraction (Hm). Unexpectedly from Hm to S1 the expression of this pre-synaptic marker decreases. In the following supernatants fractions (S2, S3, S4 and S5) a very low or no expression of synaptophysin was detected (Figure 21, A). However, observing the results for sucrose gradient protocol, we can observe that the levels of synaptophysin in synaptosomal fraction are very similar to those observed in homogenate fraction (Hm) and S1. The levels of synaptophysin on S2 fraction were very low, as expected (Figure 21, A).

As post-synaptic marker we analyzed the PSD-95 protein (Figure 21, B). Thus, for Percoll gradient protocol the expression of this protein showed the same behavior as synaptophysin. There is a decrease from Hm to the supernatants fractions (S1, S2, S3, S4 and S5). The level of PSD-95 in synaptosomal fraction was approximately 70% from those observed initially in Homogenate. For sucrose gradient protocol there was a decrease of PSD-95 expression from Homogenate (Hm) to synaptosomal fraction. From Hm to S1 only a slight decrease was observed and no expression was detected in S2 fraction. The synaptosomal fraction expresses approximately 70% of PSD-95 when compared with homogenate fraction. Finally, we also analyzed the content of mitochondria using the ATP-Synthase α (ATP-S α) (Figure 21, C). In Percoll gradient protocol we observed a decrease in expression from Hm to S1 with no expression detected in S2 and S3 fractions. For Syn fraction, we verified that the levels of ATP-S α were around 90% to those observed initially in the homogenate. For sucrose gradient protocol, we observed that the levels of ATP-S α in synaptosomal-enriched fractions are quite similar to those observed in homogenate.

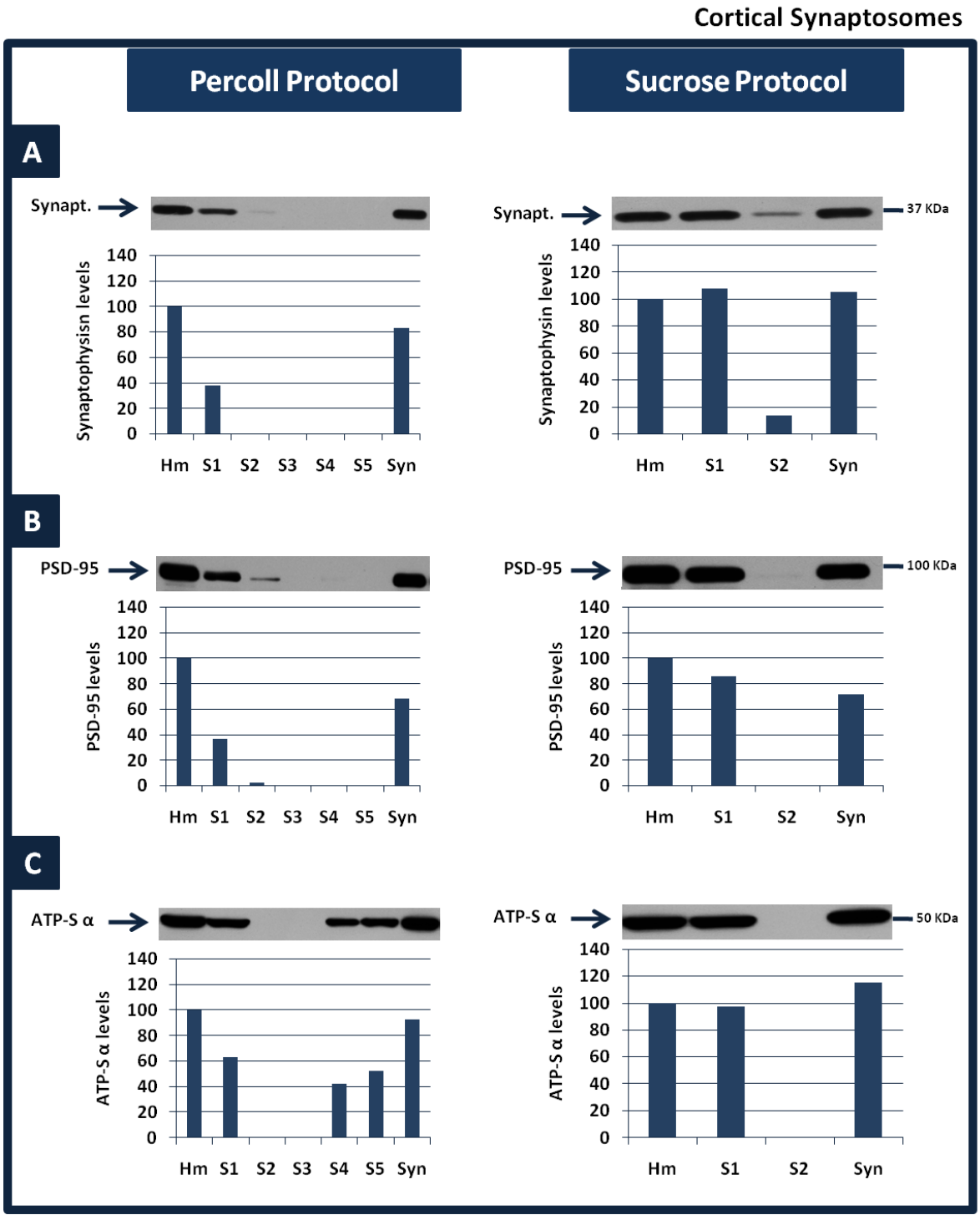

Figure 21: Comparison of Percoll gradient protocol (left) and sucrose gradient protocol (right) for the isolation of cortical synaptosomes-enriched fractions. (A) Relative expression levels of the pre-synaptic marker synaptophysin (Synapt.) in several fractions collected in both protocols. **(B)** Relative levels of post-synaptic marker PSD-95 in several fractions collected in both protocols. **(C)** Relative levels of the mitochondrial marker ATP-synthase α (ATP-S α) in several fractions collected in both protocols. Hm: homogenate, S1: supernatant from the first centrifugation; S2: supernatant from the second centrifugation; S3: supernatant from the third centrifugation; S4 and S5: supernatants from the washing steps; Syn: synaptosomal-enriched fraction. Values shown represent percentage relative to control (Hm: homogenate). Data were obtained from one experiment (n=1).

For Percoll gradient protocol, the homogenate is the fraction that has the highest level of the markers tested while in sucrose gradient protocol we verified that the levels of synaptophysin and ATP-S α in Syn fractions were very similar to those observed in homogenate. Regarding PSD-95 expression levels we observed that they decrease for around 70% of the initial values (homogenate) in both protocols.

4.1.2 Isolation of hippocampal synaptosome-enriched fractions

For the isolation of synaptosome-enriched fractions from hippocampus we used the same methodology, and the results are presented in Figure 22. The same fractions were collected for each protocol during isolation procedure, only the starting material (hippocampus) is different.

For Percoll gradient protocol, we detected a strong decrease in the synaptophysin expression from Hm to S1 and S2. Unexpectedly, in the Syn fraction we did not detect synaptophysin. The results were similar with two other markers (PSD-95 and ATP-S α) analyzed. Observing the results for sucrose gradient protocol, considering the three markers analyzed (synaptophysin, PSD-95, ATP-S α) we observed the same behavior in all fractions. The Hm and S1 fractions have the same level of expression, and S2 have no expression, as expected. In synaptosomal fraction was observed an accentuated increase in the expression of the three markers analyzed.

With this hippocampal analysis, we can observe that sucrose gradient protocol provide a higher sensitivity, allowing an enrichment of protein content of synaptosomes, particularly pre and post-synaptic proteins.

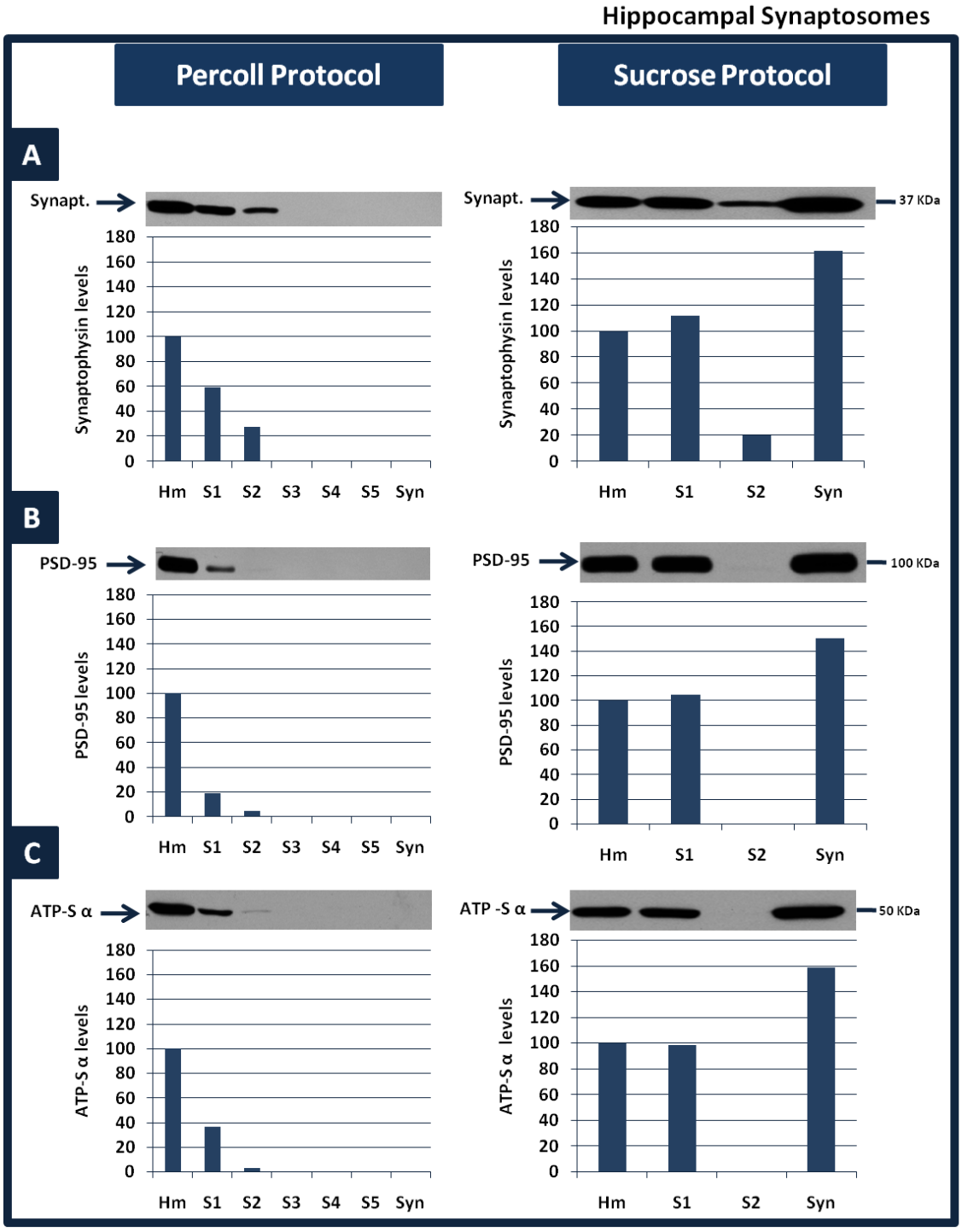

Figure 22: Comparison of Percoll gradient protocol (left) and sucrose gradient protocol (right) for the isolation of hippocampal synaptosome-enriched fractions. (A) Relative levels of the pre-synaptic marker synaptophysin (Synapt.) in several fractions collected in both protocols. **(B)** Relative levels of post-synaptic marker PSD-95 in several fractions collected in both protocols. **(C)** Relative levels of the mitochondrial marker ATP-synthase α (ATP-S α) in several fractions collected in both protocols. Hm: homogenate, S1: supernatant from the first centrifugation; S2: supernatant from the second centrifugation; S3: supernatant from the third centrifugation; S4 and S5: supernatants from the washing steps; Syn: synaptosomal-enriched fraction. Values shown represent percentage of the control (Hm: homogenate). Data were obtained from one experiment (n=1).

4.2 Effect of $Abeta_{1-42}$ treatment on synaptosome viability

To assess the degree of neurotoxicity induced in cortical and hippocampal synaptosomal-enriched fractions after the exposure to increasing concentrations of $Abeta_{1-42}$ peptide (0.25, 0.5 and 2 µM) during three hours, we performed the MTT assay. As previously described in 3.6 section the scrambled $Abeta_{1-42}$ (2µM) was also used. Therefore, two hours after the exposure of synaptosomes to $Abeta_{1-42}$, 60 µl of MTT was added to each sample (final concentration in each sample of 0,5mg/ml). After MTT addition, the samples were placed again at 37ºC (in the dark) for another hour, allowing the reduction of MTT to formazan crystals by viable synaptosomes. After this period of time, the formazan crystals were solubilized adding 0,04M HCL/isopropanol solution. When solubilized, samples were analyzed spectrophotometrically at 570 nm. MTT results for cortical and hippocampal synaptosomes are shown in Figure 23 and Figure 24, respectively. The results are expressed relative to control (without Abeta treatment).

4.2.1 MTT assay of cortical synaptosome-enriched fractions

In Figure 23 we observe that after 3 hours of exposure of cortical synaptosomes to increasing $Abeta_{1-42}$ concentrations, no significant changes in viability are observed. Moreover, when the synaptosomes were incubated with scrambled $Abeta_{1-42}$ (2 µM) no significant changes in viability were also observed.

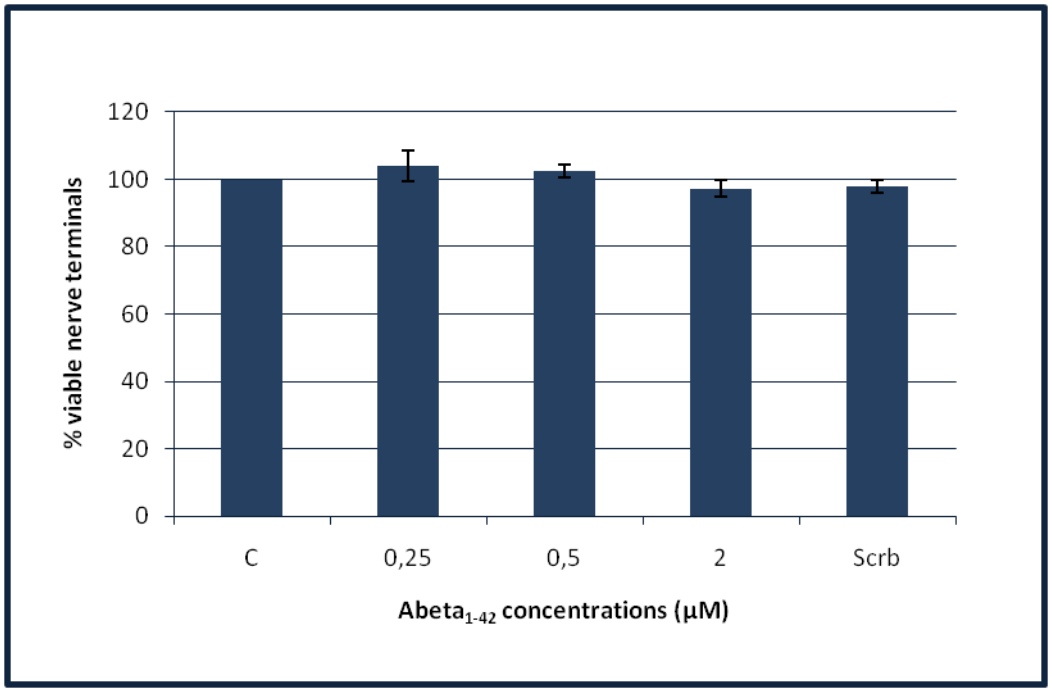

Figure 23: Viability of cortical synaptosome-enriched fractions after exposure to increasing concentrations of Abeta$_{1-42}$ (0.25, 0.5 and 2 µM) and to scrambled Abeta$_{1-42}$ (2µM) during three hours. The values are expressed in percentage relative to Control. Data were obtained from three experiments (n=3). Scrb, scrambled Abeta$_{1-42}$.

With this result, we could confirm that the exposure of cortical synaptosomes to Abeta$_{1-42}$ peptide (all concentrations tested) did not affect their viability and therefore they are physiological active.

4.2.2 MTT assay of hippocampal synaptosome-enriched fractions

The MTT assay of hippocampal synaptosome-enriched fractions produced the same pattern of results of cortical synaptosomes. There were no significant changes on synaptosome viability relative to control (without Abeta treatment) when they were incubated with the various Abeta concentrations. However, when the synaptosomes were incubated with the scrambled Abeta$_{1-42}$ (2µM) a strong reduction on their viability was observed (around 70%).

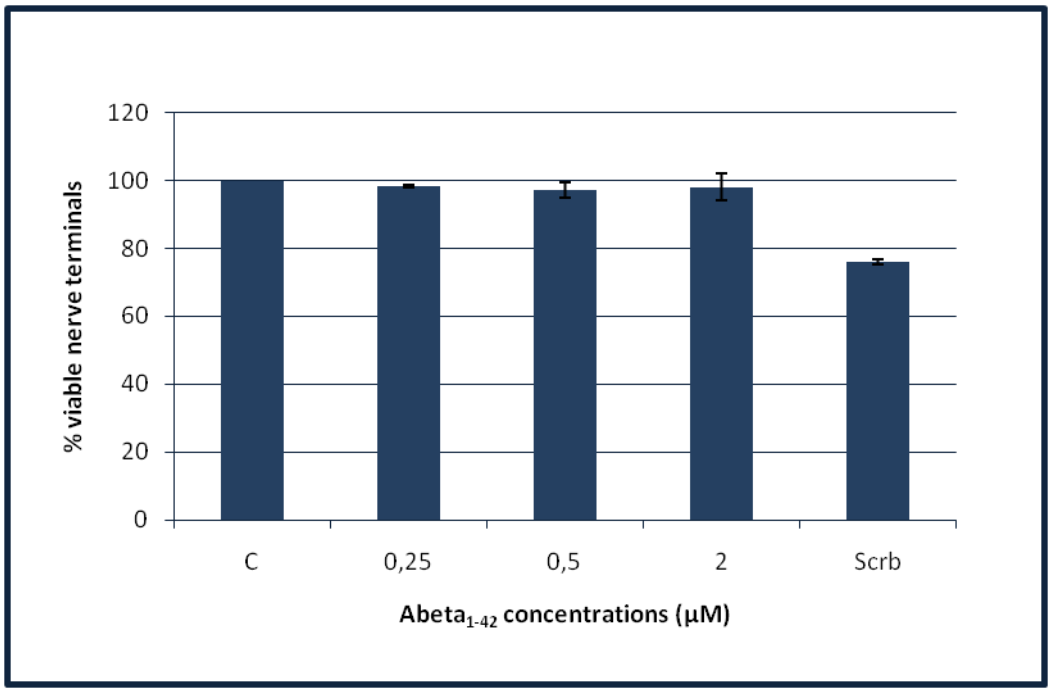

Figure 24: Viability of hippocampal synaptosome-enriched fractions after exposure to increasing concentrations of Abeta$_{1-42}$ (0.25, 0.5 and 2 µM) and to scrambled Abeta$_{1-42}$ (2µM) during three hours. The values are expressed in percentage relative to Control. Data were obtained from three experiments (n=3). Scrb, scrambled Abeta$_{1-42}$.

4.3 Role of Abeta on APP and Tau phosphorylation

4.3.1 Cortical synaptosome-enriched fractions

In order to determine the effect of Abeta on APP and Tau phosphorylation we incubated cortical synaptosome-enriched fractions with Abeta$_{1-42}$ peptide with increasing concentrations (0.25, 0.5 and 2 µM) for three hours. We also included scrambled Abeta$_{1-42}$ as a control, at a concentration of 2 µM. Following this period, cortical synaptosomes were harvested and analyzed by SDS-PAGE and immunoblotting, using for this purpose, p-APP (Thr$_{668}$) antibody, holo-APP (C-Terminal) antibody, p-Tau (Ser$_{262}$) antibody and total-Tau (Tau5) antibody. β-Tubulin was used as loading control.

4.3.1.1 APP phosphorylation in cortical synaptosome-enriched fractions

Observing the state of APP phosphorylation at Thr_{668} residue upon treatment for three hours with $Abeta_{1-42}$ peptide, APP phosphorylation seems to increase with all Abeta concentrations tested. However, is higher with 0.5µM and 2µM $Abeta_{1-42}$ concentrations (Figure 25). Regarding the levels of holo-APP we can observe that it slight decreases relative to Control. However, in order to have a clear idea of the phosphorylation pattern at Thr_{668} residue, we calculated the ratio of p-APP (Thr_{668}) versus holo-APP (C-Terminal) and the graphic representation is presented in Figure 25. Analyzing the ratio we can see that the APP phosphorylation at Thr_{668} residue increases with Abeta treatment, being more evident with higher $Abeta_{1-42}$ concentrations (0.5 and 2 µM).

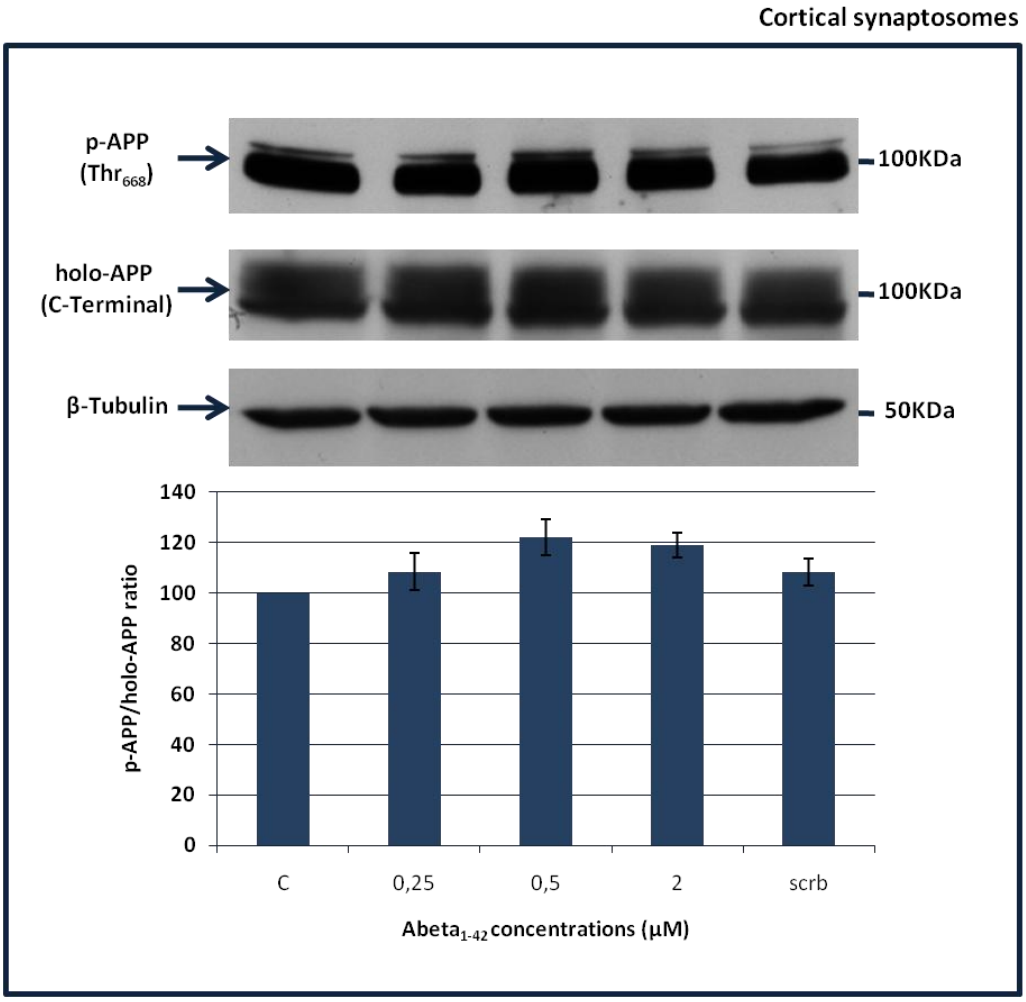

Figure 25: Abeta effects on APP phosphorylation at Thr_{668} residue. Cortical synaptosome-enriched fractions were incubated at 37°C for t(ree hours widh ancreasing concendrations of $Abeda_{1-42}$ (.25, 0.5, 2µM) afd with scrambled $Abeta_{1-42}$ (2 µM). The synaptosomes were then harvested and analyzed by SDS-PAGE and immunoblotting with p-APP (Thr_{668}) antibody, which recognizes Thr_{668} residue; holo-APP (C-Terminal) antibody which recognizes holo-APP and β-Tubulin used as loading control. The graphic represents the ratio between phospho-APP at residue Thr_{668} and holo-APP. Values shown represent percentage relative to control. Data was obtained from triplicate experiments (n=3).

4.3.1.2 Tau phosphorylation in cortical synaptosome-enriched fractions

Observing the effects of $Abeta_{1-42}$ on Tau phosphorylation (Figure 26), we can realize that the phosphorylation of Tau at Ser_{262} residue increases with higher concentrations of $Abeta_{1-42}$ (0.5 and 2µM). Regarding the levels of total-Tau we can observe that upon $Abeta_{1-42}$ treatment they did not change in all Abeta concentrations tested. We also calculated the ratio of phospho-Tau (Ser_{262}) versus total-Tau and we observed that

Abeta$_{1-42}$ treatment affect Tau phosphorylation at Ser$_{262}$ residue being this increase more evident for higher concentrations of Abeta (0.5 and 2µM).

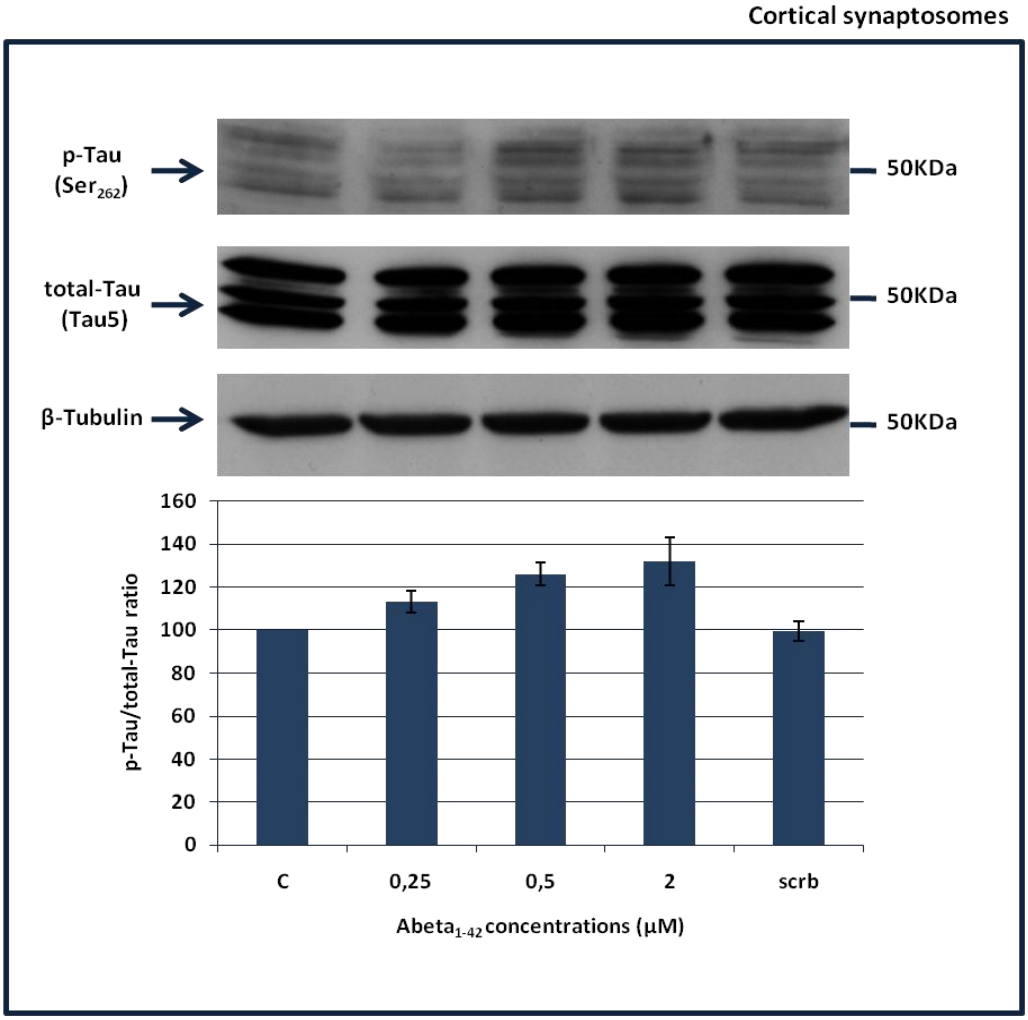

Figure 26: Abeta effects on Tau phosphorylation at Ser$_{262}$ residue. Cortical synaptosome-enriched fractions were incubated at 37°C for three hours with increasing concentrations of Abeta$_{1-42}$ (0.25, 0.5, 2µM) and with scrambled Abeta$_{1-42}$ (2 µM). The synaptosomes were then harvested and analyzed by SDS-PAGE and immunoblotting with p-Tau (Ser$_{262}$) antibody, which recognizes Ser$_{262}$ residue; total-Tau (Tau5) antibody which recognizes total-Tau and β-Tubulin used as loading control. The graphic represents the ratio between phospho-Tau at residue Ser$_{262}$ and total-Tau. Values shown represent percentage relative to Control. Data was obtained from triplicate experiments (n=3).

4.3.2 Hippocampal synaptosome-enriched fractions

To evaluate the effects of Abeta on APP and Tau phosphorylation, hippocampal synaptosome-enriched fractions were also used. The procedures were similar to those described for cortical synaptosome-enriched fractions (section 4.3.1).

4.3.2.1 APP phosphorylation in hippocampal synaptosome-enriched fractions

Analyzing the state of APP phosphorylation (Figure 27) we verified an increase in phosphorylation for the higher concentrations of $Abeta_{1-42}$ specially with 2µM. Relative to holo-APP there is no change for all Abeta concentrations tested. The phospho-APP (Thr_{668})/holo-APP(C-Terminal) ratio was calculated and interestingly present the same pattern observed for APP phosphorylation in cortical synaptosomes. In overall, we can see that exposure of synaptosomes to $Abeta_{1-42}$ affects APP phosphorylation, specifically on Thr_{668} residue, being more evident for the higher concentrations of $Abeta_{1-42}$.

In overall, we observed that upon $Abeta_{1-42}$ treatment of either cortical and hippocampal synaptosomes-enriched fractions an increase on APP Thr_{668} residue phosphorylation is observed, particularly with the two higher concentrations.

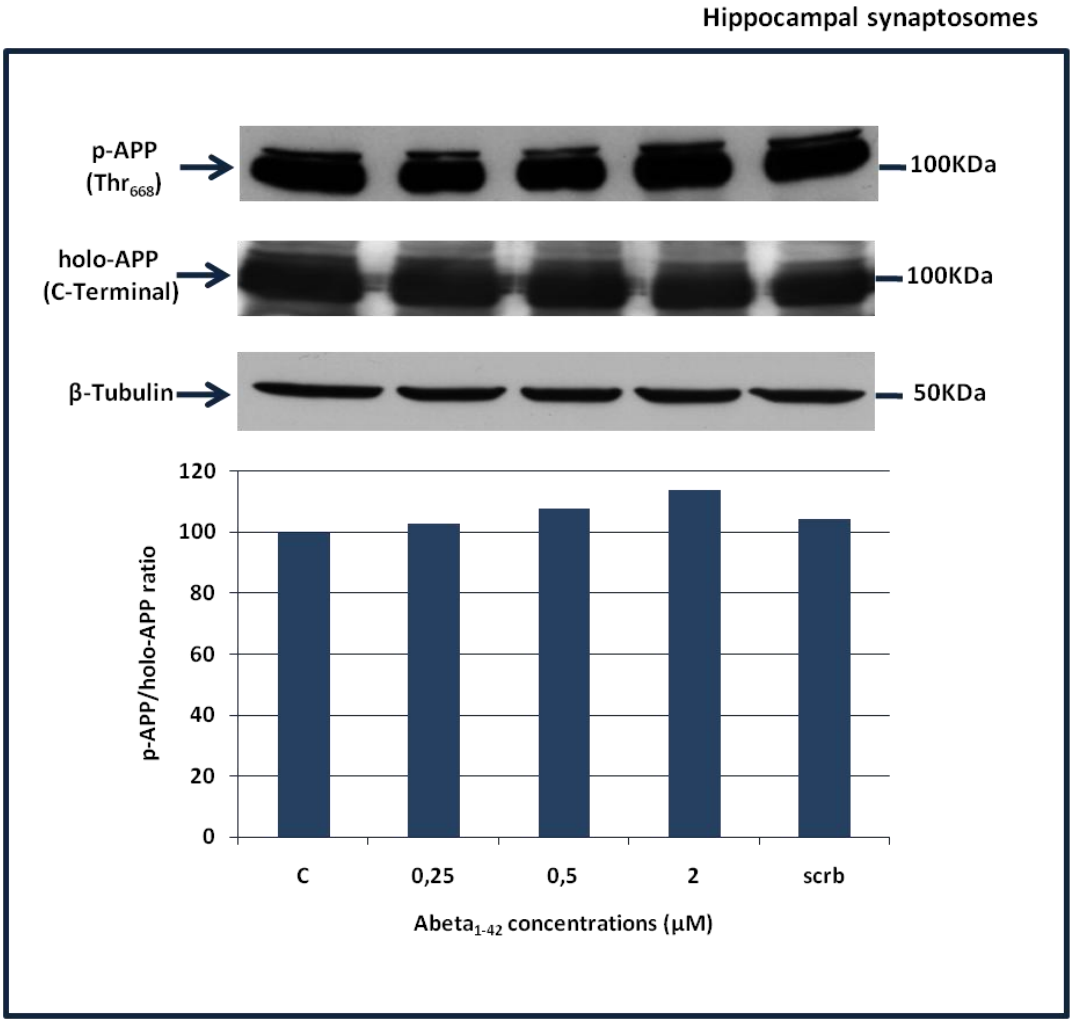

Figure 27: Abeta effects on APP phosphorylation at Thr_{668} residue. Hipocampal synaptosome-enriched fractions were incubated at 37°C for three hours with increasing concentrations of $Abeta_{1-42}$ (0.25, 0.5, 2µM) and with scrambled $Abeta_{1-42}$ (2 µM). The synaptosomes were then harvested and analyzed by immunoblotting with p-APP (Thr_{668}) antibody, which recognizes Thr_{668} residue; holo-APP (C-Terminal) antibody which recognizes holo-APP and β-Tubulin used as loading control. The graphic represents the ratio between phospho-APP at residue Thr_{668} and holo-APP. Values shown represent percentage relative to control. Data was obtained from duplicate experiments (n=2).

4.3.2.2 Tau phosphorylation in hippocampal synaptosome-enriched fractions

The levels of Tau phosphorylation at Ser_{262} residue (Figure 28), revealed an accentuated increase with 0.5µM of $Abeta_{1-42.}$ However, no effect was observed for the other Abeta concentrations tested. The levels of total-Tau were quite similar in all concentrations tested. The phospho-Tau (Ser_{262})/total-Tau (Tau5) ratio was calculated

and shows an increase in Tau phosphorylation at Ser_{262} residue upon treatment with $Abeta_{1-42}$ peptide at concentration of 0.5µM.

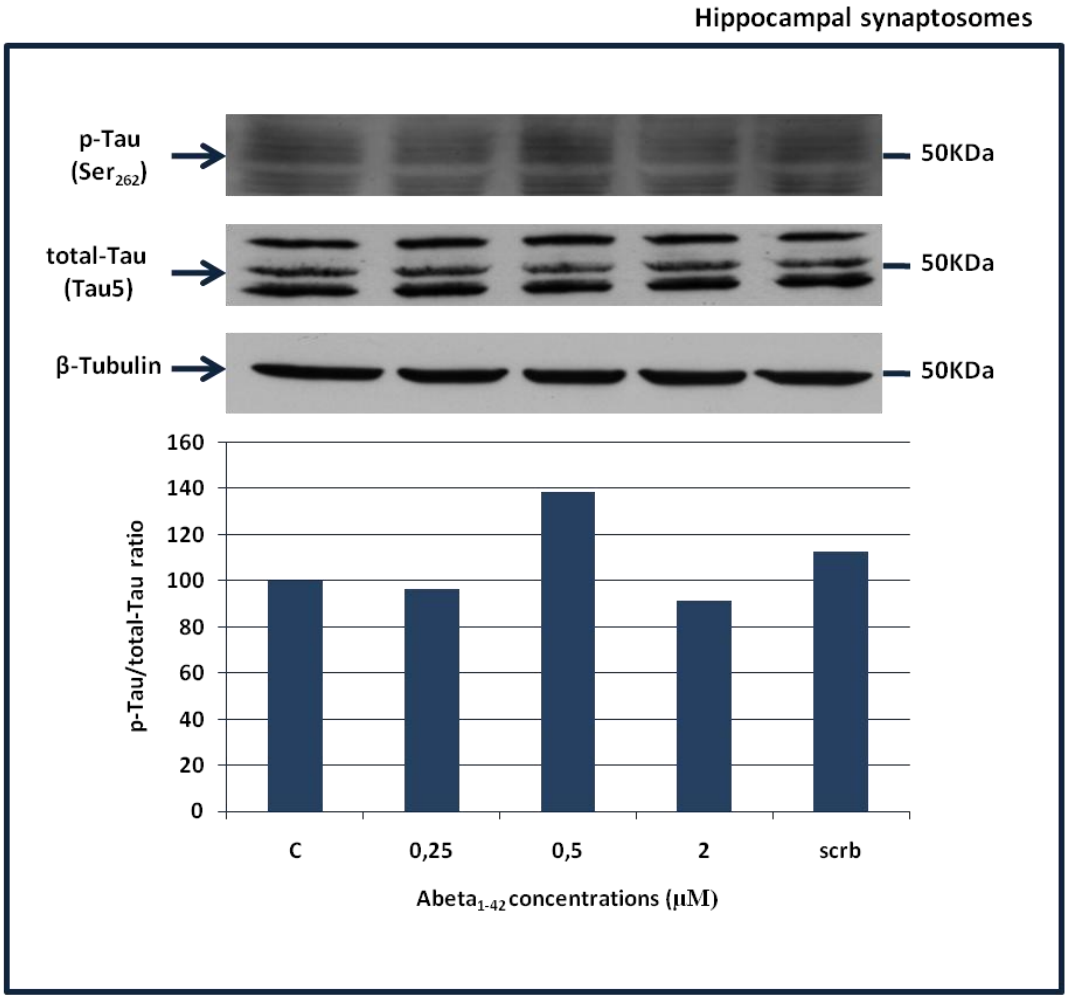

Figure 28: Abeta effects on Tau phosphorylation at Ser_{262} residue. Hippocampal synaptosome-enriched fractions were incubated at 37°C for three hours with increasing concentrations of $Abeta_{1-42}$ (0.25, 0.5 and 2µM) and with scrambled $Abeta_{1-42}$ (2 µM). The synaptosomes were then harvested and analyzed by SDS-PAGE and immunoblotting with p-Tau (Ser_{262}) antibody, which recognizes Ser_{262} residue; total-Tau (Tau5) antibody which recognizes total-Tau and β-Tubulin used as loading control. The graphic represents the ratio between phospho-Tau at residue Ser_{262} and total-Tau. Values shown represent percentage relative to Control. Data was obtained from duplicate experiments (n=2).

4.4 Protein phosphatases involved on APP and Tau dephosphorylation

In order to determine the Protein Phosphatases (PPs) involved in APP and Tau dephosphorylation, we used two well known PPs inhibitors, okadaic acid (OA) and cantharidin (CT) at different concentrations to specific inhibit PP1, PP2A and PP2B. Therefore, cortical synaptosome-enriched fractions were incubated with increasing concentrations of OA and CT, for 30 minutes and 3 hours. After incubation with these PPs inhibitors the synaptosome-enriched fractions were harvested and analyzed by SDS-PAGE and by immunoblotting with the same antibodies used for the previous section 4.3. β-Tubulin was used as loading control.

To determine the effect of OA on APP and Tau phosphorylation we used the following concentrations: 0.1, 0.25, 50, 500 and 5000nM. For Cantharidin (CT), the same methodology described for OA was used, except the concentrations: 100, 250, 500, 1000 and 10000 nM.

4.4.1 Effect of Okadaic acid and Cantharidin on APP phosphorylation

4.4.1.1 Okadaic acid and APP phosphorylation

The results regarding the effect of OA on APP phosphorylation are presented in Figure 29. We can observe that upon 30 minutes of exposure to increasing concentrations of OA, the levels of APP phosphorylation remains almost unchanged. However, three hours after OA treatment we can observe a visible increase for phosphorylation at three higher OA concentrations (50nM, 500nM and 5000nM). The levels of holo-APP did not dramatically change after 30 minutes and 3 hours of cortical synaptosomes treatment with OA. Observing the graphic representation of phospho-APP (Thr_{668})/holo-APP ratio, for 30 minutes we can see that OA did not induce significant alterations in the level of APP phosphorylation. However, at the 3 hours time-point we can observe an increase in APP phosphorylation when PP1 is inhibited (50 and 500nM). Lower concentrations of OA (0.1, 0.25nM), where PP4 and PP2A are inhibited, are not sufficient to induce alterations in the

phosphorylation levels of APP. However, exposure to 50, 500 and 5000nM of OA in fact induces a marked increase on APP phosphorylation, suggesting an involvement of PP1 on APP dephosphorylation at Thr_{668} residue since there is a reduced difference in phosphorylation between 500nM and 5000nM (where PP2B is inhibited).

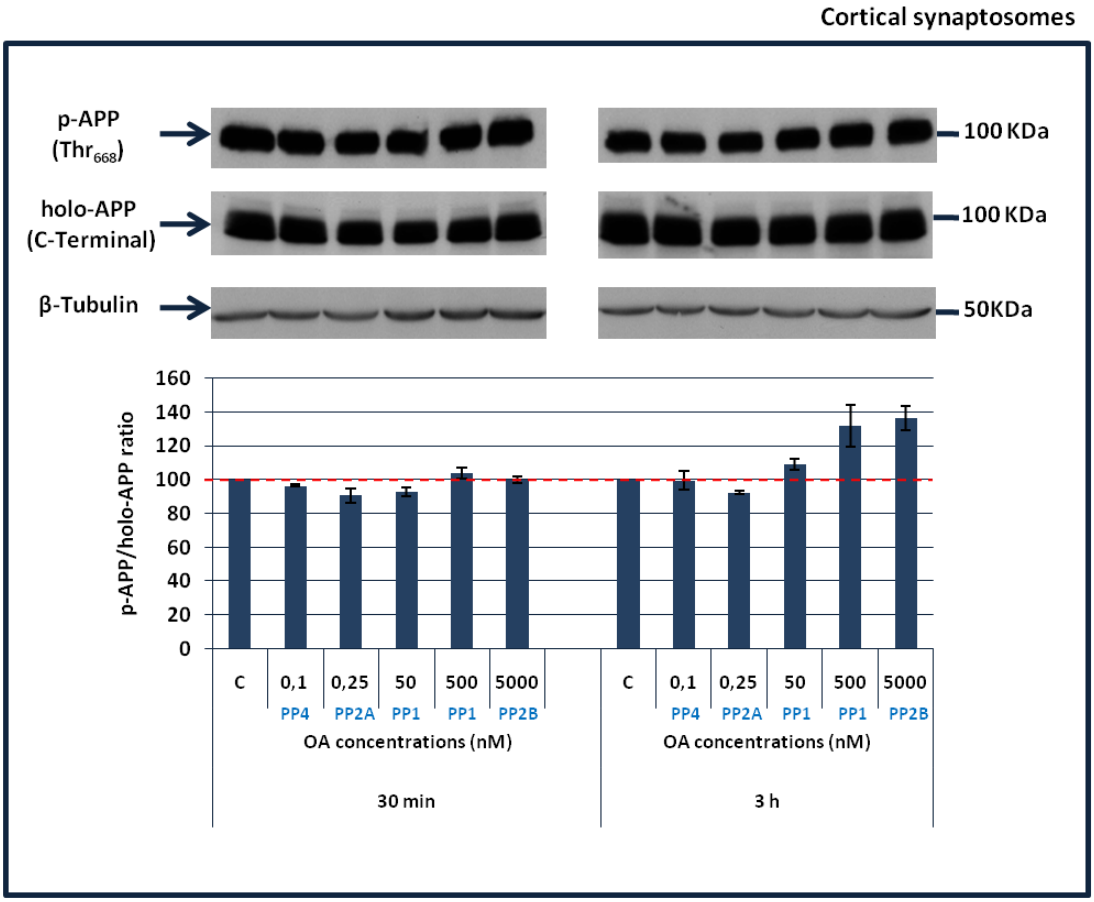

Figure 29: Effect of Okadaic acid on APP phosphorylation (Thr_{668} residue). Cortical synaptosome-enriched fractions were incubated at 37°C for 30 minutes and 3 hours with increasing concentrations of OA (0.1, 0.25, 50, 500 and 5000nM). This fraction was harvested and analyzed by SDS-PAGE and immunoblotting with p-APP (Thr_{668}) antibody, which recognizes Thr_{668} residue; holo-APP (C-Terminal) antibody which recognizes holo-APP and β-Tubulin that was used as loading control. The graphic represents the ratio between phospho-APP at residue Thr_{668} and holo-APP. Values shown represent percentage relative to control. Data was obtained from triplicate experiments (n=3).

4.4.1.2 Cantharidin and APP phosphorylation

Observing the effect of CT on APP phosphorylation, we can realize that the level of phospho-APP (Thr_{668}) for both 30 minutes and 3 hours slightly increased with higher concentrations (1000 and 10000nM). The holo-APP levels remain almost unchanged in the two time periods tested. We calculated the phospho-APP/holo-APP ratio and for 30 minutes of CT exposure is observed an increase in phosphorylation for all concentrations, although more accentuated for the three last concentrations (500, 1000 and 10000nM). This is indicative of an involvement of PP1 on dephosphorylation of APP at Thr_{668} residue. However, upon 3 hours of exposure to CT, there are no significant changes relative to phosphorylation state, only a slight tendency to increase with the two higher concentrations (Figure 30).

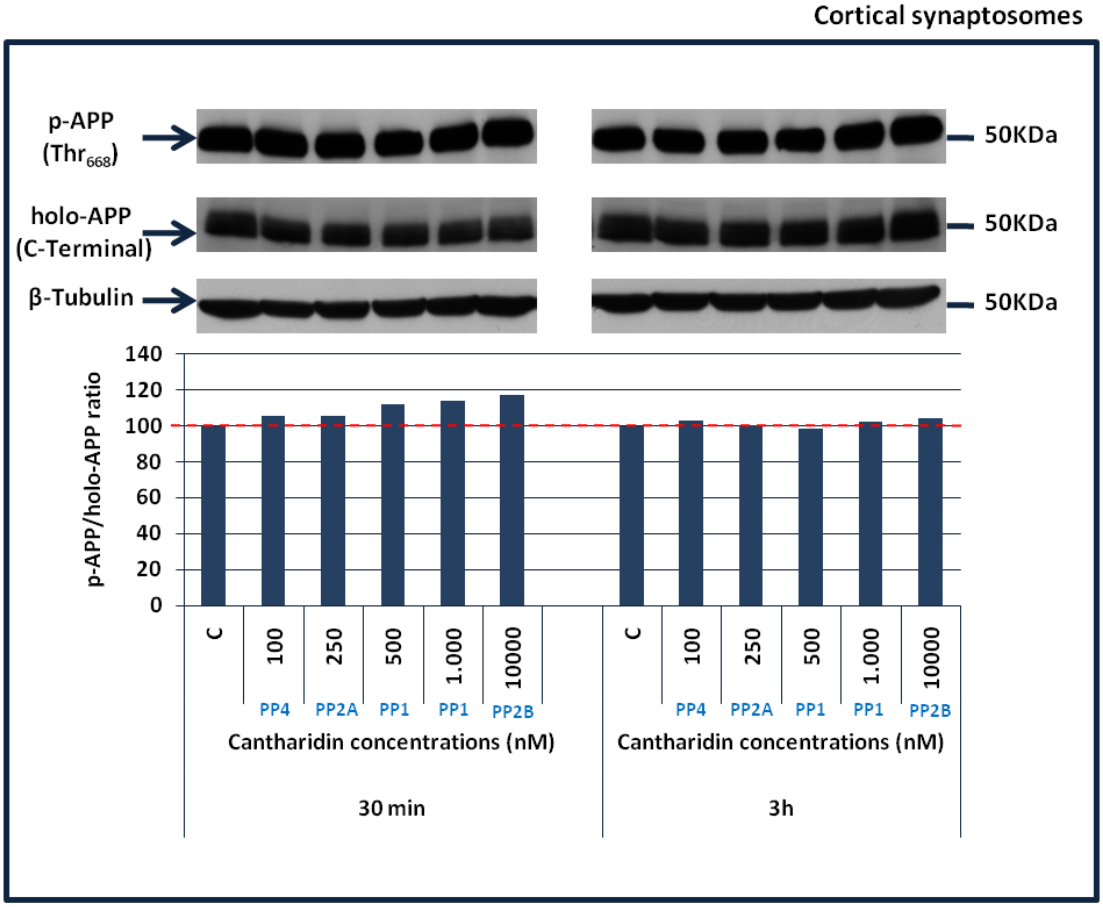

Figure 30: Effects of Cantharidin on APP phosphorylation at Thr_{668} residue. Cortical synaptosome-enriched fractions were incubated at 37°C for 30 minutes and 3 hours with increasing concentrations of CT (100, 250, 500, 1000 and 10000nM). This fraction was harvested and analyzed by SDS-PAGE and immunoblotting with p-APP (Thr_{668}) antibody, which recognizes Thr_{668} residue; holo-APP (C-Terminal) antibody which recognizes holo-APP and β-Tubulin used as loading control. The graphic represents the ratio between phospho-APP at residue Thr_{668} and holo-APP. Values shown represent percentage relative to Control. Data was obtained from duplicate experiments (n=2).

4.4.2 Effect of Okadaic acid on Tau phosphorylation

Regarding the effect of OA on Tau phosphorylation, we can observe that the levels of phospho-Tau (Ser_{262}) for both 30 minutes and 3 hours, increased with higher OA concentrations (50, 500 and 5000nM). The total-Tau did not dramatically changed for both time-point analyzed. Observing phospho-Tau/total-Tau ratio, we can see that upon 30 minutes of exposure to OA, there was an increase on Tau phosphorylation with 50 and 500nM (where PP1 is inhibited) as well as with 5000nM (where PP2B is inhibited). However, since there is no significant increase on Tau phosphorylation between the last two concentrations we can say that only PP1 is involved on dephosphorylation of this residue. The results obtained for 3 hours also indicate an involvement of PP1 in dephosphorylation of Ser_{262} (Figure 31).

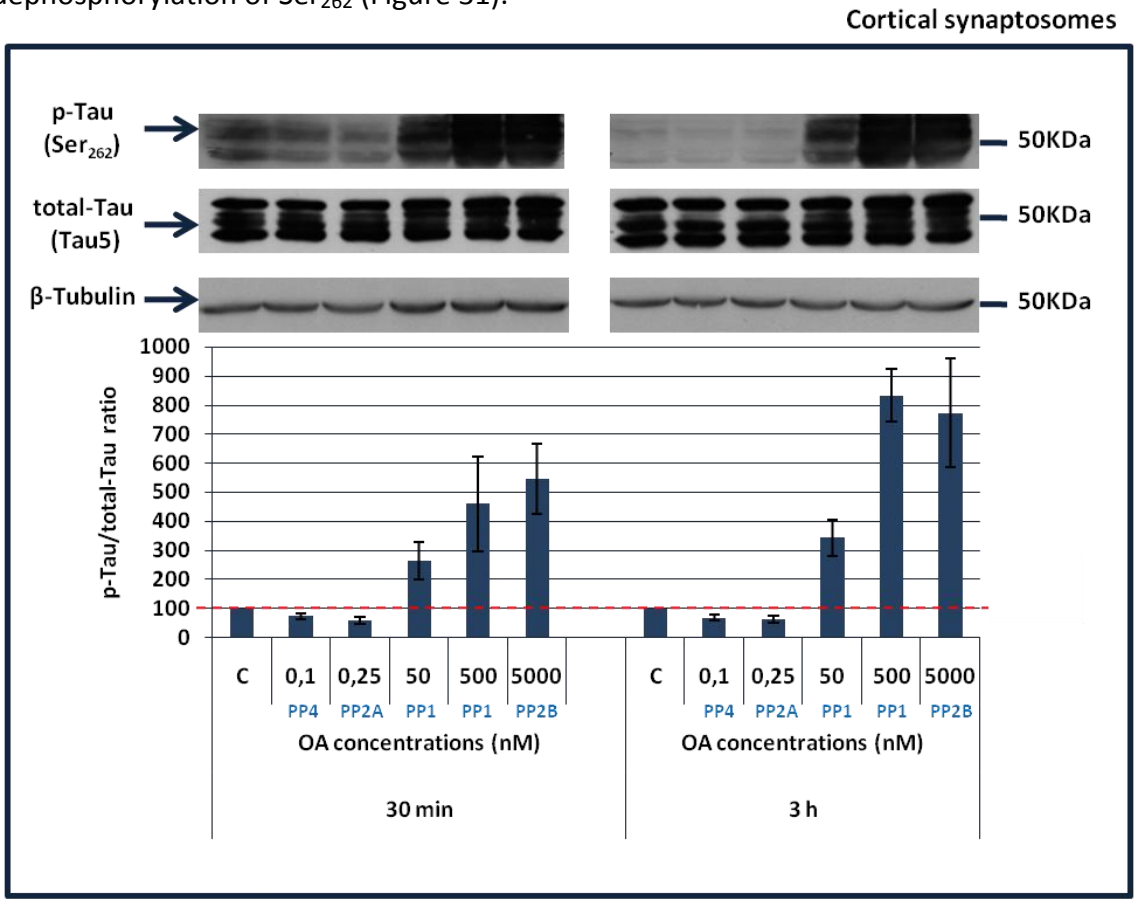

Figure 31: Effects of Okadaic acid on Tau phosphorylation at Ser_{262} residue. Cortical synaptosome-enriched fractions were incubated at 37°C for 30 minutes and 3 hours with increasing concentrations of OA (0.1, 0.25, 50, 500 and 5000nM). This fraction was harvested and analyzed by SDS-PAGE and immunoblotting with p-Tau (Ser_{262}) antibody, which recognizes Ser_{262} residue; total-Tau (Tau5) antibody which recognizes total-Tau and β-Tubulin used as loading control. The graphic represents the ratio between phospho-Tau at residue ser_{262} and total-Tau. Values shown represent percentage relative to Control. Data was obtained from triplicate experiments (n=3).

5 Discussion

Alzheimer´s disease is the most common form of dementia, having SPs and NFTs as main features. According to the amyloid cascade hypothesis, has been proposed that these two hallmarks are correlated. Abeta peptide results from the proteolytic processing of APP and can aggregate originating extracellular SPs. This peptide could deregulate some signaling cascades and also the activity of some kinases and phosphatases, leading to hyperphosphorylation of Tau originating intracellular NFTs. Thus, the study of AD pathology involves the analysis of altered expression of proteins, and for this reason AD is a good candidate for proteomic research. The possibility to use synaptosomes as an *in vitro* model to study synaptic physiology and neurochemistry makes this model system an appropriate form to investigate synaptic dysfunction pathways and therefore to study AD pathology. The main characteristics that make synaptosomes a good model are the presence of a pre-synaptic side (mainly composed by synaptic vesicles, mitochondria and cytoskeleton proteins) and also a post-synaptic side.

To enable more efficient proteomic analysis using synaptosomes some techniques have been developed for the isolation of relative pure synaptosomes from rat brain. So, the first objective of this work was the comparison of two different methodologies to isolate synaptosomes: Percoll gradient protocol and sucrose gradient protocol, from both cortex and hippocampus tissues. During the isolation procedure, for each tissue were collected several fractions (Hm: Homogenate, Sn: Supernatants fractions and Syn: Synaptosomal fractions) that were further analyzed by SDS-PAGE and immunoblotting using different markers (Synaptophysin, ATP-synthase α and PSD-95). The evaluation of immunoblots allowed the determination of the yield and purity of each protocol. For cortex, using Percoll gradient protocol we observed that there was a decrease in all markers in synaptosomal fraction relative to control (Figure 21). Although, with sucrose gradient protocol the expression of synaptophysin and ATP synthase α were very similar to those observed in Homogenate, while a decrease was observed for PSD-95 (Figure 21). The decrease in PSD-95 levels in Syn fraction could be due to the loss of post-synaptic terminals during the centrifugation steps. Regarding the hippocampal synaptosomes, for Percoll gradient protocol no expression was detected for the three markers tested on synaptosomal fraction, indicating that the amount of the previous markers present in the

sample were below the limiar of detection meaning that this procedure failure in the isolation of hippocampal synaptosomes. However, in sucrose gradient protocol we observed an increase in the expression levels of all markers tested. This increase could be explained by the presence of more contaminants on homogenate fraction that also contains nuclei, cell debries and remains of meninges. After the centrifugation steps these contaminants were removed and we obtained relatively pure synaptosomal fractions, enriched in pre-synaptic and post-synaptic markers and also with some mitochondria. Also, very evident is the fact that with the Percoll gradient protocol (either in cortex and hippocampus) a huge amount of material is lost in the first centrifugation step, affecting obviously the final yield obtained with procedure that was more critical in the hippocampus. Although, our results are in accordance with some previous reports. Gredilla et al. showed that synaptosomal fractions contain significant amounts of mitochondria, since they are present in pre synaptic side. This localization facilitates the access to energy that is critical for exocytosis/endocytosis events of synaptic vesicles, being for this reason important for the maintenance of synaptic activity and the proper function of central nervous system (Gredilla et al., 2012). This enrichment in mitochondria is also supported by McClatchy group (McClatchy et al., 2007). Regarding to synaptophysin marker there are some studies that also confirm an enrichment in synaptosomal fraction relative to whole brain preparations (Wishart et al., 2007). Finally, for PSD-95, some groups also verified an increase in the immunoreactivity of this protein in synaptosomal fraction compared with control (Hm) (McClatchy et al., 2007). Taken together, our results indicate that sucrose gradient protocol allows a more efficient purification of synaptosomes than Percoll gradient protocol. Additionally, with sucrose gradient protocol we obtained more synaptosomes than with Percoll gradient protocol. Therefore this protocol was chosen to routinely isolate cortical and hippocampal synaptosomes needed for further experiments in our laboratory. However, more independent experiments must be performed to confirm these results and additional techniques would be used to further validate the comparison of these two methodologies. Among them electron microscopy will be used to characterize these fractions.

The next aim was the evaluation of the effect of $Abeta_{1-42}$ on APP and Tau phosphorylation. Prior to that, we tested if the different Abeta concentrations used (0.25, 0.5 and 2μM) affect synaptosomal viability using a MTT assay. After the exposure of synaptosomes to $Abeta_{1-42}$ we observed that cortical and hippocampal synaptosomes were viable since no significative changes relative to control were observed. Our results are supported by Canas et al., which obtained a reduction less than 10% when exposed hippocampal synaptosomes to 0.5μM $Abeta_{1-42}$ during 2 hours (Canas et al., 2009). Another study also shows that exposure of synaptosomes to 1μM $Abeta_{1-40}$ during 5 minutes, 30 minutes, 1 hour and 4 hours do not change their viability (Uranga et al., 2010).

Since with all $Abeta_{1-42}$ concentrations tested the synaptosome-enriched fractions were viable we carried on with the following experiments and we determined the effects of $Abeta_{1-42}$ on APP and Tau phosphorylation. For this purpose, we exposed cortical and hippocampal synaptosomes to increasing concentrations of $Abeta_{1-42}$ (0.25, 0.5 and 2μM) and we verified that Abeta influences both APP and Tau phosphorylation. To study APP and Tau phosphorylation we considered two residues, Thr_{668} and Ser_{262} on APP and Tau, respectively. Thr_{668} has an important role in AD since when phosphorylated the interaction of APP with its partners is affected. Relative to Ser_{262}, this is an important residue on Tau. It is present in microtubule binding domain and so it is crucial for microtubule assembly. For this reason, phosphorylation of these residues could affect APP and Tau functions, being relevant for AD. For cortical synaptosome-enriched fractions we observed an increase in APP phosphorylation for Thr_{668} residue, considering higher concentrations of $Abeta_{1-42}$ (0.5 and 2μM) (Figure 25). For Tau phosphorylation at Ser_{262} residue it increases in a concentration-dependent manner, being much higher for 2μM (Figure 26). Relative to hippocampal-enriched fractions phosphorylation of APP at Thr_{668} residue increases with higher concentrations of Abeta (0.5 and 2μM) (Figure 27). For Tau at Ser_{262} the phosphorylation increases substantially for 0.5μM $Abeta_{1-42}$ (Figure 28), while the phosphorylation pattern for the other concentrations remains similar to control. Interestingly is that the effect of Abeta on APP and Tau phosphorylation is similar in both cortical and hippocampal synaptosomes. All together the results confirm that

$Abeta_{1-42}$ influence APP and Tau phosphorylation. The mechanism whereby Abeta influence protein phosphorylation is not full elucidated. However, is thought that Abeta is affecting some signaling cascades and in turn some PKs and some PPs, which cause abnormal protein phosphorylation (Figure 32).

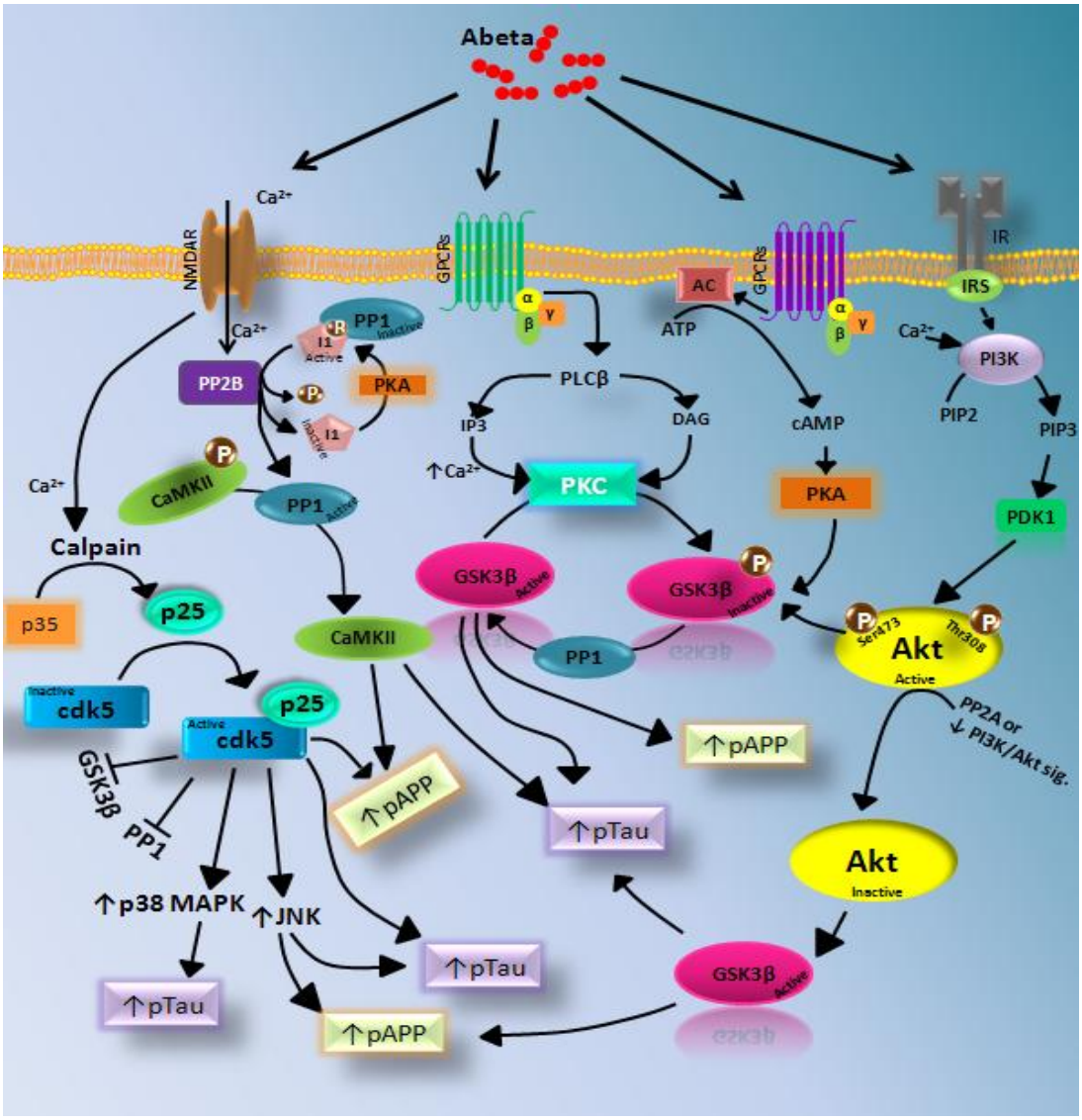

Figure 32: Schematic representation of possible signaling cascades that could be deregulated in the presence of extracellular Abeta, leading to APP and Tau phosphorylation. Abeta stimulation increases Cdk5 activity, due to the coupling of p25, increasing APP and Tau phosphorylation. Cdk5 also mediates p38 MAPK and JNK activation, which in turn could phosphorylate Tau and the latter also phosphorylate APP. The increase in Ca^{2+} influx activates PP2B, which in turn activates PP1 by dephosphorylation of inhibitor 1 (I1). Since PP1 is active, it could dephosphorylate CaMKII, being this kinase active to phosphorylate APP and Tau. The presence of Abeta could also inhibit Akt signaling, inhibiting Akt. Inactivate Akt (dephosphorylated state) is not able to phosphorylate GSK3β being this kinase active, causing the phosphorylation of APP and Tau. PP1 also plays an important role in GSK3β activation leading to an increase in phosphorylation. Although is not shown in the figure, PKA and PKC could phosphorylate Tau and the latter can also phosphorylate APP. APP phosphorylation originates senile plaques and Tau phosphorylation form NFTs, which results in neurodegeneration. NMDR: N-Methyl-D-aspartate (NMDA) receptor; GPCR: G protein coupled receptors; DAG: dyacilglycerol; PLC: phospholipase C-β; IR: Insulin receptor; AC: adenylate cyclase; PIP2: phosphatidylinositol (4,5)-biphosphate; PIP3: phosphatidylinositol (3,4,5) triphosphate; PDK1: phosphoinositide dependent kinase 1; PI3K: phosphoinositide 3 kinase.

For APP phosphorylation, specifically at Thr_{668} residue, the principal signaling cascades involved culminate with GSK3β, CaMKII and Cdk5 activation, which in turn activate JNK (Table 2 and Figure 32). These activated kinases are able to phosphorylate APP leading to more Abeta production that ultimately leads to more SPs formation. Relative to Tau phosphorylation at residue Ser_{262}, the principal signaling cascades involve CaMKII, Cdk5, GSK3 and p38 MAPK (activated by Cdk5). These kinases are able to phosphorylate Tau which may results in NFTs formation (Table 2 and Figure 32). As shown in Figure 32, APP and Tau phosphorylation could result from activation or downregulation of some signaling cascades, like PI3K/Akt. In this case, the presence of extracellular Abeta diminishes Akt phosphorylation causing the inactivation of this kinase. This inactivation causes the GSK3β activation, being this able to phosphorylate APP and Tau. A variety of second messengers (like cAMP, DAG, IP3 and Ca^{2+}) and the multiplicity of signaling cascades that are thought to be involved in AD, makes the study of this disease a difficult task.

Once established that $Abeta_{1-42}$ induces APP and Tau phosphorylation, we went on to study the protein phosphatases involved on APP and Tau dephosphorylation at Thr_{668} and Ser_{262} residues, respectively. Our experiments, using both OA and CT, revealed that the major PP involved in APP Thr_{668} residue dephosphorylation seems to be PP1. This result is in agreement with previous works performed in our laboratory where an inhibition of PP1 was observed after treatment of cortical primary neuronal cultures also with OA and CT (Oliveira, 2011).

For Ser_{262} residue of Tau, the phosphorylation increased when PP1 was inhibited with OA, suggesting an involvement of this PP in Tau dephosphorylation (Figures 31). Previous works from our laboratory also indicates PP1 as the main PP involved on Tau dephosphorylation at this residue, using cortical primary neuronal cultures treated with OA (Martins, 2011). Additionally, Rahman et al. (2006), also show a decrease in PP1 activity in AD brains and this fact is also supported by several reports (Rahman et al., 2006; Swingle et al., 2007). Experiments done with rats, which were treated with intraventricular infusions of OA also showed an increase in Tau phosphorylation, and decreased activity of PP1 (Billingsley and Kincaid, 1997).

In conclusion, these findings suggest an important role of PP1 on both APP and Tau dephosphorylation at Thr_{668} and Ser_{262} residues, respectively. Phosphorylation of APP at Thr_{668} may facilitates β-secretase activity leading to Abeta production and accumulation, which results in neuronal damage and consequently in AD. For this reason, dephosphorylation of APP by PP1 could have a protective role. Relative to Tau Ser_{262} is an important residue located on microtubule binding domain and essential to the maintenance of microtubule assembly. Thus, PP1 may also have an important role in preventing not only the disruption of microtubule assembly but also the self-assembly of Tau into PHFs.

Interestingly, previous reports from the laboratory by Vintem et al. (2009), also described an inhibition of different PP1 isoforms with Abeta ($Abeta_{1-40}$, $Abeta_{25-35}$ and $Abeta_{1-42}$) at low micromolar concentrations both *in vivo* and *ex vivo* (Vintem et al., 2009). Taken together these results suggests that Abeta inhibits PP1 probably by Cdk5 pathway (Figure 32), favoring phosphorylation of some proteins such as APP and Tau. Thus, these findings are consistent with the pathological sequential events of Alzheimer´s disease and deserve further investigation.

6 Concluding Remarks

Comparison of methodologies to isolate synaptosomes

- Sucrose gradient protocol allows a more efficient purification of synaptosomes than Percoll gradient protocol.

Abeta Effects on APP and Tau phosphorylation

- $Abeta_{1-42}$ treatment of cortical and hippocampal synaptosome enriched fractions did not affect their viability;
- $Abeta_{1-42}$ affects the phosphorylation state of APP, for both cortex and hippocampus;
- In cortex, $Abeta_{1-42}$ affects Tau phosphorylation in a concentration-dependent manner. However, in hippocampus, only 0.5µM affects the phosphorylation state;

Protein Phosphatases involved in APP and Tau dephosphorylation

- PP1 is involved in APP and Tau dephosphorylation.

7 References

Ahlijanian, M. K., Barrezueta, N. X., Williams, R. D., Jakowski, A., Kowsz, K. P., McCarthy, S., Coskran, T., Carlo, A., et al. (2000). "Hyperphosphorylated tau and neurofilament and cytoskeletal disruptions in mice overexpressing human p25, an activator of cdk5." Proc Natl Acad Sci U S A **97**(6): 2910-5.

Alonso, A. C., Zaidi, T., Novak, M., Grundke-Iqbal, I. and Iqbal, K. (2001). "Hyperphosphorylation induces self-assembly of τ into tangles of paired helical filaments/straight filaments." **98**(12): 6923-6928.

Anoop, A., Singh, P. K., Jacob, R. S. and Maji, S. K. (2010). "CSF Biomarkers for Alzheimer's Disease Diagnosis." Int J Alzheimers Dis **2010**.

Avila, J., Lucas, J. J., Perez, M. and Hernandez, F. (2004). "Role of tau protein in both physiological and pathological conditions." Physiol Rev **84**(2): 361-84.

Bai, F. and Witzmann, F. A. (2007). "Synaptosome proteomics." Subcell Biochem **43**: 77-98.

Balaraman, Y., Limaye, A. R., Levey, A. I. and Srinivasan, S. (2006). "Glycogen synthase kinase 3beta and Alzheimer's disease: pathophysiological and therapeutic significance." Cell Mol Life Sci **63**(11): 1226-35.

Barbagallo, A. P., Weldon, R., Tamayev, R., Zhou, D., Giliberto, L., Foreman, O. and D'Adamio, L. (2010). "Tyr(682) in the intracellular domain of APP regulates amyloidogenic APP processing in vivo." PLoS One **5**(11): e15503.

Bergmans, B. A. and De Strooper, B. (2010). "gamma-secretases: from cell biology to therapeutic strategies." Lancet Neurol **9**(2): 215-26.

Bielska, A. A. and Zondlo, N. J. (2006). "Hyperphosphorylation of tau induces local polyproline II helix." Biochemistry **45**(17): 5527-37.

Billingsley, M. L. and Kincaid, R. L. (1997). "Regulated phosphorylation and dephosphorylation of tau protein: effects on microtubule interaction, intracellular trafficking and neurodegeneration." Biochem J **323 (Pt 3)**: 577-91.

Buee, L., Bussiere, T., Buee-Scherrer, V., Delacourte, A. and Hof, P. R. (2000). "Tau protein isoforms, phosphorylation and role in neurodegenerative disorders." Brain Res Brain Res Rev **33**(1): 95-130.

Busciglio, J., Lorenzo, A., Yeh, J. and Yankner, B. A. (1995). "beta-amyloid fibrils induce tau phosphorylation and loss of microtubule binding." Neuron **14**(4): 879-88.

Canas, P. M., Porciuncula, L. O., Cunha, G. M., Silva, C. G., Machado, N. J., Oliveira, J. M., Oliveira, C. R. and Cunha, R. A. (2009). "Adenosine A2A receptor blockade prevents

synaptotoxicity and memory dysfunction caused by beta-amyloid peptides via p38 mitogen-activated protein kinase pathway." J Neurosci **29**(47): 14741-51.

Chua, J. J. E., Kindler, S., Boyken, J. and Jahn, R. (2010). "The architecture of an excitatory synapse." Journal of Cell Science(123): 819-823.

Chung, S. H. (2009). "Aberrant phosphorylation in the pathogenesis of Alzheimer's disease." BMB Rep **42**(8): 467-74.

Cicero, S. and Herrup, K. (2005). "Cyclin-Dependent Kinase 5 Is Essential for Neuronal Cell Cycle Arrest and Differentiation " Journal of Neuroscience **25**(42): 9658-9668.

Citron, M., Diehl, T. S., Gordon, G., Biere, A. L., Seubert, P. and Selkoe, D. J. (1996). "Evidence that the 42- and 40-amino acid forms of amyloid β protein are generated from the β-amyloid precursor protein by different protease activities." **93**(23): 13170-13175

Cong, C. X., Singh, T. J., Grundke-Iqbal, I. and Iqbal, K. (1993). "Phosphoprotein phosphatase activities in Alzheimer disease brain." J. Neurochem. (61): 921-927.

Crewes, L. and Mashliah, E. (2010). "Molecular mechanisms of neurodegeneration in Alzheimer´s disease." Human Molecular Genetics **19**(1): 12-20.

Cruz, J. C., Tseng, H. C., Goldman, J. A., Shih, H. and Tsai, L. H. (2003). "Aberrant Cdk5 activation by p25 triggers pathological events leading to neurodegeneration and neurofibrillary tangles." Neuron **40**(3): 471-83.

da Cruz e Silva, E. F. and da Cruz e Silva, O. A. (2003). "Protein phosphorylation and APP metabolism." Neurochem Res **28**(10): 1553-61.

da Cruz e Silva, O. A., Fardilha, M., Henriques, A. G., Rebelo, S., Vieira, S. and da Cruz e Silva, E. F. (2004). "Signal transduction therapeutics: relevance for Alzheimer's disease." J Mol Neurosci **23**(1-2): 123-42.

Dale Purves, G. J. A., David Fitzpatrick, William C. Hall, Anthony-Samuel Lamantia, James O. McNamara, S. Mark Williams (2004). Neuroscience, Sinauer Associates.

de Leon, M. J., DeSanti, S., Zinkowski, R., Mehta, P. D., Pratico, D., Segal, S., Clark, C., Kerkman, D., et al. (2004). "MRI and CSF studies in the early diagnosis of Alzheimer's disease." J Intern Med **256**(3): 205-23.

DeKosky, S. and Scheff, S. (1990). "Synapses loss in frontal cortex biopsies in Alzheimer´s disease: correlation with cognitive severity. ." Ann. Neurol(27): 457-464.

Deshpande, A., Win, K. M. and Busciglio, J. (2008). "Tau isoform expression and regulation in human cortical neurons." FASEB J **22**(7): 2357-67.

Dhavan, R. and Tsai, L. H. (2001). "A decade of CDK5." Nat Rev Mol Cell Biol **2**(10): 749-59.

Dunkley, P. R., Jarvie, P. E. and Robinson, P. J. (2008). "A rapid Percoll gradient procedure for preparation of synaptosomes." Nat Protoc **3**(11): 1718-28.

Dunkley, P. R. and Robinson, P. J. (1986). "Depolarisation-dependent protein phosphorylation in synaptosomes:mechanisms and significance." Prog. Brain Res. **69**: 273-293.

Fox, S. I. (2010). Human Physiology. New York, McCraw-Hill.

Gandy, S. (2005). "The role of cerebral amyloid beta accumulation in common forms of Alzheimer disease." J Clin Invest **115**(5): 1121-9.

Gandy, S., Czernik, A. J. and Greengard, P. (1988). "Phosphorylation of Alzheimer disease amyloid precursor peptide by protein kinase C and Ca2+/calmodulin-dependent protein kinase II." Proc Natl Acad Sci U S A **85**(16): 6218-21.

Gandy, S. E., Caporaso, G. L., Buxbaum, J. D., de Cruz Silva, O., Iverfeldt, K., Nordstedt, C., Suzuki, T., Czernik, A. J., et al. (1993). "Protein phosphorylation regulates relative utilization of processing pathways for Alzheimer beta/A4 amyloid precursor protein." Ann N Y Acad Sci **695**: 117-21.

Giese, K. P. (2009). "GSK-3: a key player in neurodegeneration and memory." IUBMB Life **61**(5): 516-21.

Glenner, G. G., Wong, C. W., Quaranta, V. and Eanes, E. D. (1984). "The amyloid deposits in Alzheimer´s disease:their nature and pathogenesis." Appl Pathol (2): 357-69.

Gong, C. X. and Iqbal, K. (2008). "Hyperphosphorylation of microtubule-associated protein tau: a promising therapeutic target for Alzheimer disease." Curr Med Chem **15**(23): 2321-8.

Gong, C. X., Liu, F., Grundke-Iqbal, I. and Iqbal, K. (2006). "Dysregulation of protein phosphorylation/dephosphorylation in Alzheimer's disease: a therapeutic target." J Biomed Biotechnol **2006**(3): 31825.

Gredilla, R., Weissman, L., Yang, J. L., Bohr, V. A. and Stevnsner, T. (2012). "Mitochondrial base excision repair in mouse synaptosomes during normal aging and in a model of Alzheimer's disease." Neurobiol Aging **33**(4): 694-707.

Grimes, C. A. and Jope, R. S. (2001). "The multifaceted roles of glycogen synthase kinase 3beta in cellular signaling." Prog Neurobiol **65**(4): 391-426.

Haass, C., Schlossmacher, M. G., Hung, A. Y., Vigo-Pelfrey, C., Mellon, A., Ostaszewski, B. L., Lieberburg, I., Koo, E. H., et al. (1992). "Amyloid beta-peptide is produced by cultured cells during normal metabolism." Nature **24**(359): 322-5.

He, Y., Cui, J., Lee, J. C., Ding, S., Chalimoniuk, M., Simonyi, A., Sun, A. Y., Gu, Z., et al. (2011). "Prolonged exposure of cortical neurons to oligomeric amyloid-beta impairs NMDA receptor function via NADPH oxidase-mediated ROS production: protective effect of green tea (-)-epigallocatechin-3-gallate." ASN Neuro **3**(1): e00050.

Holtzman, D. M., Bales, K. R., Tenkova, T., Fagan, A. M., Parsadanian, M., Sartorius, L. J., Mackey, B., Olney, J., et al. (2000). "Apolipoprotein E isoform-dependent amyloid deposition and neuritic degeneration in a mouse model of Alzheimer's disease." Proc Natl Acad Sci U S A **97**(6): 2892-7.

Holtzman, D. M., Fagan, A. M., Mackey, B., Tenkova, T., Sartorius, L., Paul, S. M., Bales, K., Ashe, K. H., et al. (2000). "Apolipoprotein E facilitates neuritic and cerebrovascular plaque formation in an Alzheimer's disease model." Ann Neurol **47**(6): 739-47.

Hooper, C., Killick, R. and Lovestone, S. (2008). "The GSK3 hypothesis of Alzheimer's disease." J Neurochem **104**(6): 1433-9.

Hunter, T. (1995). "Protein kinases and phosphatases: the yin and yang of protein phosphorylation and signaling." Cell **80**(2): 225-36.

Irvine, G. B., El-Agnaf, O. M., Shankar, G. M. and Walsh, D. M. (2008). "Protein Aggregation in the Brain: The Molecular Basis for Alzheimer´s and Parkinson´s Diseases." Mol Med **14**((7-8)): 451-464.

Johnson, G. V. (2006). "Tau phosphorylation and proteolysis: insights and perspectives." J Alzheimers Dis **9**(3 Suppl): 243-50.

Johnson, G. V. and Stoothoff, W. H. (2004). "Tau phosphorylation in neuronal cell function and dysfunction." J Cell Sci **117**(Pt 24): 5721-9.

Johnson, L. N. and Barford, D. (1993). "The effects of phosphorylation on the structure and function of proteins." Annu Rev Biophys Biomol Struct **22**: 199-232.

Kang, J., Lemaire, H. G., Unterbeck, A., Salbaum, J. M., Masters, C. L., Grzeschik, K. H., Multhaup, G., Beyreuther, K., et al. (1987). "The precursor of Alzheimer's disease amyloid A4 protein resembles a cell-surface receptor." Nature **325**(6106): 733-6.

Karran, E., Mercken, M. and De Strooper, B. (2011). "The amyloid cascade hypothesis for Alzheimer's disease: an appraisal for the development of therapeutics." Nat Rev Drug Discov **10**(9): 698-712.

Katzam, R. and Saitoh, T. (1991). "Advances in Alzheimer´s disease." FASEB J(4): 278-286.

Kelly, E. B. (2008). Genes & Disease. Alzheimer´s Disease, Chelsea House.

Kennedy, M. B. (1993). "The postsynaptic density." Curr Opin Neurobiol **3**(5): 732-7.

Knops, J., Gandy, S., Greengard, P., Lieberburg, I. and Sinha, S. (1993). "Serine phosphorylation of the secreted extracellular domain of APP." Biochem Biophys Res Commun **197**(2): 380-5.

Kopke, E., Tung, Y. C., Shaikh, S., Alonso, A. C., Iqbal, K. and Grundke-Iqbal, I. (1993). "Microtubule-associated protein tau. Abnormal phosphorylation of a non-paired helical filament pool in Alzheimer disease." J Biol Chem **268**(32): 24374-84.

Lee, M., Kao, S., Lemere, C. A., Xia, W., Tseng, H., Zhou, Y., Neve, R., Ahlijanian, M. K., et al. (2003). "APP processing is regulated by cytoplasmic phosphorylation." J Cell Biol **163**(1): 83-95.

Lee, M. S., Kwon, Y. T., Li, M., Peng, J., Friedlander, R. M. and Tsai, L. H. (2000). "Neurotoxicity induces cleavage of p35 to p25 by calpain." Nature **405**(6784): 360-4.

Levy-Lahad, E., Wasco, W., Poorkaj, P., Romano, D. M., Oshima, J., Pettingell, W. H., Yu, C. E., Jondro, P. D., et al. (1995). "Candidate gene for the chromosome 1 familial Alzheimer's disease locus." Science **269**(5226): 973-7.

Liu, F., Grundke-Iqbal, I., Iqbal, K. and Gong, C. X. (2005). "Contributions of protein phosphatases PP1, PP2A, PP2B and PP5 to the regulation of tau phosphorylation." Eur J Neurosci **22**(8): 1942-50.

Liu, F., Iqbal, K., Grundke-Iqbal, I., Rossie, S. and Gong, C. X. (2005). "Dephosphorylation of tau by protein phosphatase 5: impairment in Alzheimer's disease." J Biol Chem **280**(3): 1790-6.

Liu, F., Liang, Z., Shi, J., Yin, D., El-Akkad, E., Grundke-Iqbal, I., Iqbal, K. and Gong, C. X. (2006). "PKA modulates GSK-3beta- and cdk5-catalyzed phosphorylation of tau in site- and kinase-specific manners." FEBS Lett **580**(26): 6269-74.

Lublin, A. L. and Gandy, S. (2010). "Amyloid-beta oligomers: possible roles as key neurotoxins in Alzheimer's Disease." Mt Sinai J Med **77**(1): 43-9.

Lucas, J. J., Hernandez, F., Gomez-Ramos, P., Moran, M. A., Hen, R. and Avila, J. (2001). "Decreased nuclear beta-catenin, tau hyperphosphorylation and neurodegeneration in GSK-3beta conditional transgenic mice." EMBO J **20**(1-2): 27-39.

Maccioni, R. B., Munoz, J. P. and Barbeito, L. (2001). "The molecular bases of Alzheimer's disease and other neurodegenerative disorders." Arch Med Res **32**(5): 367-81.

Martins, F. d. S. (2011). "Abeta dependent tau phosphorylation." Aveiro: University of Aveiro. Master´s Dissertation.

Masdeu, J. C., Zubieta, J. L. and Arbizu, J. (2005). "Neuroimaging as a marker of the onset and progression of Alzheimer´s disease." J. Neurol. Sci. **236**: 55-64.

Masters, C. L., Cappai, R., Barnham, K. J. and Villemagne, V. L. (2006). "Molecular mechanisms for Alzheimer's disease: implications for neuroimaging and therapeutics." J Neurochem **97**(6): 1700-25.

Mathis, C. A., Klunk, W. E., Price, J. C. and DeKosky, S. T. (2005). "Imaging technology for neurodegenerative diseases: progress toward detection of specific pathologies." Arch Neurol **62**(2): 196-200.

Matsui, T., Ingelsson, M., Fukumoto, H., Ramasamy, K., Kowa, H., Frosch, M. P., Irizarry, M. C. and Hyman, B. T. (2007). "Expression of APP pathway mRNAs and proteins in Alzheimer's disease." Brain Res **1161**: 116-23.

McClatchy, D. B., Liao, L., Park, S. K., Venable, J. D. and Yates, J. R. (2007). "Quantification of the synaptosomal proteome of the rat cerebellum during post-natal development." Genome Res **17**(9): 1378-88.

Moir, R. D., Lynch, T., Bush, A. I., Whyte, S., Henry, A., Portbury, S., Multhaup, G., Small, D. H., et al. (1998). "Relative increase in Alzheimer's disease of soluble forms of cerebral Abeta amyloid protein precursor containing the Kunitz protease inhibitory domain." J Biol Chem **273**(9): 5013-9.

Neve, R. L., McPhie, D. L. and Chen, Y. (2000). "Alzheimer's disease: a dysfunction of the amyloid precursor protein(1)." Brain Res **886**(1-2): 54-66.

O´Brien, R. J. and Wong, P. C. (2011). " Amyloid Precursor Protein Processing and Alzheimer´s disease." Annual Review of Neuroscience(34): 185-204.

Oliveira, J. M. d. (2011). "Abnormal protein phosphorylation in Alzheimer´s disease." Aveiro: University of Aveiro. Master´s Dissertation.

Palay, S. L. (1958). "The morphology of synapses in the central nervous system." Exp Cell Res **14**(Suppl 5): 275-93.

Pevalova, M., Filipcik, P., Novak, M., Avila, J. and Iqbal, K. (2006). "Post-translational modifications of tau protein." Bratisl Lek Listy **107**(9-10): 346-53.

Pimplikar, S. W. (2009). "Reassessing the amyloid cascade hypothesis of Alzheimer's disease." Int J Biochem Cell Biol **41**(6): 1261-8.

Pleckaityte, M. (2010). "Alzheimer's disease: a molecular mechanism, new hypotheses, and therapeutic strategies." Medicina (Kaunas) **46**(1): 70-6.

Pocklington, A. J., Armstrong, J. D. and Grant, S. G. (2006). "Organization of brain complexity--synapse proteome form and function." Brief Funct Genomic Proteomic **5**(1): 66-73.

Priller, C., Bauer, T., Mitteregger, G., Krebs, B., Kretzschmar, H. A. and Herms, J. (2006). "Synapse Formation and Function Is Modulated by the Amyloid Precursor Protein " Journal of Neuroscience **26**(27): 7212-7221.

Rahman, A., Grundke-Iqbal, I. and Iqbal, K. (2005). "Phosphothreonine-212 of Alzheimer abnormally hyperphosphorylated tau is a preferred substrate of protein phosphatase-1." Neurochem Res **30**(2): 277-87.

Rahman, A., Grundke-Iqbal, I. and Iqbal, K. (2006). "PP2B isolated from human brain preferentially dephosphorylates Ser-262 and Ser-396 of the Alzheimer disease abnormally hyperphosphorylated tau." J Neural Transm **113**(2): 219-30.

Rebola, N., Canas, P. M., Oliveira, C. R. and Cunha, R. A. (2005). "Different synaptic and subsynaptic localization of adenosine A2A receptors in the hippocampus and striatum of the rat." Neuroscience **132**(4): 893-903.

Rogaev, E. I., Sherrington, R., Rogaeva, E. A., Levesque, G., Ikeda, M., Liang, Y., Chi, H., Lin, C., et al. (1995). "Familial Alzheimer's disease in kindreds with missense mutations in a gene on chromosome 1 related to the Alzheimer's disease type 3 gene." Nature **376**(6543): 775-8.

Ryoo, S. R., Jeong, H. K., Radnaabazar, C., Yoo, J. J., Cho, H. J., Lee, H. W., Kim, I. S., Cheon, Y. H., et al. (2007). "DYRK1A-mediated hyperphosphorylation of Tau. A functional link between Down syndrome and Alzheimer disease." J Biol Chem **282**(48): 34850-7.

Schmidt, C., Lepsverdize, E., Chi, S. L., Das, A. M., Pizzo, S. V., Dityatev, A. and Schachner, M. (2008). "Amyloid precursor protein and amyloid beta-peptide bind to ATP

synthase and regulate its activity at the surface of neural cells." Mol Psychiatry **13**(10): 953-69.

Schrimpf, S. P. and Meskenaite, V. (2005). "Proteomic analysis of synaptosomes using isotope-coded affinity tags and mass spectrometry." Proteomics(5): 2531-2541.

Sherrington, R., Rogaev, E. I., Liang, Y., Rogaeva, E. A., Levesque, G., Ikeda, M., Chi, H., Lin, C., et al. (1995). "Cloning of a gene bearing missense mutations in early-onset familial Alzheimer's disease." Nature **375**(6534): 754-60.

Sisodia, S. S. and Tanzi, R. E. (2007). Alzheimer´s Disease. Advances in Genetics, Molecular and Cellular Biology., Springer.

Slomnicki, L. P. and Lesniak, W. (2008). "A putative role of the Amyloid Precursor Protein Intracellular Domain (AICD) in transcription." Acta Neurobiol Exp (Wars) **68**(2): 219-28.

Smalla, K. D., Li, K., Smit, A. B. and Gundelfinger, E. D. (2004). "Proteomic analysis of synaptic structures " (15): 1-4.

Staple, J. K., Morgenthaler, F. and Catsicas, S. (2000). "Presynaptic Heterogeneity: Vive la difference." News Physiol Sci **15**: 45-49.

Swingle, M., Ni, L. and Honkanen, R. E. (2007). "Small Molecule Inhibitors of Ser/thr Protein Phosphatases: Specificity, Use and Common Forms of Abuse." Methods Mol Biol. (365): 23-38.

Takashima, A., Noguchi, K., Sato, K., Hoshino, T. and Imahori, K. (1993). "Tau protein kinase I is essential for amyloid beta-protein-induced neurotoxicity." Proc Natl Acad Sci U S A **90**(16): 7789-93.

Tanimukai, H., Grundke-Iqbal, I. and Iqbal, K. (2005). "Up-regulation of inhibitors of protein phosphatase-2A in Alzheimer's disease." Am J Pathol **166**(6): 1761-71.

Tanzi, R. E., McClatchey, A. I., Lamperti, E. D., Villa-Komaroff, L., Gusella, J. F. and Neve, R. L. (1988). "Protease inhibitor domain encoded by an amyloid protein precursor mRNA associated with Alzheimer's disease." Nature **331**(6156): 528-30.

Tian, Q. and Wang, J. (2002). "Role of serine/threonine protein phosphatase in Alzheimer's disease." Neurosignals **11**(5): 262-9.

Uranga, R. M., Giusto, N. M. and Salvador, G. A. (2010). "Effect of transition metals in synaptic damage induced by amyloid beta peptide." Neuroscience **170**(2): 381-9.

Vintem, A. P., Henriques, A. G., da Cruz, E. S. O. A. and da Cruz, E. S. E. F. (2009). "PP1 inhibition by Abeta peptide as a potential pathological mechanism in Alzheimer's disease." Neurotoxicol Teratol **31**(2): 85-8.

Whittaker, V. P. (1993). "Thirty years of synaptosome research." J Neurocytol **22**(9): 735-42.

Whittaker, V. P. and Gray, E. G. (1962). "The synapse: biology and morphology." Br Med Bull **18**: 223-8.

Williams, R. W. and Herrup, K. (1988). "The control of neuron number." Annu Rev Neurosci **11**: 423-53.

Wimo, A. and Prince, M. (2010). "World Alzheimer Report 2010: The Global Economic Impact of Dementia." Alzheimer´s Disease International.

Wishart, T. M., Paterson, J. M., Short, D. M., Meredith, S., Robertson, K. A., Sutherland, C., Cousin, M. A., Dutia, M. B., et al. (2007). "Differential proteomics analysis of synaptic proteins identifies potential cellular targets and protein mediators of synaptic neuroprotection conferred by the slow Wallerian degeneration (Wlds) gene." Mol Cell Proteomics **6**(8): 1318-30.

www.alzheimerportugal.org/.

Yates, D. and McLoughlin, D. M. (2007). "The molecular pathology of Alzheimer´s disease." Psychiatry: 1-5.

Zhang, Y. W., Thompson, R., Zhang, H. and Xu, H. (2011). "APP processing in Alzheimer's disease." Mol Brain **4**: 3.

Zoidl, G. and Dermietzel, R. (2002). "On the search for the electrical synapse: a glimpse at the future." Cell Tissue Res **310**(2): 137-42.

8 Appendix

I. Synaptosome isolation

→ Equipment

- Yellowline (OST 20 digital) Homogeneizer;
- Centrifuge 5810R (eppendorf);
- Centrifuge 5417R (eppendorf);
- Ultracentrifuge (Beckman Optima LE-80K, 80Ti rotor).

→ Solutions

2M Sucrose

- Sucrose 68,46g

Mix until the solute has dissolved. Adjust the final volume to 100 mL deionised H_2O and store at 4^0C.

0,5M HEPES

- HEPES 13,015g

Mix until the solute has dissolved. Adjust the final volume to 100 mL deionised H_2O and store at 4^0C.

0,01M Dithiothreitol (DTT)

- DTT 0,03085g

Mix until the solute has dissolved. Adjust the final volume to 20 mL deionised H_2O and store at 4^0C. Discard the solution if it is stored for more than 24 hours.

0,1M KCl

- KCl 0,7456g

Mix until the solute has dissolved. Adjust the final volume to 100 mL deionised H_2O and store at 4^0C.

0,01M Ethylenediamine tetraacetic acid (EDTA)

- EDTA 0,3722g

Mix until the solute has dissolved. Adjust the final volume to 100 mL deionised H_2O and store at 4^0C.

0,02M Ethylene glycol tetraacetic acid (EGTA)

- EGTA 0,7607g

Mix until the solute has dissolved. Adjust the final volume to 100 mL deionised H_2O and store at 4^0C.

0,2M Glucose

- Glucose 3,6032g

Mix until the solute has dissolved. Adjust the final volume to 100 mL deionised H_2O and store at 4^0C.

2M NaCl

- NaCl 11,688g

Mix until the solute has dissolved. Adjust the final volume to 100 mL deionised H_2O and store at 4^0C.

1M Tris

- Tris 12,114g

Mix until the solute has dissolved. Adjust the final volume to 100 mL deionised H_2O and store at 4^0C.

Homogenizing buffer – Percoll gradient protocol

- 2M Sucrose solution 8 mL (0,32 M)
- 1M Tris solution 2,5 mL (0,05 M)
- 0,02M EGTA solution 5 mL (0,002 M)
- 0,01 M DTT solution 5 mL (0,001 M)

Prepare the solution just prior to use. Adjust the pH at 7.6 and store at 4^0C.

Homogenizing buffer – Sucrose gradient protocol

- 2 M Sucrose solution 16 mL (0,32 M)
- 0,5 M HEPES solution 4 mL (0,02 M)
- 0,01 M DTT solution 10 mL (0,001 M)

Prepare the solution just prior to use. Adjust the pH to 7.4 and after add 50 µl of protease inhibitor to each 50 ml of solution. Finally, store at 4^0C.

Krebs buffer

- 2 M NaCl solution 7 mL (0,14 M)
- 0,1 M KCl solution 5 mL (0,005 M)
- 0,5 M HEPES solution 5 mL (0,025 M)
- 0,01 M EDTA solution 10 mL (0,001 M)
- 0,2 M Glucose solution 5 mL (0,01 M)

Prepare the solution just prior to use. Adjust the pH to 7.4 and store at 4^0C.

Percoll® 45% (v/v)

- Percoll 2.7 mL
- Krebs Buffer 3.3 mL

Add 2.7 mL of Percoll® to 3.3 mL of Krebs buffer, for a final volume of 6 mL. Prepare the solution just prior to use and store at 4^0C.

II. SDS-PAGE and Immunoblotting Solutions

→ Equipment

- Electrophoresis system (Hoefer SE600 vertical unit);
- Electrophoresis power supply EPS 1000 (Amersham Pharmacia Biotec);
- Transfer electrophoresis unit (Hoefer TE42).

→ Solutions

LGB (Lower Gel Buffer) (4x)

To 900 mL of deionised H_2O add:

- Tris 181.65g
- SDS 4g

Mix until the solutes have dissolved. Adjust the pH to 8.9 and adjust the volume to 1L with deionised H_2O.

UGB (Upper Gel Buffer) (5x)

To 900 mL of deionised H_2O add:

- Tris 75.69g

Mix until the solutes has dissolved. Adjust the pH to 6.8 and adjust the volume to 1L with deionised H_2O.

30% Acrylamide/0.8% Bisacrylamide

To 70 mL od deionised H_2O add:

- Acrylamide 29.2g
- Bisacrylamide 0.8g

Mix until the solutes have dissolved. Adjust the volume to 100 mL with deionised H_2O. Filter through a 0.2 µm filter and store at 4^0C.

10% APS (ammonium persulfate)

In 10 mL of deionised H_2O dissolve 1 g of APS. This solution should be prepared fresh before use.

10% SDS (Sodium Dodedilsulfate)

In 10 mL of deionised H_2O dissolve 1 g of SDS.

Loading Gel Buffer (4x)

- 1 M Tris solution (pH 6.8) 2.5 mL (250 mM)
- SDS 0.8g (8%)
- Glycerol 4 mL (40%)
- Beta-Mercaptoetanol 2 mL (2%)
- Bromofenol Blue 1 mg (0.01%)

Adjust the volume to 10 mL with deionised H2O. Store in darkness at room temperature.

1 M Tris (pH 6.8) solution

To 150 mL of deionised H_2O add:

- Tris base 30.3g

Adjust the pH to 6.8 and adjust the final volume to 250 mL.

10x Running Buffer

- Tris 30.3g (250 mM)
- Glycine 144.2g (2.5 M)
- SDS 10 g (1%)

Dissolve in deionised H_2O, adjust the pH to 8.3 and adjust the volume to 1L.

Resolving (lower) gel solution (for gradient gels, 60 mL)

	5%	20%
H_2O	17.4 mL	2.2 mL
30% Acryl/0.8% Bisacryl solution	5 mL	20 mL
LGB (4x)	7.5 mL	7.5 mL
10% APS	150 µL	150 µL
TEMED	15 µL	15 µL

Stacking (upper) gel solution (20 mL)

	3.5%
H_2O	17.4 mL
30% Acryl/0.8% Bisacryl solution	5 mL
UGB (5x)	7.5 mL
10% APS	150 µL
10% SDS	200 µL
TEMED	25 µL

1x Transfer Buffer

- Tris 3.03g (25 mM)
- Glycine 14.41 (192 mM)

Mix until solutes dissolution. Adjust the pH to 8.3 with HCl and adjust the volume to 800 mL with deionised H_2O. Just prior to use add 200 mL of methanol (20%).

10X TBS (Tris buffered saline)

- Tris 12.11g (10 mM)
- NaCl 87.66 (150 mM)

Adjust the pH to 8.0 with HCl and adjust the volume to 1L with deionised H_2O.

10x TBS T (TBS+Tween)

- Tris 12.11g (10mM)
- NaCl 87.66g (159 mM)
- Tween 20 5 mL (0.05%)

Adjust the pH to 8.0 with HCl and adjust the volume to 1L with deionised H_2O.

Membrane stripping solution (500 mL)

- Tris-HCl (pH 6.7) 3.76 g (62.5 mM)
- SDS 10g (2%)
- Beta-mercaptoetanol 3.5 mL (100 mM)

Dissolve Tris and SDS in deionised H_2O and adjust with HCl to pH 6.7. Add the mercaptoethanol and adjust volume to 500 mL.